7-2021

Synthesis of Single-Modal and Dual-Modal Targeted Molecular Imaging Agents for MRI-NIR Imaging of Breast Cancer

Basant Kaur
bk7452@rit.edu

Synthesis of Single-Modal and Dual-Modal Targeted Molecular Imaging Agents for MRI-NIR Imaging of Breast Cancer

Basant Kaur

A thesis submitted in Partial Fulfillment of the Requirements for the Degree

Master of Science in Chemistry

Supervised by

Dr. Hans Schmitthenner

School of Chemistry and Materials Science

The College of Science

Rochester Institute of Technology

July, 2021

Signature of the Author _____

Accepted by _____

Director, M.S. Degree Program Date

SCHOOL OF CHEMISTRY AND MATERIALS SCIENCE
COLLEGE OF SCIENCE
ROCHESTER INSTITUTE OF TECHNOLOGY
ROCHESTER, NEW YORK

CERTIFICATE OF APPROVAL

M.S. DEGREE THESIS

The M.S. Degree Thesis of Basant Kaur has
been examined and approved by the thesis
committee as satisfactory for the thesis required for
the M.S. degree in Chemistry.

_____
Dr. Hans Schmitthenner, Thesis Advisor

_____
Dr. Maureen Ferran

_____
Dr. Joseph J. Hornak

_____
Dr. Scott Williams

_____
Date

Abstract

Our research is focused on the early and accurate detection of breast cancer (BrCa) by molecular imaging. Breast cancer is the most common type of cancer among women. Each year about one in eight women will be diagnosed, and over 500,000 deaths occur from breast cancer globally. To improve chances of survival, breast cancer must be diagnosed and treated at an early stage. Conventional imaging uses mammography, magnetic resonance imaging (MRI), and ultrasound. Limitations in these can result in false-positive results or undetected tumors. It is vital to create more sensitive imaging methods to diagnose BrCa, to reduce false-positives and to guide therapy. A new approach to targeted molecular imaging agents (TMIAs) for BrCa will be described for single-modal and dual-modal imaging by fluorescence and MRI. To target these imaging agents, we employed a new BrCa-targeting peptide called 18-4. This peptide was synthesized by solid phase peptide synthesis (SPPS) followed by conjugation of a near infrared dye, Cy5.5-1S, utilizing a new modular method developed in our lab, to form M3, an imaging agent for BrCa. The modular method was then utilized to construct a single-modal agent containing the MRI-contrast agent metal gadolinium. Lastly, a dual modal targeted imaging agent containing both Gd and Cy5.5-1S for dual modal fluorescence-MRI of BrCa was synthesized. This is the first example of a dual-modal TMIA that is synthesized entirely by SPPS, where the imaging agents are brought in on the side chain of amino acids that coupled as part of the solid phase synthetic approach.

Acknowledgements

I would like to express my deepest appreciation to my research advisor, Professor Dr. Hans Schmitthenner for all his support and help throughout this research project. Even through the most difficult times of this project, his insightful feedback pushed me to sharpen my thinking and overcome the hurdles in this work.

I am also grateful for all of my group members in the molecular imaging laboratory at RIT who helped and supported me. I would like to specifically thank a former group member, Xinyu Xu, who provided the groundwork for this project. Osarhuwense Otasowie deserves to be recognized, for her help with the gadolinium MRI contrast agent. Julia Crandall, for her help with synthesis of the NIR Cy5.5 puzzle piece. A special thanks to Matt Law, who helped me along the way of my journey. Matt helped with the mystery of Fmoc deprotection step, which was an important discovery for the M3-TMIA synthesis.

I would like to acknowledge Dr. Kamaljit Kaur from Chapman University for providing our group with the breast cancer peptide 18-4 and for her help in mentoring to synthesize 18-4 peptide. Additionally, I would like to thank the RIT College of Science, specifically the School of Chemistry and Material Science for providing me with academic support during my graduate studies here at RIT. I would also like to thank my committee members: Dr. Maureen Ferran, Dr. Joseph Hornak, and Dr. Scott Williams. Thank You for all your support with my research.

Last but not least, I would like to thank my family and friends, who supported me greatly during my time here at RIT as a graduate student. I am grateful for my family, who have been there for me every step of my educational journey and encouraged me to explore new opportunities in life. This journey would not have been possible without their support.

Abbreviations

AA (Amino Acids)
ACN (Acetonitrile, an organic solvent used in HPLC)
BrCa (Breast Cancer)
B_0 (magnetic felid)
CFM (confocal fluorescence microscopy)
CT (computerized tomography)
DCM (Dichloromethane)
DSS (A linker in targeting molecular imaging agents)
DIPA (diisopropyl ethyl amine, also called DIEA, used as a base in coupling reactions)
DMF (Dimethylformamide, a solvent for peptide coupling)
Fmoc (fluorenylmethyloxycarbonyl chloride)
FID (free induction decay)
Gd (gadolinium)
HATU (a common peptide coupling reagent)
HPLC-MS (high-performance liquid chromatography-mass spectrometry)
HR-MS (high-resolution mass spectrometry)
KRT1 (keratin-1)
MRI (magnetic resonance imaging)
MeOH (Methanol an organic solvent used in HPLC)
Mtt (Methyltrityl, a protecting group that is easily removed with mild acid)
NIR (Near-infrared)
NMR (nuclear magnetic resonance spectroscopy)
OMI (Optical molecular imaging)
PET (Positron-emission tomography)
PDT (Photodynamic Therapy)
PhiPr (a protecting group that is remove with mild acid)
RP-HPLC (reverse phase-high performance liquid chromatography)
RF (radio-frequency)
ROS (reactive oxygen species)
SPPS (solid-phase peptide synthesis)
SNR (signal-to-noise ratio)
TNM (tumor node metastasis)
TMIAs (targeting molecular imaging agents)
TFA (Trifluoroacetic acid)
TSTU (a common peptide coupling reagent)
tBu (t-butyl, a protecting group that is remove with mild acid)

Abbreviations of Amino Acids in peptide 18-4

Amino Acids	Three Letter Abbreviations	One Letter Abbreviations
Alanine	Ala	A
Glutamic Acid	Glu	E
Glutamine	Gln	Q
Leucine	Leu	L
Lysine	Lys	K
Phenylalanine	Phe	F
Tryptophan	Try	W
Tyrosine	Tyr	Y
Norleucine	Nle	X

Table of Contents

List of Figures

List of Schemes

List of Tables

Chapter 1. Introduction

1.1 Breast Cancer Background

It has been reported that each year globally, about 458,000 deaths occur from breast cancer (BrCa).[1] BrCa must be treated at an early stage to decrease the mortality rate.[2] Cancer is caused by genetic mutations of DNA and or RNA, which can occur under an unhealthy cell environment.[3] Patients with a family history of BrCa are at higher risk for BrCa.[4] Some other risks for BrCa include age, genetics (abnormal gene mutations), being overweight, smoking, and lack of exercise.[4] There are two kinds of tumors, which include benign and malignant.[5] The cells in a benign tumor are non-cancerous and are not dangerous.[5] Moreover, benign cells have a similar appearance to healthy cells and do not metastasize (spread to other parts of the body).[5] BrCa is known as a malignant tumor that can metastasize.[5]

For BrCa, a staging system known as tumor-node-metastasis (TNM) is used for diagnosis.[6] Staging is the analysis of the tumor's (T) size and location.[6] The second step of diagnosis is determination of node (N), which identifies if the tumor has spread to the lymph nodes and how many.[6] Lastly, metastasis (M) or stage IV diagnosis is used to determine if the tumor has spread to other parts of the body (lungs, liver, bones, brain, or chest wall).[6] The process of metastasis can occur by migration through circulation, where cancer cells travel to healthy cells by the lymph vessels or blood vessels.[7] The stage of BrCa or staging is used to identify the location, growth, and spreadability of cancer.[6]

Utilizing this system, there are five stages of cancer, ranging from stage zero through stage IV.[6] A lower stage number indicates that it has spread less through the body.[6] Stage zero is known as noninvasive, which means that the tumor does not spread or damage other organs.[6,8]

However, stages I through IV are known to be invasive breast cancer.[6] Stage I is known as a very early stage, where cancer has grown larger within the breast, and the tumor can be up to 20 mm large.[8] Stage II is known as the localized stage, where the tumor has spread to the lymph nodes and is about 20-50 mm in size.[8] Stage III is known as the regional spread (larger than 50 mm), where the tumor may have spread to more than one lymph node or the skin.[8]

Lastly, Stage IV is the most severe and is known as distant spread cancer.[8] Currently, to determine the stage of cancer, two diagnosis methods are used, including the clinical stage and the pathologic stage.[8] The initial step of diagnosis is the clinical stage, which uses a physical exam, biopsy, and imaging testresults.[8] Since the clinical-stage testing does lead to inaccurate results, sometimes further testing is required.[8] To determine the stage precisely, the pathologic stage is used, a process that removes the tissue surgically for pathological testing.[8]

1.2 Current Imaging methods for breast cancer

While mammography and ultrasound are the primary diagnostic imaging methods for detection of breast cancer, a more powerful imaging method for diagnosis of breast cancer is magnetic resonance imaging (MRI), which uses a magnetic field, and radio waves.[9] Mammography and ultrasound used in conjunction with MRI for confirmation and accurate spatial mapping of BrCa. A significant advantage of MRI over other imaging diagnoses is that it has minimal risks, in comparison to mammography, which has a risk for radiation.[10] The x-rays in mammography are known as ionizing radiation and in large amounts, can cause damage to cells and lead to cancer.[11] A limitation with the current imaging diagnosis of US, Mammography and MRI is that these can result in false-positive results.[12]

In a false-positive test result, the imaging method shows the benign tissue incorrectly to be cancerous tissue.[9] Therefore, such results can lead to further testing (MRI-guided breast biopsy), which causes the patient to go through unnecessary pain and expense. Moreover, there has been an increasing number of biopsies for breast cancer due to false-positive results.[13] Also, MRI screening is unable to determine the stage of BrCa in a patient due to the limited specificity.[12] Therefore, it is essential to create efficient imaging methods to diagnose breast cancer and to reduce the false-positive rate.[12]

In this study, the goal was to diagnose and pinpoint the location of breast cancer cells by using targeting molecular imaging agents (TMIAs). The purpose of the TMIAs is to concentrate the imaging agent at the site of cancer selectively Thus, with the use of TMIAs, MRI diagnosis will be able to differentiate between cancer and benign tissues, which will rule out false-positive results. Furthermore, this approach will improve the staging of breast cancer. Current staging by for breast cancer requires further diagnosis such as removal of tissue via surgery.[6,8] Addition of TMIAs to MRI imaging will lead to a precise diagnosis for staging because the TMIAs will distinctly identify cancer cells, including those which have spread to lymph nodes or throughout the body.

1.3 Molecular Imaging

Advancements in molecular imaging has provided new hope for early cancer detection, cancer treatment, monitoring therapy response and disease recurrence in the future.[14] Molecular imaging allows *in vivo* visualization and characterization of cellular biological processes.[14] Older technologies were able to only identify the structure and morphology of a disease.[14] Molecular imaging is able to identify biochemical and intracellular pathways, which can help determine the disease development and progression.[14] It is a therefore a means to

provide functional imaging. Using targeted probes for functional imaging we can extend the question “what is there?” to “what is happening there?”

There are some advantages of molecular imaging compared to other imaging techniques.[14] Molecular imaging can provide early cancer detection because it can evaluate cellular abnormalities along with physical abnormalities, which can identify the stage of the disease.[14] Also, molecular imaging can detect functional variation in tissue, which can potentially help with identification of lesions.[14] Lastly, in current imaging methods there is a limitation to the capability of measuring the effectiveness of drugs. Molecular imaging can be used to advance this process and has become a valuable tool in drug development and discovery.[14] Moreover, another advantage is that it can be used for gene therapy, where the genetic changes that are caused by the treatment can be evaluated.[14]

Of the various imaging modalities available, optical molecular imaging (OMI), which is based on fluorescence of dyes, is non-invasive and provides high sensitivity (single-molecule level) with minimal invasion.[14] Furthermore, OMI has low screening risk does not use ionizing radiation to generate an image.[14] A disadvantage of OMI is that whole body imaging is not possible. In OMI, the probe is a visualizing agent that is used to characterize and quantify biological processes.[15] A probe may also be defined as a contrast agent, tracer, and molecular beacon.[15] Probes for OMI consists a fluorochrome, which is attached covalently by a linker to a targeting moiety that ultimately provides a visualization method on the target of interest as shown in Figure 1.[14,15]

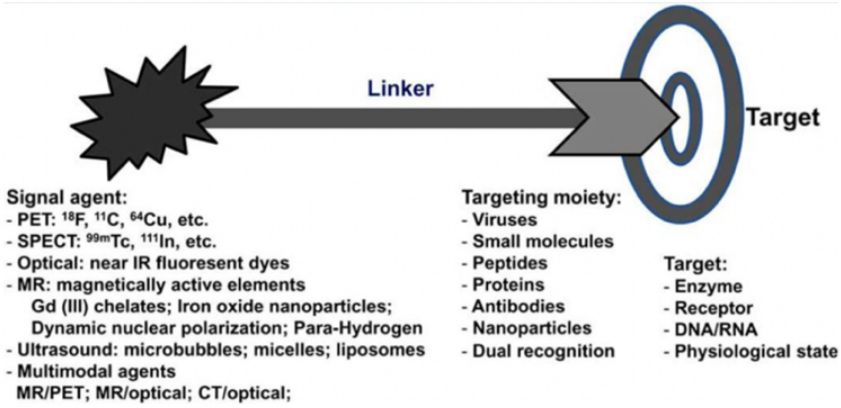

***Figure 1**. Optical Molecular Imaging Probes*[15]

Reprinted with permission from Chen,K.; Chen, X. Design and Development of Molecular Imaging Probes. *Curr. Top. Med. Chem.* **2010**, *10* (12), 1227.

Imaging probes can be made more effective by attaching to them a targeting moiety, which binds selectively to a specific biological target of interest.[15] In this study the targeting moiety is a breast cancer peptide and the target is a breast cancer receptor. This will be attached to an optical imaging probe to design a targeted molecular imaging agent (TMIA).

Molecular imaging probes have the advantage of high binding affinity to the target along with high specificity to the target.[15] The probes interact with only the specific target of interest, such as a membrane receptor, an enzyme, or cellular DNA.[15] Moreover, the highly specific binding can reduce the uptake of non-specific biological molecules, which will help to quantify only the targeted molecules in the cell.[15]

1.3.1 Confocal fluorescence microscopy (CFM) and NIR Dyes

Within the field of OMI, confocal fluorescence microscopy (CFM) is a microscopic technique provides three-dimensional (3D) optical resolution.[16] An advantage of CFM microscopy is that it produces high-contrast images even with a thinly layered specimen.[17] A laser beam is scanned

across the sample (also known as point-by-point), which causes the fluorophores in the specimen to absorb energy.[16,17] As a result, the fluorophores fluoresce and emits light in the near infrared (NIR) region of the spectrum at a longer wavelength (about 30 nm longer) than the excitation wavelength.[16,17] Moreover, near-IR fluorescence emission is ideal for *in vivo* imaging because it has strong tissue penetration (1-2 cm).[18,19]

The wavelength range for NIR fluorescence imaging is from 700 nm to 1000 nm.[18] The NIR probes have good water solubility, which prevents the aggregation of the dye in tissues and biological systems.[18] There are two types of NIR probes, which includes inorganic and organic molecules.[18] Some of the inorganic NIR probes (nanometer-sized) used in vitro and vivo biological imaging are quantum dots and nanoparticles.[18] However, some nanoparticles such as quantum dots have a disadvantage because the heavy metals ingredients (Cd, Se) can potentially lead cytotoxicity (cell death).[18] Moreover, nanoparticles have a disadvantage because they are prepared at a small scale and are expensive.[18] In addition, nanoparticles can exhibit non-specific binding, thereby lighting up more than the tumor and in some cases the whole body.

Comparatively, small organic molecules (under 3,000 MW units), are ideal as a NIR probe and can be synthesized at a larger scale.[18] The organic NIR dyes are suitable to be conjugated (covalently or noncovalently) with different biological molecules, which includes proteins, DNA primers, amino acid, peptides, antibodies and nucleotides.[18] There are some limitations to the NIR conventional dyes, which includes poor depth penetration, poor hydrophilicity, and low quantum yield.[18] Dye types such as cyanine dyes, squaraines, phthalocyanines, porphyrin derivatives, and BOD-IPY (boron dipyrromethane) dyes are newly developed organic NIR dyes

that are used for biomedical imaging and have shown to improve fluorescence intensity and sensitivity.[18]

A cyanine dye is an organic dye that is composed of two aromatic systems, which contain heterocycles linked by a polymethine bridge. The two aromatic systems are known as indolenine groups.[18] Some of the common cyanine dyes (Cy) that are used for NIR fluorescence are trimethine cyanine (Cy3, Cy3.5), pentamethine cyanine (Cy5, Cy5.5), and heptamethine cyanine (Cy7, and Cy7.5).[18,20] These dyes absorb at different wavelengths in the NIR region, where the Cy3 dyes absorbs in the visible region and the Cy5 dyes absorb in the near-infrared region (>700 nm).[18] A dye known as indocyanine green (ICG), absorbing between 600 and 900 nm and emitting between 750 and 950 nm is a mainstay in OMI. With an established reputation in the clinic, many cyanine dye systems have since been designed to emulate this, but with the added feature of adding a functional group that enables joining the dye to a biological targeting system. Lastly, the Cy7 dyes absorbs at 750 nm.[18]

Our molecular imaging lab collaborates with Dr. Ferran and Dr. Sweet from the Biology department to produce confocal fluorescence microscopy (CFM) images for TMIAs. To label peptides in our lab, the CFM dye used is known as the cyanine 5.5 (Cy 5.5) NHS ester dye. In particular, the Cy 5.5 dye was chosen because the highest laser available at RIT for the CFM has excitation at 633 nm, which has emission range between 650 nm and 750 nm. The difference between Cy5.5, which is utilized for in-vitro imaging such as CFM, and Cy7 which is suitable for in vivo imaging is shown in Figure 2. The main reason to utilize higher wavelength dyes such as Cy7 in animal studies is that they absorb light well beyond the absorption of Hemoglobin.

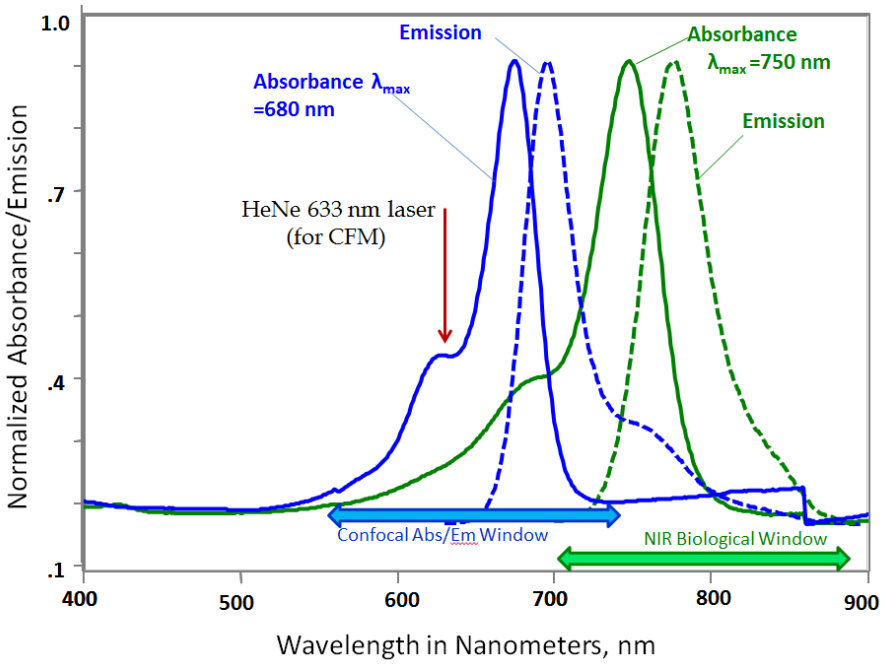

Figure 2. *Absorbance and emission spectra for Fluorescent Near Infrared (NIR) dyes, maximum absorbance occurs at 680 nm*

Apart from structural differences that result in different wavelengths, the cyanine dyes are divided into two groups based on solubility, which includes non-sulfonated and sulfonated dyes.[20] And both are used to label biomolecules, such as proteins and DNA.[20] A disadvantage to the non-sulfonated cyanine dye is that they have low aqueous solubility.[20] The sulfo-dyes are water soluble and the of addition of a sulfonate group (SO_3^-) at the aromatic ring facilitates the solubility of the cyanine dye in aqueous phase.[20] The negative charge of on the sulfonate group decreases the aggregation of the dye molecules in water.[20] In particular, the single-sulfonated cyanine 5.5 (Cy 5.5-**1S**) dye was used in this study as shown in Figure 3.

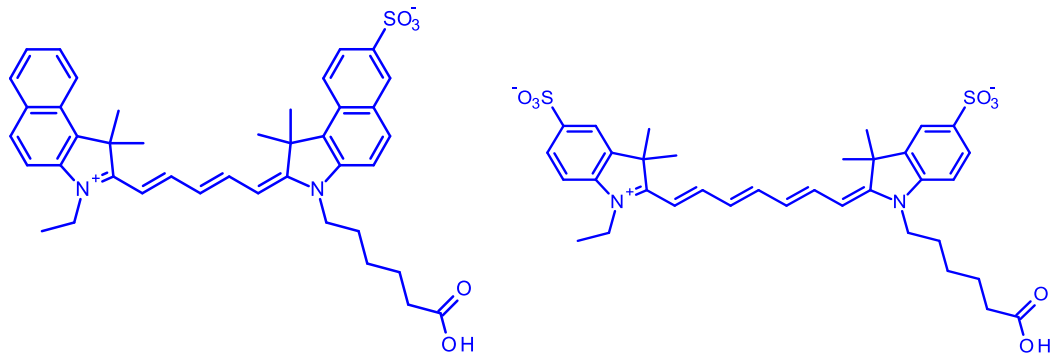

***Figure 3**. Structure of Cyanine 5.5 (1S) dye and Cy 7.*

1.4 Magnetic Resonance Imaging (MRI)

Magnetic resonance imaging (MRI) is a tomographic imaging technique commonly used in medical clinical practice.[21] In 1952, Bloch and Purcell were awarded the Nobel Prize for discovering the magnetic resonance phenomenon.[22] A MRI scanning machine was introduced by a physician Damadian and later in 1969 he was the first to perform a full human body scan to diagnose cancer.[23] Moreover, Damadian discovered MRI distinguishes between tumors and normal tissue because they have different relaxation times.[23] MRI generates three-dimensional (3D) images and is noninvasive and unlike other imaging techniques MRI is considered a safe imaging method because it does not use ionizing radiation.[24]

All of the components on MRI scanner are controlled by the computer.[21] The MRI scanner is composed of three main components, which includes large magnet, gradient coils, and radio frequency (RF) coils (shown in Figure 4).[21] To image the body, MRI uses a strong magnetic field, which is ten thousand times greater than the Earth's magnetic field.[24]

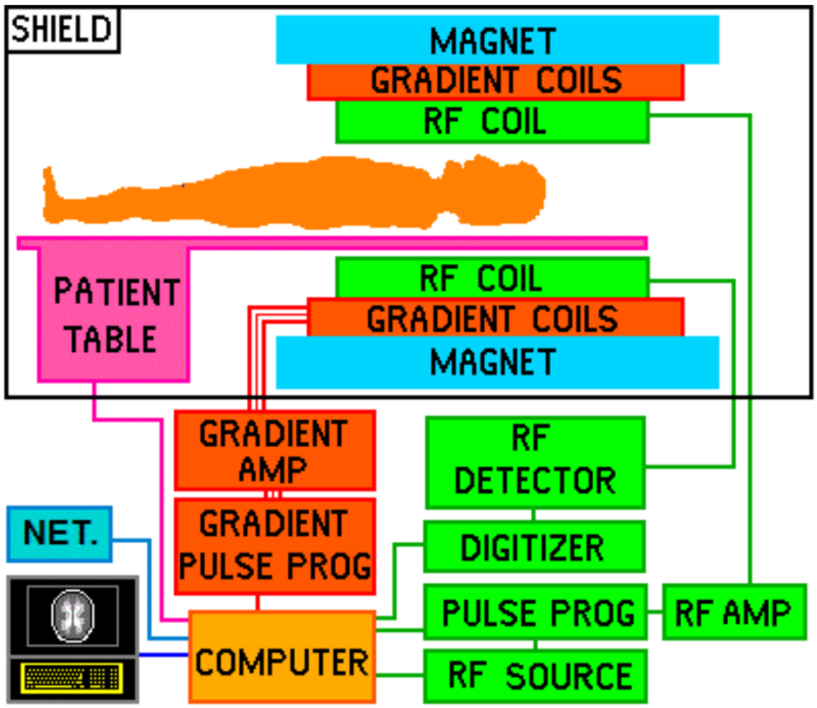

***Figure 4**. Schematic representation of MRI Scanner*[21]

Reprinted with permission from Hornak. J.P. *The Basics of MRI*; Interactive Learning Software, Henietta, NY, 2012.

The type of magnet used in MRI is known as the superconducting magnet, which is an electromagnet composed of superconducting wire.[21] Liquid helium is used to cool the superconducting wire to absolute zero (0 K).[21] To produce an image MRI produces a magnetic felid (B_0) at about 1.5 to 3 Tesla.[21,25] Moreover, there are gradient coils in the MRI that are at room temperature, which are within the magnet that produce B_0 in the X, Y, and Z directions.[21] Lastly, in the MRI scanner the RF coil are present within the gradient coils.[21] A B_1 magnetic field is produced by the RF coil, which is used to rotate the spins by 90°, 180° in the XY plane.[21]

The imaging property responsible for MRI is water and fat present in the human body.[21] Water and fat molecules are abundant in hydrogen atoms (approximately 63% in the body).[21]

Mainly the nuclei of the hydrogen atom is responsible for producing an NMR signal.[21] The hydrogen atoms have a property known as nuclear spin.[21,26] When there is no magnetic flied present the hydrogen spins are randomly aligned in the body.[26] However, after MRI provides a strong magnetic felid (B_0) the spins of the protons are aligned with magnetic field.[26]

Firstly, the nucleus of the protons has angular momentum and it spins or rotates around the B_0 axis, called precession, which results in a net magnetization.[21,26] The rotation velocity or rate around direction of the protons is known as the Larmor frequency.[26]

Secondly, the protons that have a nuclei spin are excited with a second radio frequency (RF) magnetic field B_1, which is applied perpendicular to the external magnetic field (B_0).[26] When a RF is applied in short pulses, which last about microseconds.[26] The energy level of the nucleus transitions from higher to lower energy from the process of absorption. After the radiofrequency is turned off, it results in magnetic vectors to return to the resting state, which results in a relaxation signal that can be detected.[26] The process of relaxation occurs when after the absorption of the RF pulse, the nuclei spin returns to thermal equilibrium.[26] The precession magnetization from the RF coil generates a radio wave, which is known as the free induction decay (FID) time domain signal.[26] The RF pluses are applied multiple times, which generate multiple FIDs and as a result the FIDs are averaged to enhance signal-to-noise ratio (SNR).[26] Lastly, to obtain an MRI image the signal-averaged FID is transformed by a method called Fourier transformation.[26] An image is derived from software manipulations of this Fourier transform and various tissues are depicted in different shades of color.

Chapter 2. Modular Approach

2.1 Modular approach for Imaging Agent Synthesis

Targeted molecular imaging agents (TMIAs) are synthesized by coupling amino acids with imaging agents attached to the side chains.[27] The peptide-based TMIAs can be synthesized with amino acids that have a combination of single-modal or dual-modal metals and dyes, which can be attached in first or last step of the synthesis.[27] Our lab's focus is to provide medical researchers with ready to access single or dual modal TMIAs. In our lab, a new approach to synthesize TMIAs was developed, which is known as the modular method. Using modular method offers many advantages, where dyes and metals can be mixed and matched.

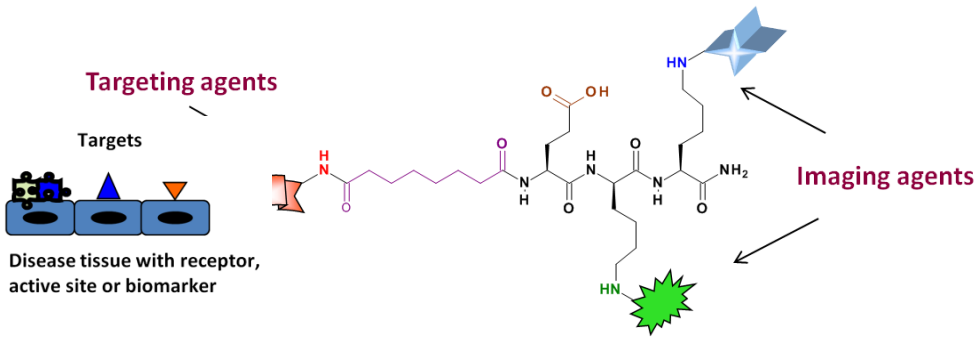

Figure 5. *Past approach for the synthesis of TMIAs using solution phase*[28]

In the modular synthesis, a puzzle piece is synthesized first. A puzzle piece is composed of an imaging group (metal or dye) placed on the side chain of lysine group (shown in Figure 5). Previously, to synthesize a TMIA, the modular method was used, where the two imaging modules are coupled first. Following the coupling of imaging agents, a linker group such as disuccinyl suberate (DSS) is added (as shown in Figure 5). Lastly, the targeting group is coupled on the left side is conjugated to this system. The targeting group can be any drug, antibody, or peptide. In our group the past TMIAs that have been synthesized were by solution phase peptide synthesis, which has some disadvantages.[28] In solution phase synthesis, each intermediate at every step

requires purification, which is a time-consuming step.[28] Moreover, dyes may degrade during the purification process and also the additional purification steps lead to a lower yield.[28]

Some of the imaging agents that can be attached to peptides include those developed for confocal fluorescence microscopy (CFM), Near-infrared (NIR), MRI, Positron-Emission tomography (PET), and Photoacoustic Imaging (PAI).[28] The main goal of this study was to synthesize TMIAs composed of the MRI contrast agent gadolinium (Gd) and the NIR (Cy5.5-1S) dye as (shown in Figure 6).

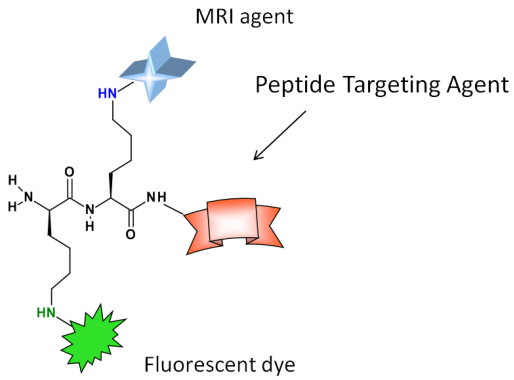

Figure 6*. Current approach for the synthesis of TMIAs using solid phase*[28]

Also shown in Figure 6, in this study, the TIMA was synthesized in the opposite direction. The BrCa targeting agent (a peptide) was synthesized first, which was followed by attaching the imaging agents (Gd agent and Cy5.5 dye) last. This synthesis stems from the targeting peptide and since the imaging modules are amino acids, it allows to make a longer peptide where the last two amino acids are the imaging modules.

Furthermore, in this case, solid phase peptide synthesis (SPPS) was used to produce the TMIA because it has many advantages. The SPPS is a faster synthesis process because there is no need to purify each intermediate, therefore is not a lost in yield. It is a much-preferred method

in peptide synthesis, because it allows us to marry the imaging agent and peptide chemistry together in an efficient manner.

2.2 Single and Dual-Modal Imaging

TMIAs can be synthesized as single-modal, dual-modal, or multi-modal imaging agents. As shown in Table 1, there are advantages and disadvantages of single modal MRI and fluorescence imaging.[29] Single modal fluorescence imaging (FI) alone is not useful for breast cancer diagnosis because FI has low temporal and spatial resolution.[29] However, FI is suitable for diagnosis because it has tissue penetration up to 1-2 cm deep) and is favorable because it has high sensitivity and high specificity.[29] Unlike many techniques in imaging, FI is conducted with relatively inexpensive instrumentation.

Table 1. Fluorescence and MRI Advantages and Disadvantages[30]

	FI	**MRI**
Spatial Resolution	Low	High
Sensitivity	High	Low
Penetration Depth	Shallow	Deep
Traumatic	Noninvasive; Nonradioactive	Noninvasive; Nonradioactive

FI has the ability of obtaining detailed biological information at a subcellular level.[29] Compared to other imaging techniques FI has a major advantage because it can be used during surgery. Doctors could use fluorescent cancer markers during a lumpectomy (removal of breast tumor), where the laser light is used to light up the targeted cancer cells and remove the tumor.[30]

MRI is used to view internal anatomical structures and tissue, a produces high contrast images.[29] Compared to FI, which generates blurry images, MRI has the advantage of producing clear and detailed morphological images with high spatial resolution.[29] But MRI is not very

sensitive. A major advantage of MRI over FI is that MRI is used for breast cancer diagnosis because it has deep tissue penetration.[29]

In molecular imaging, combining different modalities can be advantages because it can produce complementary information over single modal alone.[29] Dual modal is a powerful technique for disease diagnosis and treatment that will improve detection sensitivity and accuracy.[31] To synthesized a dual-modal TMIA, two different imaging agents are combined to produce one imaging agent. Using single-modal fluorescence agent for FI is limited with tissue penetration and is not useful for diagnosis but is useful for surgery and remove cancer at the site.[29] However, the combination of both MRI and FI will provide quantitative and tomographic information.[31]

In the past FI/MRI dual-modal imaging probes have been synthesized and applied in clinical practice.[29] The dual modal FI-MRI agents that have been synthesized were derived from nanoparticles, which have many disadvantages. [29]Nanoparticles can bind non-specifically in the body, especially in the liver and kidneys.[29] Also, nanoparticles are much larger in size to be used as a drug.[29] Moreover, due to the large size of nanoparticles they have poor tissue penetration and can only tag the surface of the tissues.[29] Lastly, nanoparticles have a disadvantage as TMAI because many types of nanoparticles cannot accumulate inside of tumor as efficiently as small molecules for amplification of tissue detection.[29]

To make dual-modal imaging agents, another reported study has combined a NIR dye with chelated gadolinium-based MRI contrast agent.[31] However, the imaging agents synthesized in this report was not targeted for cancer cells.[29] The agent instead relied on increased illumination

in an acidic environment. Since the interior of cancer cells are acidic, it was proposed to light up the cells using dyes that are non-targeted, but can change color based on changes in pH.

In contrast to this approach, our approach is based on dual-modal imaging agents which can be molecularly targeted specifically to breast cancer cells by utilizing an agent that is known to bind selectively to membrane receptors on those cells.

Chapter 3. Cancer Treatment

3.1 Current Treatment of Breast cancer

A stretch goal of this study was to treat cancer by the use of related TMIAs, synthesized by a similar route. This is a project currently being carried out in our lab by Sara Shaut and Matt Law. Conventional treatment for cancer is chemotherapy, which uses chemotherapeutic agents.[32] Chemotherapeutic agents can inhibit the rapid growth of cancer cells.[33] However, a significant disadvantage of chemotherapy is the potential risk of uptake by healthy cells.[33,34] The cell death from chemotherapy treatment can occur in many organs in the body, which includes the heart, kidneys, bladder, lungs, and nervous system.[33]

Another issue with the current drug delivery is the uncertainty of the chemotherapy agents' binding specificity; they should bind only to the breast cancer cells.[32] The agents are not selective for cancer cells, and therefore they don't particularly accumulate at the site of cancer.[34] By use of a TMIA, the agent will only attach at the cancer site and protect the healthy cells due to the binding specificity of the TMIAs. In the future, fluorescent TMIAs, several of which are in development now, will be used to assist in "light directed surgery". The agent can be given to the patient before surgery, which will light up only the cancer cells allowing for directed treatment.

3.2 Photodynamic Therapy (PDT) for cancer

A new method known as photodynamic therapy (PDT) is used to treat cancer.[35] An agent known as photosensitizing (PS) agent is injected, which is absorbed into the cells all over the body.[35] The purpose of the photosensitizing agent also known as a photosensitizer (drug) is to kill the cancer cells upon the exposure to a laser light.[36] However, the non-targeted photosensitizing agent can remain in normal cells in approximately 24 to 74 hours.[35] Also, PDT has shown to

damage tumor blood vessels, which prevents cancer because cells become deficient of nutrients.[35]

3.2.1 Photosensitizer mechanism for killing cancer cells

The electrons are unstable energy in the excited state (shown in Figure 7), and return to the ground state by emitting a photon and this process is known as fluorescence.[37] Radiative transition is described as the absorption or emission of photon, demonstrated as straight lines.[37] Non-radiative transitions are described as the energy transferred between different degrees of freedom of a molecule or to the surroundings, demonstrated as wavy lines.[37] Fluorescence and phosphorescence occur as radiative transitions.[37] Nonradiative transitions include, intersystem crossing, internal conversion, and vibrational relaxation.[37]

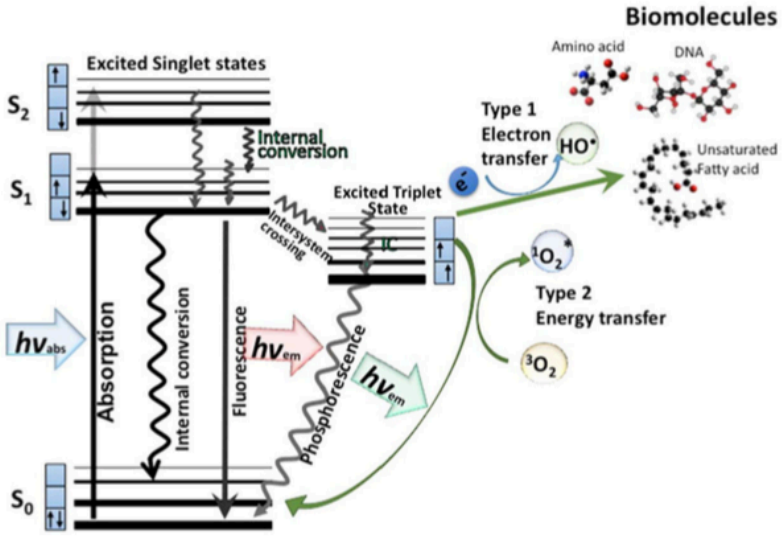

Figure 7. *Jablonski Diagram that shows the formation of reactive oxygen species (ROS) induced from photosensitizer agent*[38]

Reprinted with permission from Abrahamse, H. New Photosensitizers for Photodynamic Therapy. *Biochem. J.* **2016**, *473* (4), 347.

Due to collision of the electrons in the excited state there is a loss of energy through the transitions, which causes the emission wavelength in fluorescence to be longer than the excitation wavelength.[37]

In the ground state the photosensitizer is a singlet since it is composed of two electrons with opposite spins.[38] The electrons in the photosensitizer transition from the singlet state (low-energy orbital) to the excited state (higher-energy orbital) by absorbing energy from a photon (light).[38] The photosensitizer is unstable in the singlet excited-state, which causes it to lose energy and that can through the process of fluorescence (emission of light) or internal conversion (heat production or non-radiative decay).[38] The process of phosphorescence is the transition of the electrons from the triplet state (more stable) to the ground state, which occurs at a longer life (microseconds).[38] The photosensitizer transitions of the electrons do not occur with the phosphorescence but with intersystem crossing, which causes a stable excited triplet state (parallel spin).[38]

There are two types of chemical process that occur for the photosensitizer molecule, and that includes the Type I photochemical and Type II photochemical process.[38] In the Type II photochemical reaction, the electrons in the triplet state collide with molecular oxygen (O_2) in the cell, and energy is transferred due to the longer lifetime of the triplet state.[38] Upon collision of the electron a reactive singlet oxygen ($O_2^{\bullet}$) is formed, as shown in Figure 7.[38] In Type I photochemical reaction an electron transfer reaction leads to form a reactive oxygen species (ROS).[38]

The photosensitizer is successful is killing cancer cells because ROS is toxic to cells.[39] In the body, free radicals cause to the damage from a process known as oxidative stress. In this

study, a photosensitizer will be used to treat breast cancer and only the cancer cells will be killed because of the targeting agent present in the TIMAs. Breast cancer cells treated with the photosensitizer will be treated with a laser to kill the cells. Lastly, the treatment analysis will be done in the future by MRI and CFM to ensure that the cancer cells died.

While this stretch goal did not become part of this research, the synthetic methods developed in this study can be applied to the attachment of other dyes, including photosensitizer (PS) dyes to peptides in much the same manner as imaging dyes reported here. The same technique of attaching the puzzle piece containing the dye onto the growing peptide chain in SPPS could be applied to attaching PS dyes to produce targeted agents for PDT of BrCa.

Chapter 4. Peptides as Targeting Molecules

4.1 Peptides Advantages and Disadvantages

Previously, studies have shown that peptides can be used as targeting molecules and in addition, they have many advantages.[32] A significant advantage is that peptides are small and compact (1000-3000 amu), which allows them to circulate throughout the vascular system easily and penetrate the cells quickly.[28] Another advantage of using peptides as TMIAs is due to their clearance properties.[40] The clearance property of a drug is the ability of a drug to be excreted from the body.[40]

The process by which peptides enter the cell is known as endocytosis, where the cell ingests large particles from the extracellular environment.[41] The process of endocytosis occurs in two steps, initially the peptide binds to the receptor of the BrCa cell.[42] The binding location of the peptide to the cancer cells occurs at the receptor site of the cell.[42] The receptor known as keratin-1 (KRT1) on the breast cancer cells is recognized by the targeting agent (peptide) and attaches to it.[42] Lastly, the cell targeting agent is engulfed into the BrCa cell.[41,42]

Moreover, the peptide includes simple design and practical synthesis. Peptides are made up of individual amino acids (AA), which contain a carboxylic acid group, an R group, and a hydrogen atom.[43] For example, two AAs bonded with a peptide bond is known as a dipeptide.[43] The left side of the peptide is known as the N-terminus (amine end), and the right side of the peptide is known as the C-terminus (carboxylic acid end).[43] Lastly, the synthesis of peptides is practical, since one amino acid can be added to the peptide at a time.

Another advantage of using peptides as TMIAs is due to bioavailability characteristics and their clearance properties.[40] Upon injection, peptides naturally circulate in the bloodstream and

can readily enter tissues and readily bind to membrane rectors. Small peptides under a molecular weight of 3,000 are most idea in this regard. While an orally available drug should be under a MW of 500, an injectable imaging agent of MS 3,000 or smaller is still advantageous over larger agents such as antibodies or nanoparticles in terms of bioavailability and clearance properties.

However, a significant disadvantage of peptides is that they can otherwise degrade in the body naturally through a process known as proteolysis.[32] The enzymes that are responsible for the degradation (or cleavage) of the peptides are proteases (found naturally in the body), including trypsin and chymotrypsin.[28] These are prevalent primarily in the digestive system but also in the bloodstream. Specifically, the cleavage occurs at the peptide bond, which is a linkage of an amide bond to a carboxyl group in a peptide. A peptide that doesn't undergo the process of degradation, or proteolysis, is known to have proteolytic stability.

Fortunately, the process of proteolysis can be stabilized by synthesizing incorporating D amino acids in key locations on the peptides through the method known as solid-phase peptide synthesis (SPPS).[44] All amino acids exist naturally in the L-residue form (natural form), which commonly leads to degradation in the body.[44] In natural peptides, the amino is recognized by the proteases, which leads to the cleavage of the peptide.

4.2 Peptide Nomenclature and Stereochemistry

In SPPS, peptides may be synthesized to incorporate the unnatural D form of an amino.[32] The peptides that are synthesized with D-amino acids in critical positions will have increased proteolytic stability because the protease enzyme does not recognize D-residue (unnatural form) peptides.[32] The side chain of an amino acid in a natural peptide (all L amino acids) is depicted by the following stereochemistry: when the angle of the two bonds to the side chain carbon is a up,

the natural stereochemistry is shown by a solid wedged line (out of the page), and when the angle made by the same to bonds to the side chain carbon is down, the natural configuration is dash wedged line (behind the page).[32] When peptides that are synthesized with SPPS are contain unnatural amino acids, as shown in Figure 8. The stereochemistry of the R group is the opposite, replacing the solid wedge up with dash and when in the down position, the dashed wedge is replaced by a solid wedge down.[32]

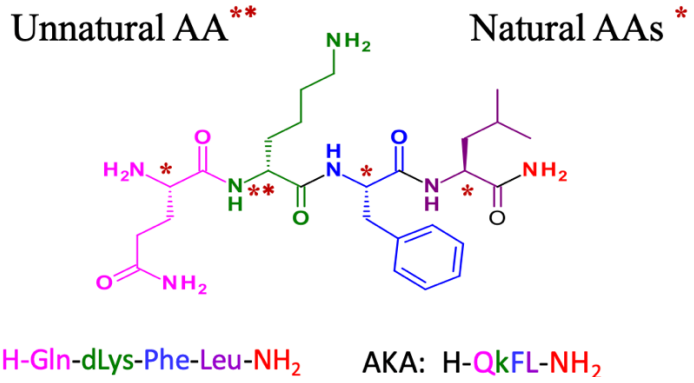

Figure 8. *Peptide Nomenclature. Unnatural AA's are denoted as D (dLys) and lower case in one letter*

4.3 Stereochemistry and Stabilization of Peptide 18-4 against proteolysis.

Previously, at the Chapman University, Dr. Kaur was successful at synthesizing a peptide with SPPS that had proteolytic stability.[32] As shown in Figure 8, peptide 18-4 has two unnatural amino acids that are D-residue, which includes norleucine and lysine.[32] These two positions imparted strong stability against proteases. It was determined that the peptide 18-4 (D-residue) did not undergo degradation in the presence of proteases, because the enzymes in the body do not recognize the unnatural peptides.[42] It is often necessary to only change the stereochemistry of amino acids involved with peptide bonds that are more vulnerable to proteolysis. Furthermore, D- amino acids can impart stability to peptide bonds in each direction.

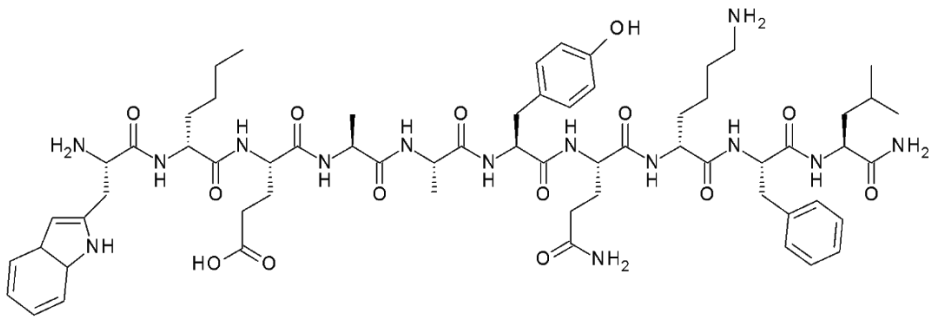

Figure 9. *Peptide 18-4 (H-Trp-dNle-Glu-Ala-Ala-Tyr-Gln-dLys-Phe-Leu-NH_2) synthesize by SPPS*[32]

Furthermore, the binding specificity of the targeting agent to the breast cancer cells was tested in mice in Dr. Kaur's study.[32] Mice with breast cancer tumors were treated (intravenously) with the targeting agent.[32] The results confirmed that the peptide specifically bound to the tumor site and not to healthy cells.[32] It was concluded that the peptide has high-affinity binding for the breast cancer cells.

In Dr. Kaur's study, the ability of peptide degradation (proteolytic stability) was examined by placing the synthesized peptide 18-4 (D-residue) in human serum, and assaying the lifetime of the intact peptide by HPLC.[32] The results established that the peptide 18-4 was resistant to degradation.[32]

4.4 Peptide 18-4 as a Selective Targeting Molecule

As a result, peptide 18-4 is a selective targeting molecule for breast cancer because it can be easily taken up by the cancer cells. In this study, peptide 18-4 was synthesized and used as a targeting molecule. An advantage of the synthesized peptide 18-4, also known as decapeptide (10 amino acids) is that it has enhanced bioavailability.[32] Drug bioavailability is the concentration of drug that reaches the bloodstream.[45]

Dr. Kaur began on the studies with peptides that were composed of 12 amino acids, which resulted in lower bioavailability due to size.[32] With the goal of increasing bioavailability and decreasing size, Kaur reduced the size by eliminating non-essential amino acids. The results led to peptide 18-4 which was smaller in size, increased in proteolytic stability which would led to higher bioavailability.[32] Essentially the primary responsibility of the target molecule (peptide 18-4) is to deliver the imaging agent to the cell, then hopefully undergo endocytosis to accumulate inside the cell.

In further studies, Kaur found that the 18-4 bound to several types of BrCa cells including TN cancel cells including MDA-MD-231, MDA-MB-435, and MCF-7. Moreover, these cells resulted in a higher affinity for the 18-4 peptide.

4.5 Preliminary CFM Results

One of the methods used to treat breast cancer is known as cancer hormonal therapy, which includes three hormones, estrogen, progesterone, and HER2.[46] In triple-negative breast cancer, the receptors for all three hormones are tested negative.[47] The three hormones used to inhibit the growth of tumor, and triple-negative breast cancer are ineffective by treatment by any of the three-hormones (hence the name triple-negative).[47] Furthermore, triple-negative breast cancer is the most aggressive cancer because it metastasizes faster and has a higher chance of spreading.[47] In our design, it was hypothesized that TMIAs based on 18-4 will bind to the triple-negative breast cancer (MDA-MD-231 BrCa) cells as well as the hormone receptor active lines MCF-7.

The TMIA, Cy5.5-18-4 or M2, synthesized in our lab, was tested with CFM in our Biology department at RIT by Dr. Irene Evans. The cellular uptake of the TMIAs into the breast cancer

cells was be tested by growing MDA-MD-2331 BrCa cells in-vitro. Non-cancerous cells were used as a control, and it was expected that in CFM they will not fluoresce (light up) because the cells will not take up the TMIAs.

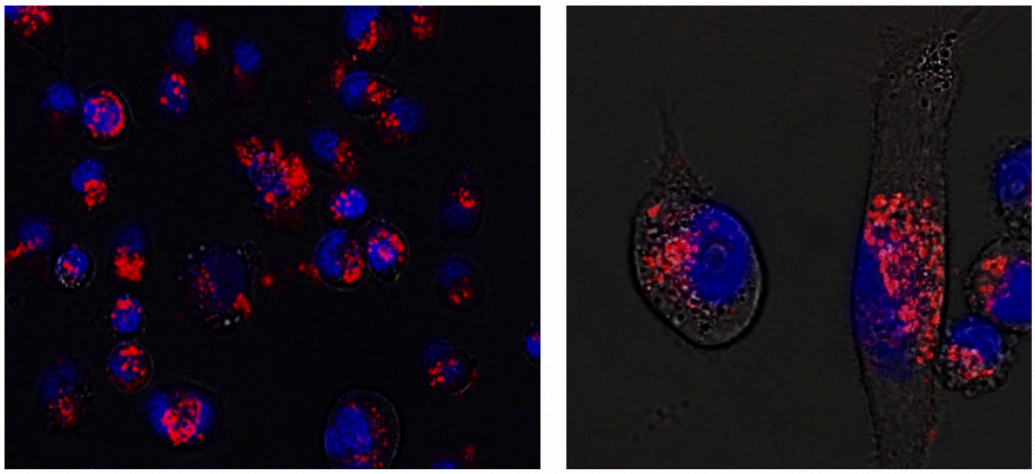

Figure 10. *CFM images of Triple negative MDA-MD-2331 BrCa cells stained with M2 TMIA in collaboration with Dr. Irene Evans, GSOLS, RIT*

It was predicted that the cancerous cells should fluoresce because the TMIAs bind only to the cancer cells specificity. The imaging of the breast cancer cells were found to indeed increase in fluorescence intensity compared to the normal cells), as shown in Figure 10. The magnification of the MDA-MD-231 cells stained with the M2 TIMA clearly showed endocytosis, a mechanism whereby the imaging agent is engulfed by the cell membrane and is internalized into the cell. The red color indicates the fluorescence where the TIMA is bound in the cell. The blue color indicates the breast cancer cell nuclei, which occurred from staining by Nuc blue. The CFM image of the cancer cells verified the hypothesis, that the 18-4 peptide – Cy5.5 conjugate selectively binds to the breast cancer cell receptor KRT1 found on the cell membrane. This had been observed earlier with a similar agent by Dr. Kaur, but it was important to verify this in our own lab with our own

agent. It is our further hypothesis that by accumulation of the TMIA inside the cell that the fluorescence intensity should be amplified versus TIMA's that are bound to the membrane only.

4.6 Solid Phase Peptide Synthesis (SPPS)

A peptide is defined as flexible long chain with 2-50 amino acids, which can be part of a protein structure naturally in the body or a stand-alone biomolecule such as a neurohormone.[44,48] Solid phase peptide synthesis (SPPS) is step-wise coupling reaction that results from the formation of a peptide bond between two amino acids.[48] There are several advantages of solid phase chemistry: the reactions are simple, fast and all reactions are carried out in a single reaction vessel.[44] Secondly, solid phase chemistry is efficient because large amount product is not lost through isolation and purification of intermediates.[44] Moreover, in solid phase byproducts or excess reactants can be removed during the washing step.[28,44] Through this process another large advantage is that peptides prepared by SPPS can be exceedingly pure (well above 95 % pure) even after multiple-step syntheses.

In this study SPPS was used to synthesize a BrCa peptide known as 18-4 (decapeptide). The SPPS method was initially developed in our lab by Xinyu Xu and Matt Law. After a ten-step synthesis it is remarkable that a pure product and good yield was obtained, which is a major advantage of the SPPS. An overview and a step-by-step of the coupling reaction for the synthesis of 18-4 peptide by SPPS is shown in Scheme 1. The amino acids are shown in a three-letter abbreviation, and in this synthesis one amino acid was coupled at a time until the final decapeptide was achieved. Also, some amino acids require a protecting group (shown in red below). At the end of the synthesis all the protecting groups and the polymer attached were removed with acid.

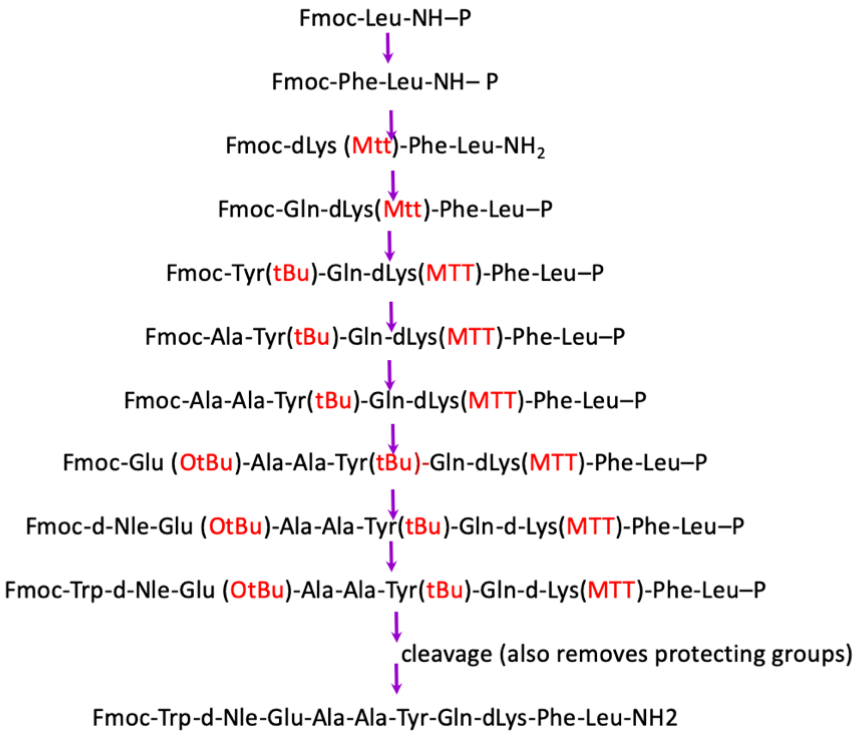

Scheme 1. *Solid Phase synthesis (SPPS)- developed by Xinyu Xu, Matt Law and Basant Kaur*[28]

Step-by-step SPPS of the first three amino acids found in the BrCa 18-4 peptide is shown in detail in Scheme 2. The peptide is synthesized by a coupling mechanism of the amino acids from the C-terminal (right side of the peptide chain) to N-terminal (left side of the peptide chain).[48] The initial step of the synthesis requires the following reactants: an amino acid with the fluorenylmethyloxycarbonyl chloride (Fmoc) and an amine group on the resin (polymer).[48] The Fmoc is a protecting group, which is used to protect the nitrogen on the amine functional group (which is on the amino acid) from reacting in the solution.[48]

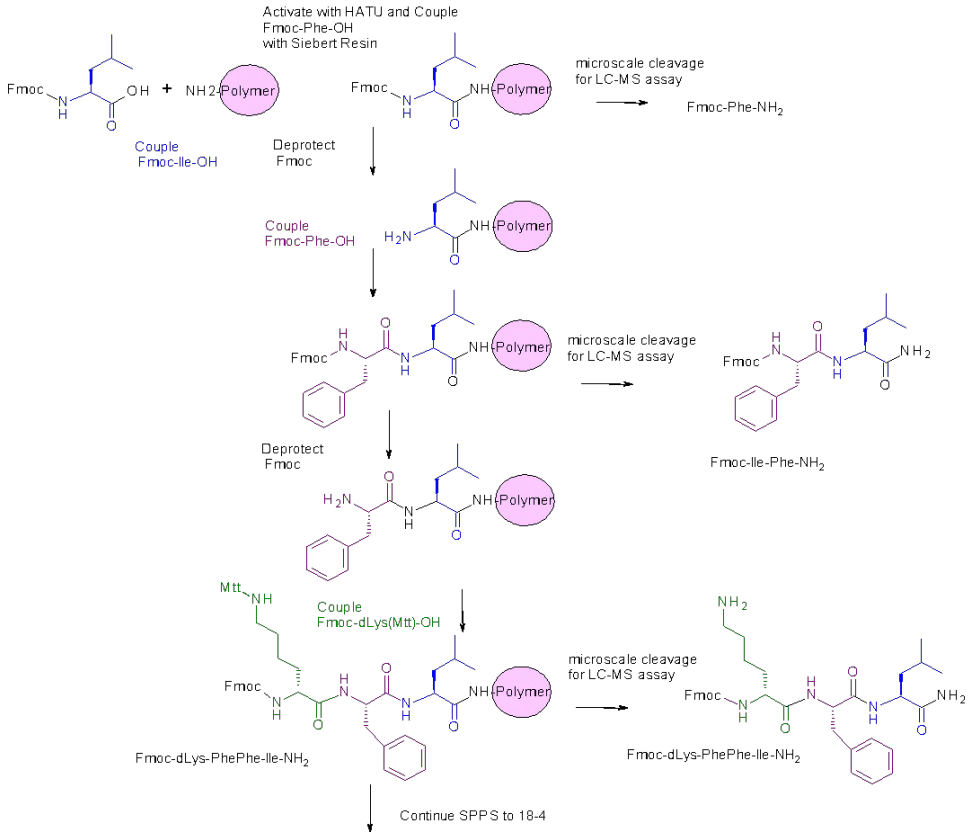

Scheme 2. *Solid Phase Peptide Synthesis (SPPS) of first tripeptide in 18-4*[28]

In the first step the polymer and first amino-acid is coupled, where the free acid group is activated, then reacts with the free amine on the polymer (shown in Scheme 2).[48,49] The second step of SPPS is known as the deprotection step, where the Fmoc group attached with the amino acid is removed.[49] The Fmoc group is stable in acidic conditions, and is removed by a weak base.[50] To remove the Fmoc group a secondary amine known as piperidine is used, which results in a free N-terminus amine.[28] The coupling process is continued by the addition of an amino acid to the free N-terminus amine.[28] The following steps including coupling, deprotection, coupling of next amino acid, which leads to the elongation of the peptide.[49] In the final step the resin is cleaved from the peptide and in this study, the process of SPPS was used to prepare the breast cancer peptide 18-4 (H-Trp-dNle-Glu-Ala-Ala-Tyr-Gln-dLys-Phe-Leu-NH_2), which is also known as the targeting agent as shown in Figure 9.

In this study, reverse phase-high performance liquid chromatography- mass spectrometry (LC-MS) was used to test the purity of the peptide 18-4. HPLC can separate a mixture based on polarity, electrical charge, and molecular size.[51] In RP-HPLC, the mixture is separated according to polarity.[51] The column in the RP-HPLC contains two phases, the stationary phase (packing of the column) that is nonpolar and the mobile phase (aqueous solution) that is polar.[51] The HPLC chromatogram was used to determine the different fractions of peptide 18-4 present in the sample. The mass spectra gives a precise measurement of molecular mass in the electrospray positive (ES+) spectra. If the sample is multiply charged, as often happens, it appears at the "half mass" according to the formula (M+n)/n. Our peptides are often seen at M+2/2 due to protonation at two sites.

To fully utilize LC-MS characterization, our group has developed a "micro-cleavage" HPLC assay at each step during the SPPS. In the past, peptide chemist generally carried out the synthesis to completion and evaluate the intermediates on the resin by a colorimetric test which indicates the presence of a free amine after the coupling reaction to ensure its completion. Micro-cleavages ensured the identification of the intermediate products along the way in the synthesis of 18-4 peptide, and confirmed that not only is there no free amine of the prior peptide, but that the protecting groups are intact, and that complete coupling has occurred. This allows conformation of complete coupling which provides the confidence to continue the synthesis to the next step. The detailed steps and methods of the SPPS reactions will be explained in the following sections.

Chapter 5. Solid Phase Peptide Synthesis Methods

5.1 Selection of Resin Material for SPPS

The most common acid linker resin in SPPS is known as the Wang resin, which requires concentrated TFA (90-95%) for peptide cleavage.[52] The Wang resin afford the C-terminal acid group. When a C-terminal amide is required, the Rink amide resin is most often utilized. Some other resin used are rink acid, 2-chlorotiyl chloride, hydrazine, and sulfonamide.[44] Some factors that are important to consider when selecting a resin for SPPS induces, loading levels, swelling capacity, peptide product (acid, amide, ester, alcohol, and hydrazide), and cleavage conditions.[44,52]

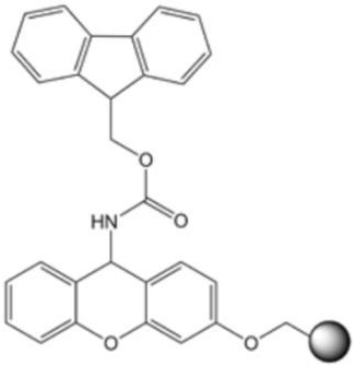

Figure 11. *Structure of Sieber resin*[28]

In Dr. Kaur's work, she used Rink resin for the BrCa 18-4 peptide synthesis, which requires strong TFA cleavage conditions. The TMIAs that we synthesize in our lab contain near infrared dyes (NIR dyes) and MRI contrast agent (Gd), which are not stable in pure TFA and can decompose in strong acid conditions.[28] In our lab, Xinyu Xu discovered that the Sieber resin is the most efficient for our TMIA synthesis.[28] In the past, it was discovered that the NIR dyes are stable in 1-2% TFA conditions.[28] For all our TMIAs synthesis we used the Sieber resin, which can be cleaved with 1% TFA and is a suitable condition for the NIR dyes. Figure 11 shows the structure of the

Sieber resin, which is a mild acid-labile linker and is composed of an amine protected by an Fmoc group.[28]

5.2 Fmoc Deprotection Mechanism

In SPPS, a common protecting group that is used to protect the backbone N-terminal nitrogen from reaction in solution is known as fluorenylmethyloxy carbonyl (Fmoc).[28] The Fmoc group is used in organic synthesis and is known as base-labile protecting group, which can be removed under mild basic conditions such as piperidine.[48]

In a more recent development in our lab, to remove the Fmoc group, 2% of 1,8-Diazabicyclo [5.4.0] undec-7-ene (DBU), 5% of piperazine and 93% of DMF was used.[28] The deprotection of the Fmoc group is shown in Scheme 4. The mechanism is shown below, where the hydrogen located on the β-carbon is highly acidic, therefore a week base such as piperazine plucks the hydrogen and causes the cleavage to occur (CO_2 is formed as a byproduct).[53]

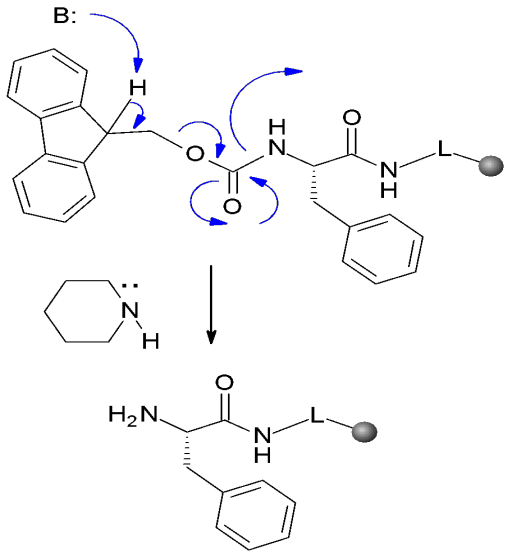

Scheme 3. *Mechanism of Fmoc Deprotection*[28]

5.3 SPPS Step-by-Step Guide for Breast Cancer Peptide 18-4

An in depth step-by-step experimental guide for the SPPS used to synthesize the BrCa 18-4 peptide is shown below. This method was originated in our molecular imaging lab (MIL) by Xinyu Xu and optimized further in the present study. For each step in SPPS, the resin and solvent scale is shown in Table 2. The following recipe below includes main synthesis in this research which started with 850 mg scale of Sieber resin.

Table 2. *Resin and solvent scale for SPPS (The steps refer to the sections below).*

Resin (mg)	**Step 1, 3,5- DMF and Step 7- DCM Wash**	**Step 2- Deprotection for 5 min**	**Step 4- DMF to HATU and AA**	**Step 8- 1% TFA for 30 min**
100	2 mL for 30 sec	1 mL	2 mL	1 mL
400	8 mL for 1.5 min	4 mL	8 mL	1 mL
500	10 mL for 2 min	4 mL	10 mL	1 mL
850	16.5 mL for 2.5 min	8.5 mL	16.5 mL	1 mL
1000	20 mL for 3 min	10 mL	20 mL	1 mL

5.3.1 SPPS Recipe: Step 1. Pre-Swelling

Obtain the initial mass of a large reaction vessel and a stir bar. Weigh out exactly 850 mg of the Sieber resin and transfer it to the SPPS vessel.[28] To begin the pre-swelling process, add 16.5 mL of N,N-Dimethylformamide (DMF) into the reaction vessel by a syringe.[28] Allow the resin to stir for 20 minutes and drain the vessel using air pressure.[28] Note the pre-swelling step is only required for the before the first amino acid is added. Following the addition of the first amino acid, wash the reaction vessel with 16.5 mL of DMF for 2.5 and repeat the washing step for 2 more times.

5.3.2 SPPS Recipe: Step 2. Fmoc Deprotection

To make 100 mL of the Fmoc Deprotection solution mix the following into a brown glass bottle, 2% of 1,8-Diazabicyclo [5.4.0] undec-7-ene (DBU), 5% of piperazine and 93% of DMF (shake well before use).[28] Add 8.5 mL of the Fmoc deprotection solution into the reaction vessel and allow it to stir for 5 mintues.[28] Repeat the Fmoc deprotection for two more times for 5 minutes each. The Fmoc deprotection step is repeated total of three times for 15 minutes in total to ensure that all of the resin is completely deprotected.

5.3.3 SPPS Recipe: Step 3. Washing after Deprotection

To ensure that the reaction vessel environment does not contain the basic Fmoc deprotection solution, the resin is washed with DMF.[28] For 850 mg of resin, add 16.5 mL of DMF to the reaction vessel, stir for 2.5 minutes and drain the DMF.[28] Repeat the washing step of the resin with the DMF 2 more times for 2.5 minutes each.[28]

5.3.4 SPPS Recipe: Step 4. Coupling Amino Acids

Tare a 20 mL scintillation vial, weigh out 2.0 equivalents of the first amino acid in the BrCa 18-4 peptide.[28] In another 20 mL scintillation vial, weight out 1.9 equivalents of (1-[Bis(dimethylamino) methylene]-1H-1,2,3-triazolo[4,5-b] pyridinium 3-oxid hexafluorophosphate) or HATU, the coupling reagent used in SPPS.[28] To dissolve the amino acid and the HATU in solution, to each scintillation vial add 16.5 mL of DMF.[28] Next, to the vial containing the amino acid, add 10 equivalents of N, N-Diisopropylethylamine (DIEA) and shake well.[28] Lastly, transfer the HATU mixture into the amino acid vial (containing the DIPEA) and stir for about 5 minutes. Lastly to couple the amino acid to the resin, add the activated solution to the reaction vial and stir for 45 minutes.[28]

5.3.5 SPPS Recipe: Step 5. Washing after Coupling

After 45 minutes of stirring, drain the reaction vial by using air pressure.[28] To wash the vial, add 16.5 mL of DMF stir for 2.5 minutes and drain the DMF.[28] Repeat the washing step of the resin with the DMF 2 more times for 2.5 minutes each.[28]

5.3.6 SPPS Recipe: Step 6. Coupling of the next amino acid

Before coupling the next amino acid, repeat the Fmoc deprotection and the washing step with DMF (step 2 and 3). Next, to couple the following amino steps repeat steps 5 and 7. If plan to continue the synthesis the next day, after the coupling step wash the reaction vial with 16.5 mL of DMF stir for 2.5 minutes DMF (repeat 2 times).[28] And, lastly wash the vial with 16.5 mL of DCM for 2.5 minutes DCM (repeat 2 times). Dry the reaction vail well and store it away in the freezer.[28]

Before staring the deprotection step, allow the reaction vial to warm up to room temperature and repeat step 1 through 4.

5.3.7 SPPS Recipe: Step 7. Final Wash

Add 16.5 mL of DMF stir for 2.5 minutes and drain the DMF.[28] Repeat the washing step of the resin with the DMF 2 more times for 2.5 minutes each.[28] Wash the reaction vial again with DCM. Add 16.5 mL of DCM stir for 2.5 minutes and drain the DCM.[28] Repeat the washing step of the resin with the DCM 2 more times for 2.5 minutes each.[28] Label the reaction vial and store it in the -20^{o}C freezer.

5.3.8 SPPS Recipe: Step 8. Micro Cleavage

To make 1% TFA cleavage solution, use DCM use as a solvent.[28] To perform a micro-cleavage for the conformation of an intermediate product, take small amount of product from the reaction vial and transfer it to a HPLC vial with a stir bar. Add 1 mL of the 1% TFA cleavage solution to the HPLC vial and allow it to stir for 30 minutes. Make a filter by adding small amount of glass wool to a pipette. Obtain a small dry flask, and filter the 1 mL of the product through the peptide and wash the filter with about 1 mL of DCM. Lastly, rotovap the filtered product and to assay it add few drops of methanol to the flask and transfer to a space-saver vial. And evaluate the molecular weight and UV-VIS chromatogram of each intermediate and final product in the LCMS.

Chapter 6. Puzzle pieces (Imaging Modules)

6.1 Puzzle Pieces for TMIAs

To synthesize the TMIAs, a new method known as the modular method, developed in our lab, was applied to attachment of imaging agents to peptides.[54] In this method, the targeting peptide is synthesized first, followed by conjugation of the imaging modules used for MRI and NIR imaging. The imaging modules are also called puzzle pieces. To synthesize the puzzle pieces, the imaging groups are placed on the side chain of a lysine amino acid early in the synthesis. Later in the synthesis the puzzle pieces (with NIR dye and Gd-DOTA) are coupled to the breast cancer peptide 18-4 by using SPPS.

6.1.1 Gd-DOTA Puzzle Piece for MIR Imaging

The contrast agent gadolinium (Gd) used in MRI, is known to have toxic effects when the free metal is released in the body.[55] To improve Gd bioavailability and excretion in the body a chelated organic structure is used.[55] Dodecane tetraacetic acid (DOTA) is a complexing agent (see Scheme 4), which is used in cancer imaging.[56] By chelating Gd using DOTA, this release is reduced to such a minimal degree that it allows the use of Gd-DOTA (Dotarem) to be utilized as a contrast agent.[56] However, there is speculation that even tiny amounts of free Gd is formed by kinetic de-metalation or trans-metalation by other metals in the bloodstream.

To minimize the safety risks further, the concentration of Gd agent per inject can be vastly reduced by using targeting agents. Moreover, by using TMIAs the concentration of Gd will be increased at the tumor site compared to normal cells. To apply the modular method to contrast

agents for MRI, the Gd-DOTA puzzle piece reaction is below, which is a one pot synthesis and was developed in our lab.[28,56]

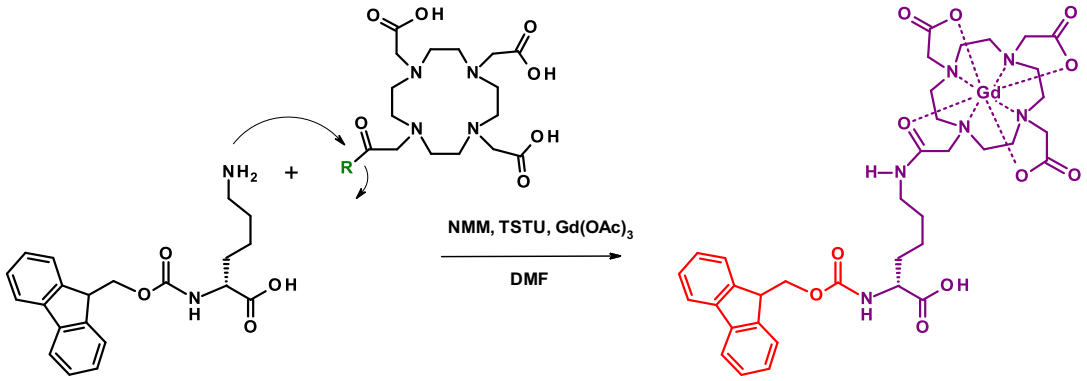

Scheme 4. *Modular Synthesis of lysine puzzle piece with Gd-DOTA.*[56] *were R – Osu (otherwise known as the mono-NHS ester of DOTA.*

6.1.2 Near Infrared (NIR) Dye Cy5.5 Puzzle Piece

Previously, in our lab, the first Cy5.5 dye puzzle that was synthesized was composed of three sulfonates.[28] As shown below, the Cy5.5 dye is drawn in blue and the Fmoc group on the lysine amino acid is drawn in black.[28] To synthesize the puzzle piece, the Cy5.5 was activated by using the coupling agent TSTU, which results in the NHS ester (a good leaving group). Then it was coupled or conjugated to the side chain amine in a protected lysine.

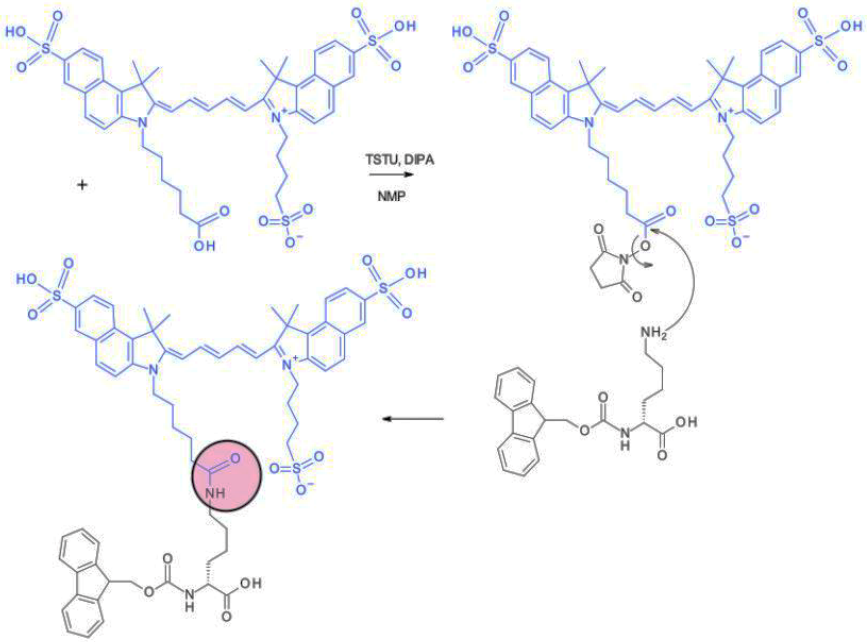

***Scheme 5**. Synthesis of Puzzle Piece with three sulfonates NIR Cy5.5 Dye*[28,57]

In a previous experiment in our lab, Xinyu Zu coupled a tri-peptide (Fmoc-Met-Ile-Phe-NH_2) to the NIR Cy5.5 puzzle piece that was synthesized with three sulfonate groups.[28] Disappointingly, that the dye was unable to be cleaved from the resin at the last step of the synthesis.[28] To cleavage the dye from the resin different methods were tested such as using stronger acid (TFA) concentration, different solvents, and increased cleavage time.[28] However, the cleavage methods were unsuccessful and it was concluded that, having three sulfonate groups=, the Cy 5.5 dye stuck on the resin irreversibly.[28]

To improve the cleavage step of the Cy 5.5 dye to the resin, Xinyu used another dye puzzle piece (shown below).[28] This puzzle piece contained the non-sulfonated version of the dye, which was lipophilic and easier to remove from the resin during the cleavage step.[28]

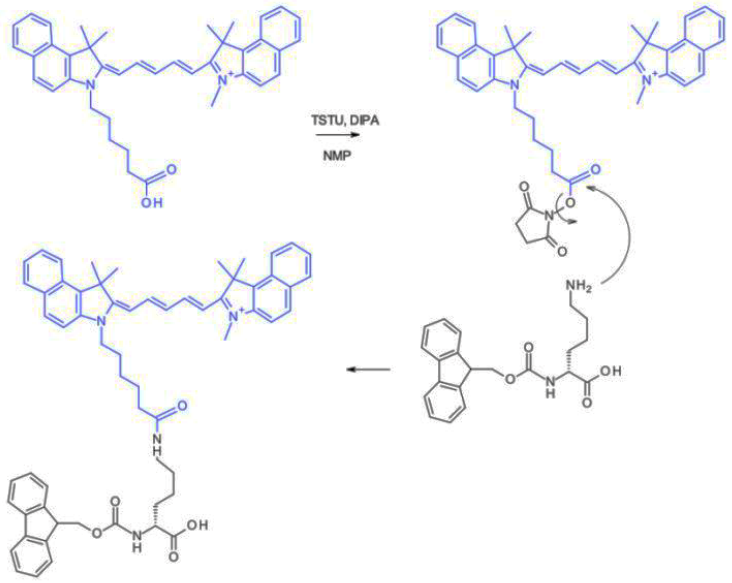

***Scheme** 6. Synthesis of Puzzle Piece with non-sulfonated NIR Cy5.5 Dye*[28,57]

The non-sulfonated NIR Cy5.5 dye puzzle piece was composed of a free acid on the right side, which can be used to conjugate to the rest of the peptide in SPPS. In the past, the SPPS was used to synthesize the breast cancer peptide 18-4 and was coupled to the non-sulfonated NIR Cy5.5 dye puzzle piece, which resulted in the TMIA product, named M2, shown in Figure 12.[28] The non-sulfonated version of the dye, when attached to the peptide, was able to be cleaved and isolated at the last step with 1% TFA.[28]

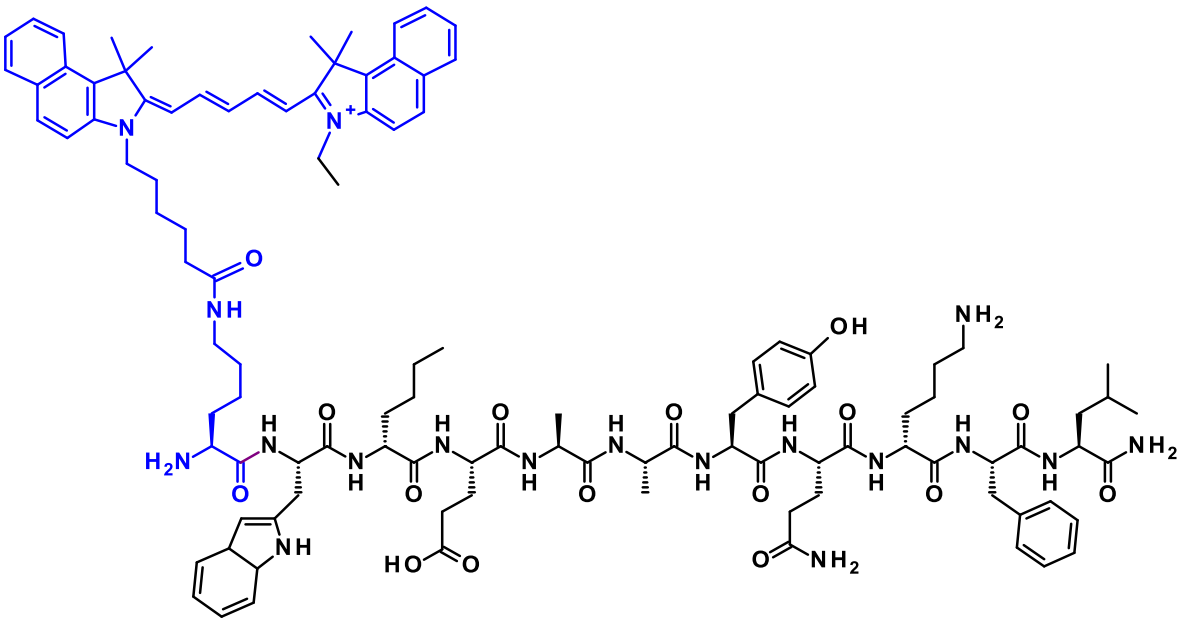

***Figure 12**. Deprotected Breast Cancer peptide 18-4 with non-sulfonated Cy5.5 dye (TMIA-M2), prepared by Xinyu Xu and Matt Law*[28]

A main drawback to the non-sulfonated Cy5.5 dye is that it has low solubility because the dye is highly lipophilic. Therefore, when making samples for biological testing (CFM imaging) the M2 TMIA product requires 5-10% of DMSO, which is not an ideal cellular environment for humans but is okay for in vitro testing. In this work, to increase the water solubility of the Cy5.5 dye, the sulfonated version of the dye was used. As shown below, the mono-sulfonated NIR Cy5.5 dye puzzle piece has a net charge of zero on the dye system, but the negative charge on the sulfonate group will assist the dye solubility in aqueous solution.

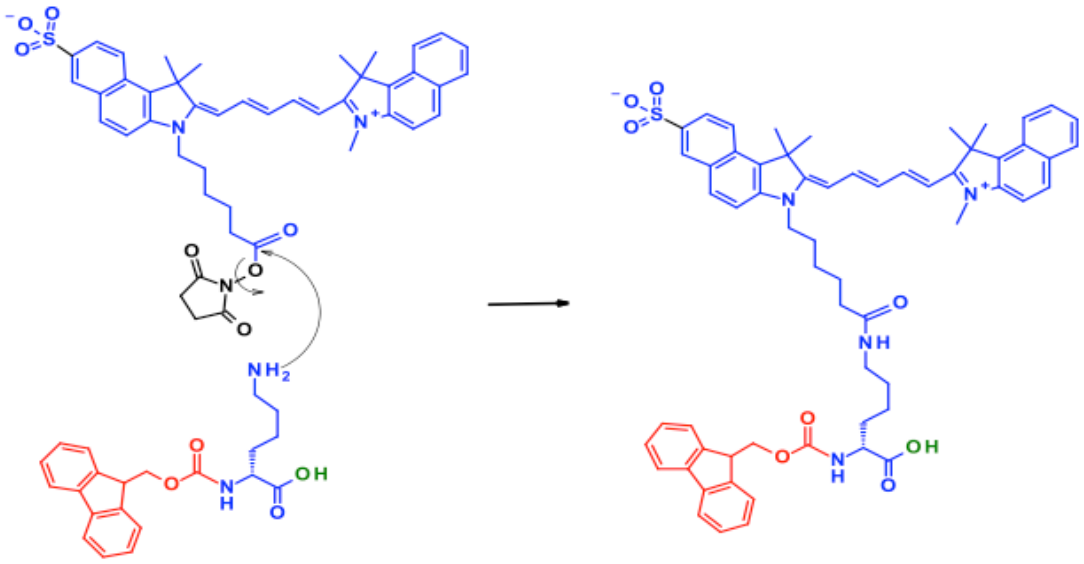

***Scheme 7**. Synthesis of Lysine Puzzle Piece with one sulfonate NIR Cy5.5 Dye*[57]

Chapter 7. Results and Discussion

7.1 Breast Cancer Targeting peptide 18-4

The first goal of this work was to use SPPS to produce the breast cancer peptide 18-4, discovered by Dr. Kaur. The stucture of 18-4 after it's synthesis on the resin, as shown in Figure 13. The peptide is composed of three protecting groups inducluding a phenylisopropyl (PhiPr) on glutamic acid, t-butyl (tBu) ether on tyrosine, and methyl trityl (MTT) on lysine. In the earlier work of Xinyu Xu, a t-butyl ester was utilized on the glutamic acid position. We found that the PhiPr was more readily deprotected during the cleavage step and is therefore preferred.

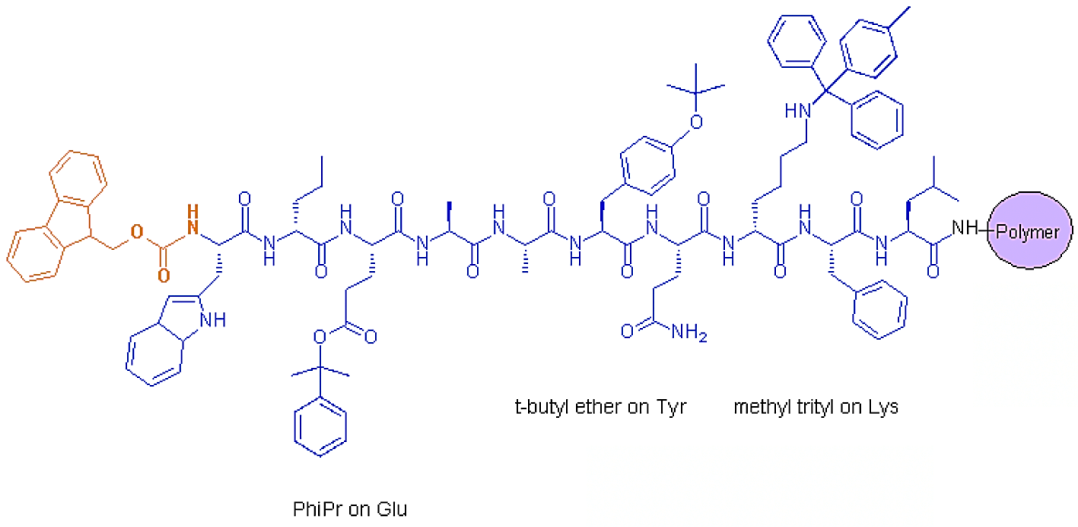

Figure 13. *Structure of breast cancer peptide 18-4 (with protecting groups) on resin*

Using the SPPS method developed in our lab by Xinyu Xu and Matt Law, and further modified in this research project, the breast cancer peptide 18-4 was sucessfully synthesized by using the step-by-step experminental SPPS guide expained in Chapter 5.

At each intermeditate step of the synthesis, a small amount of the peptide was cleaved wih 1% TFA and was assayed with LC-MS. The molecular weight at each intermediate step was

verified by comparing masses obtained with those in Table 3. The protecting group MTT on d-lysine and PhiPr on glutamic acid are removed rapidly during the cleavage process. However, the t-butyl on tyrosine was the protecting group to be removed last and required longer time (overnight) to be cleaved.

To verify the identity and purity of the peptide 18-4, high-performance liquid chromatography-mass spectrometry (LC-MS) was used. Also, to prove the exact molecular formula of peptide and the TIMAs, high-resolution mass spectrometry (HR-MS) was used. Table 3, shows all the possible intermeditate (monopetide-decapeptide) forms of the breast cancer peptide 18-4 (with and without protecting groups) with the calculated molecular weights and half mass.

Ths LC-MS results for all of the breast cancer peptide 18-4 intermediate and products from the LC-MS are shown in Appendix I, with the parent intermediate peptide numbered (no numbers on the multiple protected forms) which shows the purity of product and verfies the correct molecular weight and half mass. For example, the final 18-4 peptide (compound 10 in Appendix 1) in its Fmoc protected form, Fmoc-trp-dNle-Glu-Ala-Ala-Tyr Gln-dLys-Phe-Leu-NH_2 displayed the expected LC-MS results (MW 1488.70 $M+H^+$).

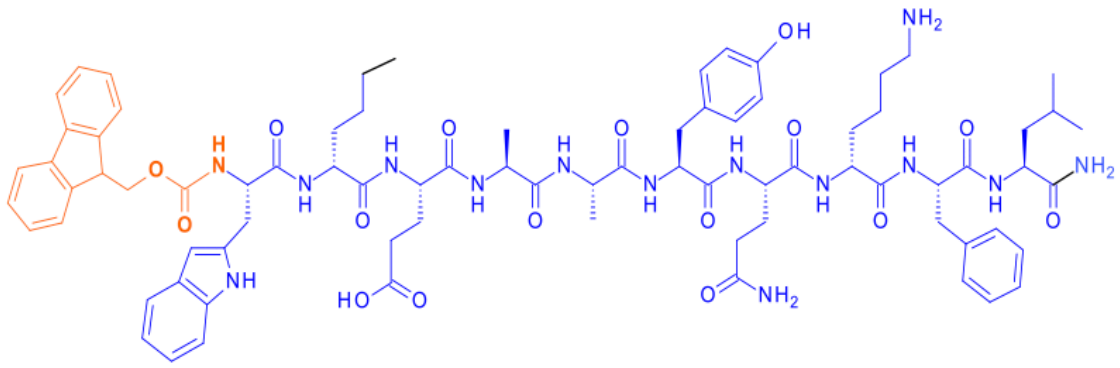

Figure 14. *Stucture of the Breast Cancer Fmoc Peptide 18-4 (10) with no protecting groups (compound numbers are displayed in Appendix 1 and Table 3)*

In Table 3, the molecular weight of each intermediate in it's protected, partially protected, and fully deprotected form is listed, along with the "half mass" that is often apparent in mass spectrometry. The half mass is defined as (M+2)/2 which is when the two protons add to the molecule to produce a charge of two. As the mass observed in MS is M/Z, where M is molecular weight and Z is the charge, the molecular weight may often be observed at half mass. This is particularly useful for very large molecules that may be beyond the range of conventional mass spectrometers (over 2,000 amu).

Table 3. *Molecular Weight of Fmoc Protected Peptide 18-4 Intermediate Products*

Compounds	Molecular Weight (g/mol)	Half Mass (g/mol)
Fmoc-Leu-NH_2 **(1)**	352.2	177.1
Fmoc-Phe-NH_2	386.2	194.1
Fmoc-Phe-Leu-NH_2 **(2)**	499.2	250.6
Fmoc-d-Lys (Mtt)-Phe-Leu-NH_2	883.5	442.8
Fmoc-d-Lys-Phe-Leu-NH_2 **(3)**	627.3	314.7
Fmoc-Gln-d-Lys-Phe-Leu-NH_2 **(4)**	755.4	378.7
Fmoc-Tyr(tBu)-Gln-d-Lys-Phe-Leu-NH_2	974.5	488.3
Fmoc-Tyr-Gln-d-Lys-Phe-Leu-NH_2 **(5)**	918.5	460.3
Fmoc-Ala-Tyr(tBu)-Gln-d-Lys-Phe-Leu-NH_2	1045.6	523.8
Fmoc-Ala-Tyr-Gln-d-Lys-Phe-Leu-NH_2 **(6)**	989.5	495.8
Fmoc-Ala-Ala-Tyr(tBu)-Gln-d-Lys-Phe-Leu-NH_2	1116.6	559.3
Fmoc-Ala-Ala-Tyr-Gln-d-Lys-Phe-Leu-NH_2 **(7)**	1060.5	531.3
Fmoc-Glu (PhiPr)-Ala-Ala-Tyr-Gln-d-Lys-Phe-Leu-NH_2	1307.6	654.8
Fmoc-Glu-Ala-Ala-Tyr(tBu)-Gln-d-Lys-Phe-Leu-NH_2	1245.6	623.8
Fmoc-Glu (PhiPr)-Ala-Ala-Tyr(tBu)-Gln-d-Lys-Phe-Leu-NH_2	1363.7	682.8
Fmoc-Glu-Ala-Ala-Tyr-Gln-d-Lys-Phe-Leu-NH_2 **(8)**	1189.6	595.8
Fmoc-d-Nle-Glu-Ala-Ala-Tyr-Gln-d-Lys-Phe-Leu-NH_2 **(9)**	1302.7	652.4
Fmoc-d-Nle-Glu (PhiPr)-Ala-Ala-Tyr-Gln-d-Lys-Phe-Leu-NH_2	1420.7	711.3
Fmoc-d-Nle-Glu-Ala-Ala-Tyr(tBu)-Gln-d-Lys-Phe-Leu-NH_2	1358.7	680.4
Fmoc-d-Nle-Glu (PhiPr)-Ala-Ala-Tyr(tBu)-Gln-d-Lys-Phe-Leu-NH_2	1476.8	739.4
Fmoc-Trp-d-Nle-Glu-Ala-Ala-Tyr-Gln-d-Lys-Phe-Leu-NH_2 **(10)**	1488.7	745.4
Fmoc-Trp-d-Nle-Glu (PhiPr)-Ala-Ala-Tyr-Gln-d-Lys-Phe-Leu-NH_2	1606.8	804.4
Fmoc-Trp-d-Nle-Glu-Ala-Ala-Tyr(tBu)-Gln-d-Lys-Phe-Leu-NH_2	1544.8	773.4
Fmoc-Trp-d-Nle-Glu((PhiPr)-Ala-Ala-Tyr(tBu)-Gln-d-Lys-Phe-Leu-NH_2	1662.8	832.4

7.2 Fmoc Deprotected Breast Cancer Targeting peptide 18-4

The Fmoc protected breast cancer peptide 18-4 (Compound 11) was deprotected, by the method described in Chapter 5.3.2 to remove the Fmoc. Lastly the peptide was cleaved with 1% TFA, which resulted in the final product as shown below in Figure 15. The product, NH_2-Trp-d-Nle-Glu-Ala-Ala-Tyr(tBu)-Gln-d-Lys-Phe-Leu-NH_2 (compound 12) shown below was composed of t-butyl on tyrosine (LC-MS results 1323.55 m/z $[M+H]_+$, 662.51 m/z $(M+2H^+)/2$).

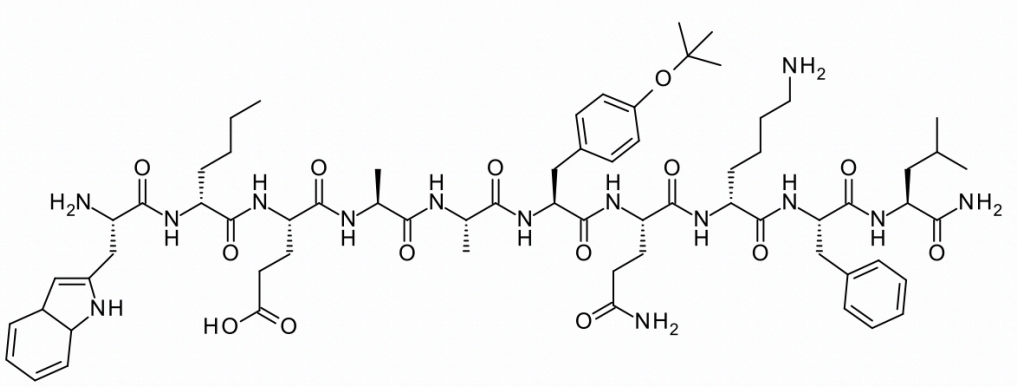

Figure 15. *Stucture of the Breast Cancer Peptide 18-4 with t-butyl protecting group on tyrosine (12)*

Table 4. Molecular Weight of Fmoc deprotected Peptide 18-4 Products

Compounds	Molecular Weight (g/mol)	Half Mass (g/mol)
NH_2-Trp-d-Nle-Glu-Ala-Ala-Tyr-Gln-d-Lys-Phe-Leu-NH_2	1266.67	634.33
NH_2-Trp-d-Nle-Glu-Ala-Ala-Tyr(tBu)-Gln-d-Lys-Phe-Leu-NH_2	1322.73	662.36
NH_2-Trp-d-Nle-Glu (PhiPr)-Ala-Ala-Tyr-Gln-d-Lys-Phe-Leu-NH_2	1384.75	693.37
NH_2-Trp-d-Nle-Glu (PhiPr)-Ala-Ala-Tyr(tBu)-Gln-d-Lys-Phe-Leu-NH_2	1426.80	714.4

7.3 Synthesis of Single-Modal Breast Cancer TMIA for MRI

The second goal of this research was to synthesize a single-modal breast cancer TMIA for MRI, where the contrast agent Gd-DOTA was used. The synthesis of the TMIA for MRI is shown in Scheme 8 where the first step was to deprotect the Fmoc on the 18-4 peptide by using the method in Chapter 5.3.2. Note the following synthesis was performed on the resin in solid phase synthesis. Next, the Gd puzzle piece (Fmoc-dLys (Gd-DOTA)-OH) was coupled by following the method mentioned in Chapter 5.3.6. As a result, the fully9 protected form of Fmoc-Gd-DOTA-18-4-NH_2 TMIA was produced as the penultimate intermediate.

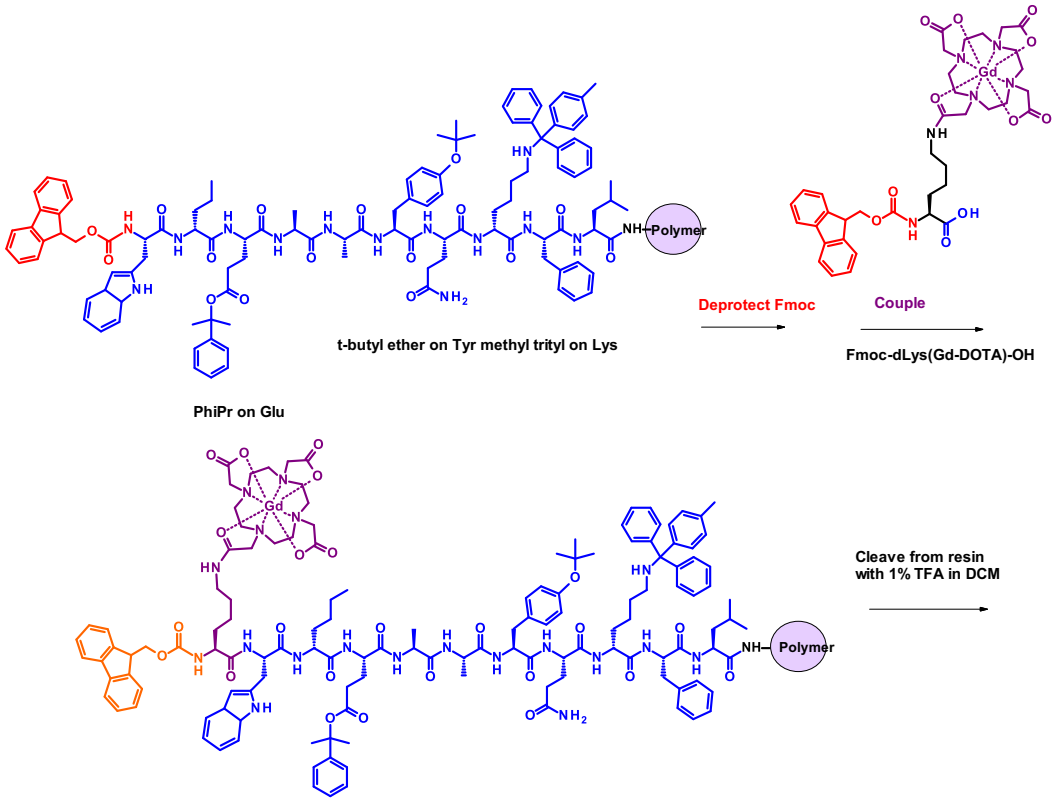

Scheme 8. *Synthesis of Single-Modal Imaging Module for MRI, Fmoc-Gd (DOTA)-18-4-*

Trp-d-Nle-Glu-Ala-Ala-Tyr-Gln-d-Lys-Phe-Leu-NH_2

7.4 Fmoc Protected Gd-DOTA labelled breast cancer peptide 18-4 TMIA Product

The second goal to synthesize a single modal TMIA for MRI was successfully achieved and was assayed with LC-MS. To test the Fmoc protected Gd-DOTA labelled breast cancer 18-4 TMIA agent was cleaved with 1% TFA. The final product, Fmoc-Gd (DOTA)-Trp-d-Nle-Glu-Ala-Ala-Tyr(tBu)-Gln-d-Lys-Phe-Leu-NH_2 is shown below, (LC-MS Results 1080.30 m/z ($M+2H^+$)/2), HRMS Results: 1079.96950 m/z ($M+2H^+$)/2), water adduct also seen at 1087.9636 m/z).

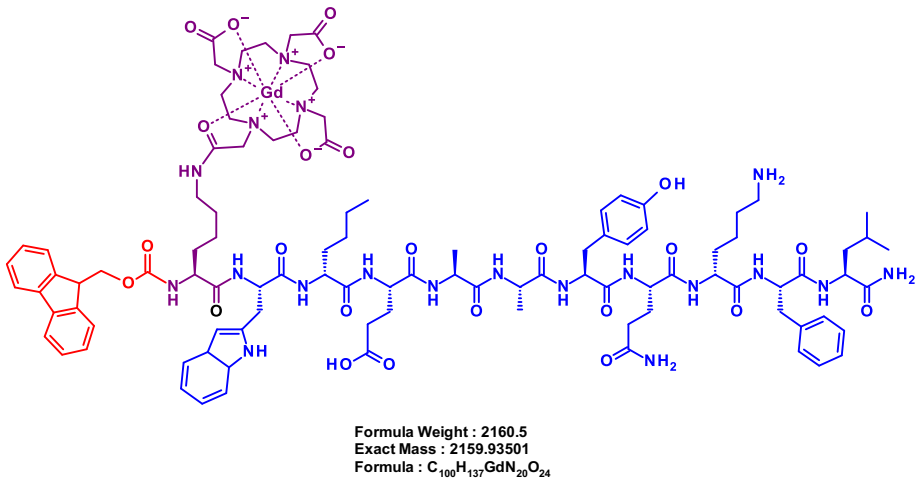

Figure 16. *Stucture of the Fmoc protected Gd(DOTA) lablled Breast Cancer Peptide 18-4 Single-Modal TMIA Agent*

Table 5. *Molecular Weight of Fmoc Protected NH_2-Gd (DOTA)-18-4-NH_2 Products*

Compounds	Molecular Weight (g/mol)	Half Mass (g/mol)
Fmoc-d-Lys(Gd-DOTA)-Trp-d-Nle-Glu-Ala-Ala-Tyr-Gln-d-Lys-Phe-Leu-NH_2	2159.93	1080.5
Fmoc-d-Lys(Gd-DOTA)-Trp-d-Nle-Glu-Ala-Ala-Tyr(tBu)-Gln-d-Lys-Phe-Leu-NH_2	2216.18	1109.09
Fmoc-d-Lys(Gd-DOTA)-Trp-d-Nle-Glu(PhiPr)-Ala-Ala-Tyr-Gln-d-Lys-Phe-Leu-NH_2	2278.19	1140.09
Fmoc-d-Lys(Gd-DOTA)-Trp-d-Nle-Glu(PhiPr)-Ala-Ala-Tyr(tBu)-Gln-d-Lys-Phe-Leu-NH_2	2334.26	1168.13

7.5 Fmoc Deprotected Gd (DOTA) labelled breast cancer peptide 18-4 TMIA Product

To obtain the final TMIA product, the Fmoc group on the Gd (DOTA) labelled breast cancer peptide 18-4 was removed using the method mentioned in Chapter 5. Note that the tbutyl group required longer cleavage time (overnight), other protecting groups were removed easily with 30-minute cleavage.

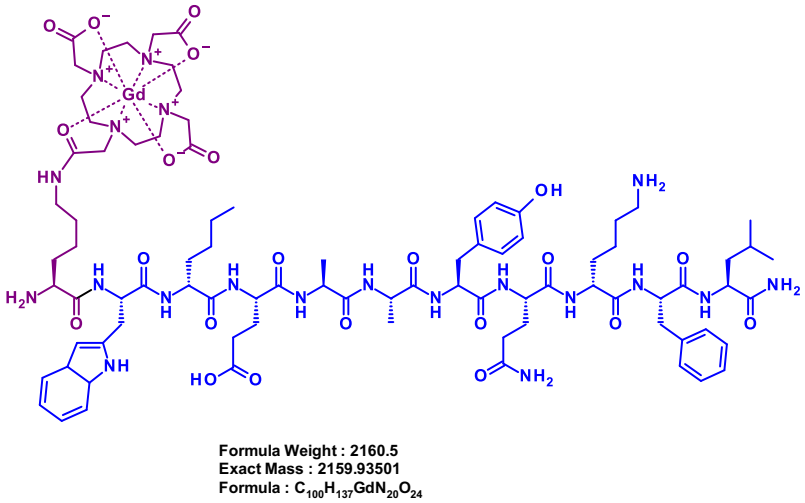

Figure 17. *Stucture of the Fmoc deprotected Gd(DOTA) lablled Breast Cancer Peptide 18-4 Single-Modal TMIA Agent*

Table 6. *Molecular Weight of Fmoc deprotected NH_2-Gd (DOTA)-18-4-NH_2 Products*

Compounds	Molecular Weight (g/mol)	Half Mass (g/mol)
NH_2-d-Lys(Gd-DOTA)-Trp-d-Nle-Glu-Ala-Ala-Tyr-Gln-d-Lys-Phe-Leu-NH_2	1935.85	968.92
NH_2-d-Lys(Gd-DOTA)-Trp-d-Nle-Glu-Ala-Ala-Tyr(tBu)-Gln-d-Lys-Phe-Leu-NH_2	1991.91	996.95
NH_2-d-Lys(Gd-DOTA)-Trp-d-Nle-Glu(PhiPr)-Ala-Ala-Tyr-Gln-d-Lys-Phe-Leu-NH_2	2053.93	1027.96
NH_2-d-Lys(Gd-DOTA)-Trp-d-Nle-Glu(PhiPr)-Ala-Ala-Tyr(tBu)-Gln-d-Lys-Phe-Leu-NH_2	2109.99	1055.99

To test the deprotected Fmoc Gd-DOTA labelled breast cancer, the Gd- 18-4 probe for MRI was cleaved with 1% TFA. The final product, NH_2-Gd (DOTA)-Trp-d-Nle-Glu-Ala-Ala-Tyr(tBu)-Gln-d-Lys-Phe-Leu-NH_2 is shown below, (LC-MS Results 996.26 m/z m/z $(M+2H^+)/2$). AS expected, the UV-Vis diode array resulted in no characteristic peak at 262 nm for the Fmoc protecting group. And the peak at 270 nm, represents the absorbance of tryptophan and tyrosine amino acids present in the peptide 18-4.

7.6 Synthesis of Single-Modal Breast Cancer TMIA with NIR Cy5.5 Dye Puzzle Piece (M3-TIMA)

The third goal of this research was to synthesize a single-modal breast cancer TMIA for NIR fluorescence, where the NIR Cy5.5(1S) dye was used. Note the following synthesis was performed on the resin in solid phase synthesis. The synthesis of the Cy5.5(1S)-TMIA is shown below, where the first step was to deprotect the Fmoc on the 18-4 peptide by using the method in Chapter 5.3.2. Next, the Cy5.5(1S) puzzle piece (Fmoc-dLys (Cy5.5-1S)-NHS ester) was coupled by following the method mentioned in Chapter 5.3.6. As a result, the Fmoc-Cy5.5(1S)-18-4-NH_2 TMIA was produced a product.

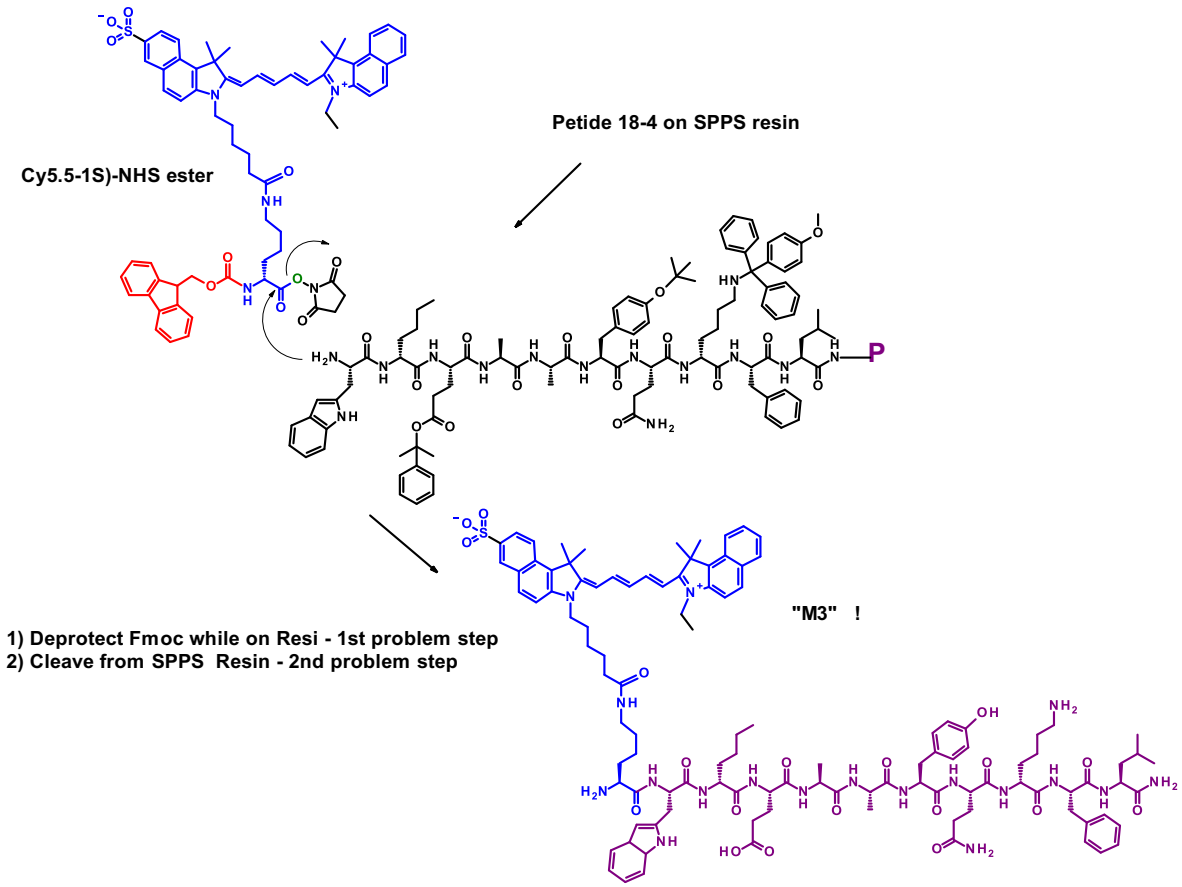

Scheme 9. *Synthesis of Single-Modal Imaging Module for CFM, NH_2-Cy5.5(1S)*-Trp-d-Nle-Glu-Ala-Ala-Tyr-Gln-d-Lys-Phe-Leu-NH_2 (M3 Product)

7.6.1 Single-Modal Breast Cancer TMIA with NIR Cy5.5 Dye Puzzle Piece Reaction Failed

All the following steps mentioned in the previous section were carried out, however the synthesis was not a success. The single modal TMIA agent for NIR dye was not produced, instead the product shown below was produced from the synthesis. The following product resulted a LC-MS peak of 1323 m/Z, and the derived structure of the product was speculated to be the structure shown below.

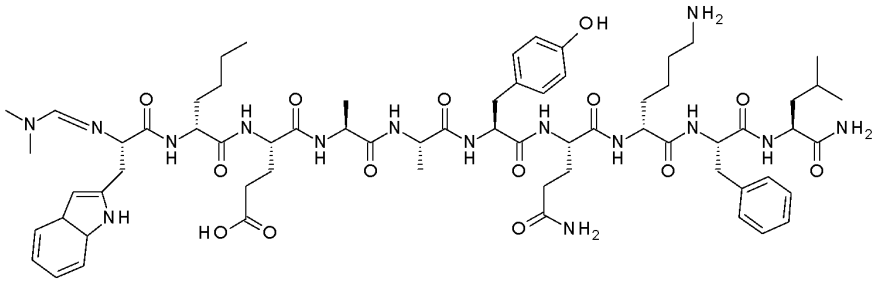

Figure 18. *A product from the M3 failed synthesis due to excess coupling agents*

The suspected impurity structure in Figure 18 was a result of the peptide reacting with the coupling agents (TBTU or TSTU) itself used in SPPS. As shown in the Figure below, both of the agents contain two dimethyl amines attached to a carbon between them as an activating group, which can react with the peptide. It was concluded that the product was result from the excess of TSTU or TBTU, therefore the solution was to not use an excess of the coupling agents. As a result, for SPPS the TSTU was reduced to 1.2 equivalents.

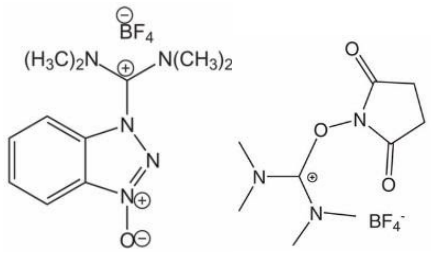

(a) **(b)**

Figure 19. *Structure of coupling agents used in SPPS (a) TBTU (b) TSTU*

7.6.2 Optimization in the Fmoc Deprotection Step of SPPS

Another resaon of the M3-TMIA reaction failed was due to the Fmoc deprotection step in SPPS. As mentioned in Chapter 5.3.2 to deprotect the Fmoc, a mixture of DBU and piperazine was used for all the pervious deprotection steps. However, Matt Law discovered that theses

deprotection reagents (shown below) cause degradation of the Cy5.5(1S) dye. To test the stability of the dye in the deprotection solution, a seprate reaction was done. To the Cy5.5(1S) dye, the deprotection was added and the dye changed color from blue to yellow, which indicated that the piperazine or DBU was causing the dye to degrade.

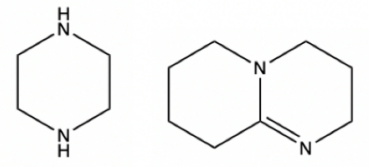

(a) (b)

Figure 20. *Structure of Fmoc Deprotection agents used in SPPS (a) Piperazine (b) DBU*

Another stability test for the dye in the deprotection solution was performed. To the Cy5.5(1S) dye, a new deprotection solution (DEA) was added and the dye did not change color from blue to yellow. As a solution for all the future Fmoc deprotection steps the new 10% DEA (shown below) was used.

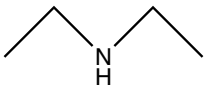

Figure 21. *Structure of Fmoc Deprotection agent DEA*

7.6.3 Optimization of SPPS steps to improve Single-Modal M3-TMIA Synthesis

After multiple failed reactions, we determined that each step of the SPPS needed to be evaluated. So, a step-by-step strategy to improve the synthesis for M3-TIMA product was carried out. Each step was studied carefully and new methods were developed and put in place, as shown in the Figure 22.

7.6.3.1 Optimization of Fmoc Deprotection and Washing After Fmoc Deprotection Step

Based on the results described above, when the Cy5.5 was present, several of the SPPS needed critical changes. The first optimization performed was on the second step of the SPPS, where a new Fmoc-deprotection reagent was tested. Using diethyl amine (DEA) instead of the DBU/piperidine method, prevented the Cy5.5(1S) dye degradation. Previously 5% of DEA was tested, which did not completely remove the Fmoc group. However, it was found that 10% of DIEA was satisfactory for Fmoc-deprotection. Before continuing the synthesis, it was important to assay a small amount of the deprotected peptide with LC-MS to prove the deprotection was successful.

In addition, after the deprotection step, the washing step was also important to optimize. To ensure that the peptide on resin was not degraded by the basic DEA solution, the reaction vial was washed well and pH of the eluent was carefully monitored until it was no longer basic. To check the PH of the eluent, a damp pH paper was used. These changes are shown in the first step in Figure 22 which summarizes all of the important optimization steps.

1. **Pre-Swelling**

2. **Fmoc Deprotection**

   Use 10% DEA and test de-Fmoc Peptide
   (previously used 5% piperizine/DBU)
   And Prove Fmoc Deprotection

3. **Washing After Deprotection**

   Wash well until eluant is no longer basic

4. **Coupling Amino Acids**

   Prove activation of the dye (with butyl amine quench)
   Check PH of the Cy5.5(1S) dye before Coupling
   Add at least 40 equivalence of DIEA

5. **Washing After Coupling**

6. **Final Wash**

   Wash Well with DMF and DCM

7. **Cleavage**

   Check Dye Stability in TFA

Figure 22. *Steps Taken to Improve Single-Modal M3 TMIA Synthesis*

7.6.3.2 Optimization of Coupling Amino Acid, Final Wash, and Cleavage Step

In addition to optimization of the Fmoc deprotection, it was discovered that optimization was also required for the amino acid coupling step. As mentioned in Chapter 5.3.2, to activate the dye DIPEA is used. It was discovered that the pH of the puzzle piece Cy5.5 (1S) dye with the DIPEA was not basic, and when it is not basic, the free amine can be partially protonated preventing it from being a nucleophile.

Therefore, checking the pH of the Cy5.5(1S) dye before adding it to the reaction vial for coupling was a very important step. Compared to other SPPS synthesis performed in the past, which required 10 equivalence of DIPEA. The puzzle piece Cy5.5(1S) dye required at least 40 equivalence to be basic. Moreover, to ensure the activation of the puzzle piece Cy5.5(1S), the puzzle piece containing the DIPEA was stirred at least 5-10 minutes.

To prove the activation of the puzzle piece by TSTU to form the intermediate active NHS ester, a test known as the butyl amine quench was performed, and the reaction is shown below.

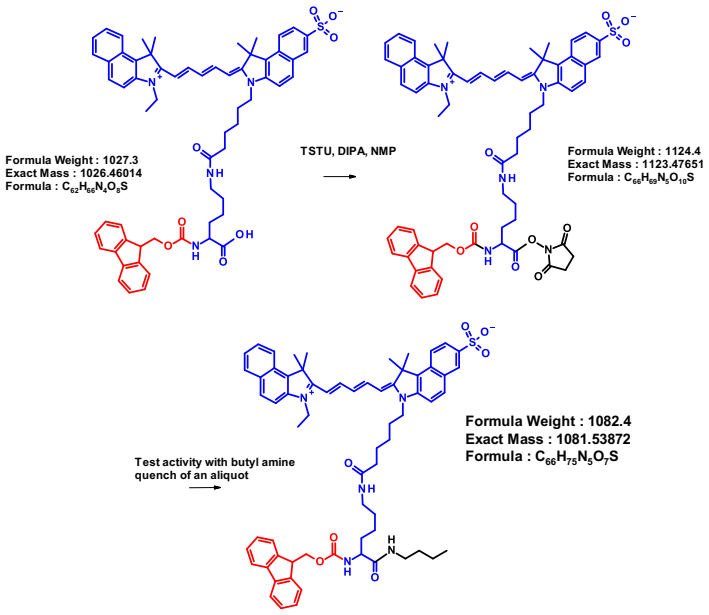

Scheme 10. *Butyl Amine Quench of the Cy5.5(1S) Puzzle Piece Reaction*

To test the identity and purity of the puzzle piece containing the Cy5.5(1S) dye, LC-MS analysis was performed (LCMS Results: Negative Ion 1025.39 m/z $[M+H]_+$, Positive Ion 1027.35 m/z $[M+H]_+$). To test the activation of the puzzle piece by TSU, a butyl amine quench reaction was carried out prior to it's addition and evaluated by LC-MS. A small amount (1-2 drops) of the activated Cy5.5(1S) puzzle piece (after 5 minutes of stirring) was added to a space saver vial, along with 1-2 drops of butyl amine. And the aliquot was assayed, (LCMS Results: Positive Ion 1082.33 m/z $[M+H]_+$).

Additionally, after the coupling of an amino acid, removal of reagents was ensured by washing the reaction vial three times with DMF and DCM.

Lastly, the stability of the Cy5.5(1S) dye was tested in 1% TFA to ensure it would be stable to the mildly acidic cleavage conditions. To the puzzle piece Cy5.5(1S) dye, about 5 mL of 1% TFA was added. It was found that the dye was stable and did not degrade in 1% TFA. Therefore, it was concluded that our reaction did not fail due to stability issues of the dye during the cleavage step.

7.6.3.3 New Continuous Flow Cleavage Method for M3 Product

The last step of the SPPS known as the cleavage step, also required improvements because the product had low yield. Normally, as mentioned earlier, to remove the t-butyl protecting group, the product was cleaved overnight. However, we observed the blue color was sticking to the resin and predicted that the TMIA sticks to the resin, possibly due to the dye adhering to the resin in the 1% TFA and the product could not be removed. Longer cleavage times did not improve results as the TMIA appeared to bind to the resin. Therefore, it leads to more dye stuck to resin as observed in the filter (glass wool) during the cleavage process and resulted in less color being eluted from the resin.

A proposed method to improve the elution of the dye analyte was to use a flow of fresh 1% TFA and collecting the sample continuously, which will allow the product to have less time to bind with the resin. As a result, more color came off the resin compared to the pervious cleavage method. About 200 mL of 1% TFA was used in this method. Note, that the Fmoc was removed prior to the continuous TFA cleavage method.

Lastly, to remove the t-butyl protecting group, the eluent was left in the hood to complete the deprotection of the acid labile protecting group, especially the t-butyl ether on tyrosine which was always the last group to come off (the MTT being the first and labile group). It was concluded that this method was a winner, which results in higher yield of the product.

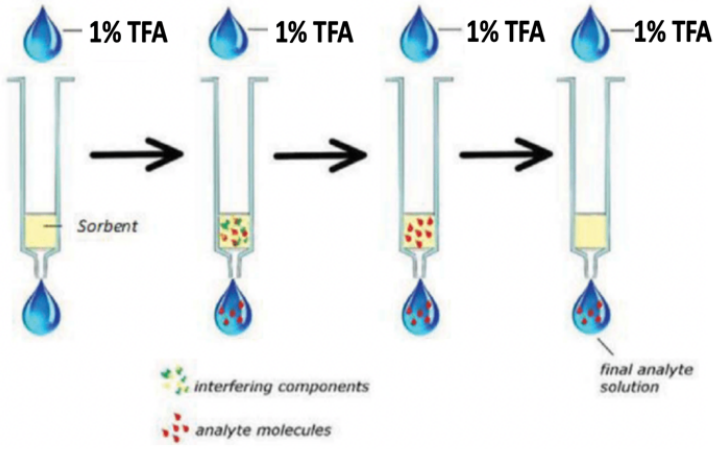

Figure 23. Schematic *Representation of the Continuous TFA Cleavage Flow Method*

7.6.4 Fmoc Deprotected Cy5.5(1S) labelled breast cancer peptide 18-4 TMIA Product (M3-TMIA)

After optimizing the SPPS, the goal to synthesize the single-modal M3-TMIA product, for NIR fluorescence and OMI imaging of BrCa, shown in Figure 24, was successfully achieved and was assayed with LC-MS.

In the initial (non-continuous flow) method of cleavage with 1 % TFA, the de-protected Fmoc Cy5.5(1S) labelled breast cancer 18-4 TMIA agent M3, NH_2-Cy5.5(1S)-Trp-d-Nle-Glu-Ala-Ala-Tyr-Gln-d-Lys-Phe-Leu-NH_2 (first line in Table 7 below) was the resulting product, (LC-MS in negative ion, 1025.72 m/z $(M+2H^+)/2$ and positive ion 1027.60 m/z $(M+2H^+)/2$). As expected, the UV-Vis diode array resulted in no characteristic peak at 262 nm for the Fmoc protecting group. And the peak at 270 nm, shows the absorbance of tryptophan and tyrosine amino acids, which are present in the peptide 18-4.

In the improved, continuous TFA flow method yielded a much better yield of the same product, M3 (LC-MS Results: negative ion 1026.04 m/z $(M+2H^+)/2$, positive ion 1027.66 m/z $(M+2H^+)/2$), HRMS Results: positive ion 1027.468 m/z $(M+2H^+)/2$).

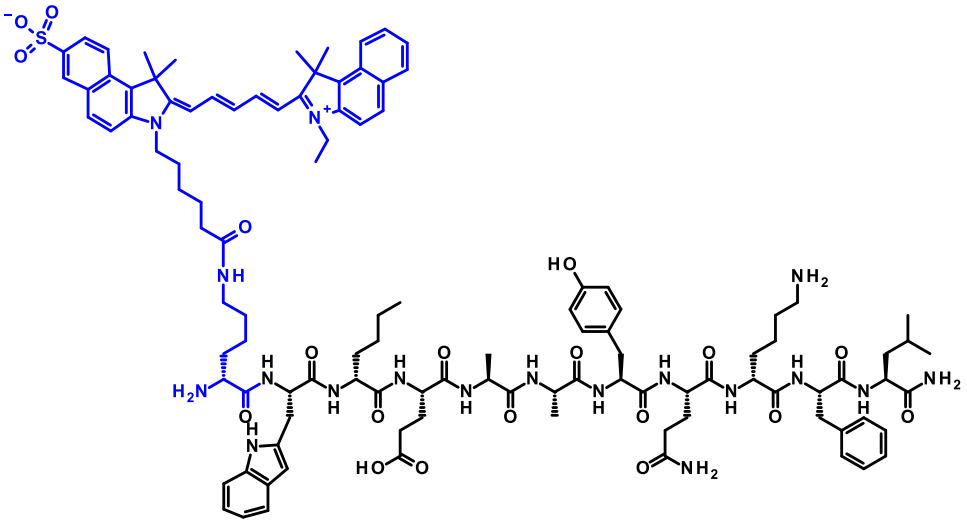

Figure 24. *Stucture of the Fmoc deprotected Cy5.5(1S) lablled Breast Cancer Peptide 18-4 Single-Modal TMIA Agent (M3 Product)*

Table 7. *Molecular Weight of Fmoc deprotected NH_2-Cy5.5(1S)-18-4-NH_2 Products*

Compounds	Molecular Weight (g/mol)	Half Mass (g/mol)
NH_2-d-Lys (Cy5.5)-Trp-d-Nle-Glu-Ala-Ala-Tyr-Gln-d-Lys-Phe-Leu-NH_2	2053.05	1027.52
NH_2-d-Lys (Cy5.5)-Trp-d-Nle-Glu-Ala-Ala-Tyr(tBu)-Gln-d-Lys-Phe-Leu-NH_2	2111.13	1056.56
NH_2-d-Lys (Cy5.5)-Trp-d-Nle-Glu (PhiPr)-Ala-Ala-Tyr-Gln-d-Lys-Phe-Leu-NH_2	2173.15	1087.57
NH_2-d-Lys (Cy5.5)-Trp-d-Nle-Glu (PhiPr)-Ala-Ala-Tyr(tBu)-Gln-d-Lys-Phe-Leu-NH_2	2229.21	1115.60

7.7 Synthesis of Dual-Modal TMIA (Fmoc-Gd (DOTA)-Cy5.5(1S)-18-4-NH_2)

The last goal of this research was to synthesize a dual-modal breast cancer TMIA for NIR fluorescence and MRI, containing both the NIR Cy5.5(1S) dye and the MRI contrast agent Gd. It is important to note that this is the first time (to our knowledge) that the modular method was utilized to introduce two different imaging modules (puzzle pieces) onto a peptide using SPPS. In this case, therefore, the entire synthesis of the dual modal TMIA was performed on the resin in solid phase synthesis.

The synthesis of the Gd (DOTA)-Cy5.5(1S)-TMIA is shown below, where the first step was to deprotect the Fmoc on the 18-4 peptide by using the method in Chapter 5.3.2. Next, the Cy5.5(1S) puzzle piece (Fmoc-dLys (Cy5.5-1S)-NHS ester) was coupled by following the method mentioned in Chapter 5.3.6. As a result, the Fmoc-Cy5.5(1S)-18-4-NH_2 TMIA was produced an intermediate product, which was followed by the removal of the Fmoc group. And lastly the Gd (DOTA) puzzle piece was coupled next, which resulted in the final dual-modal product.

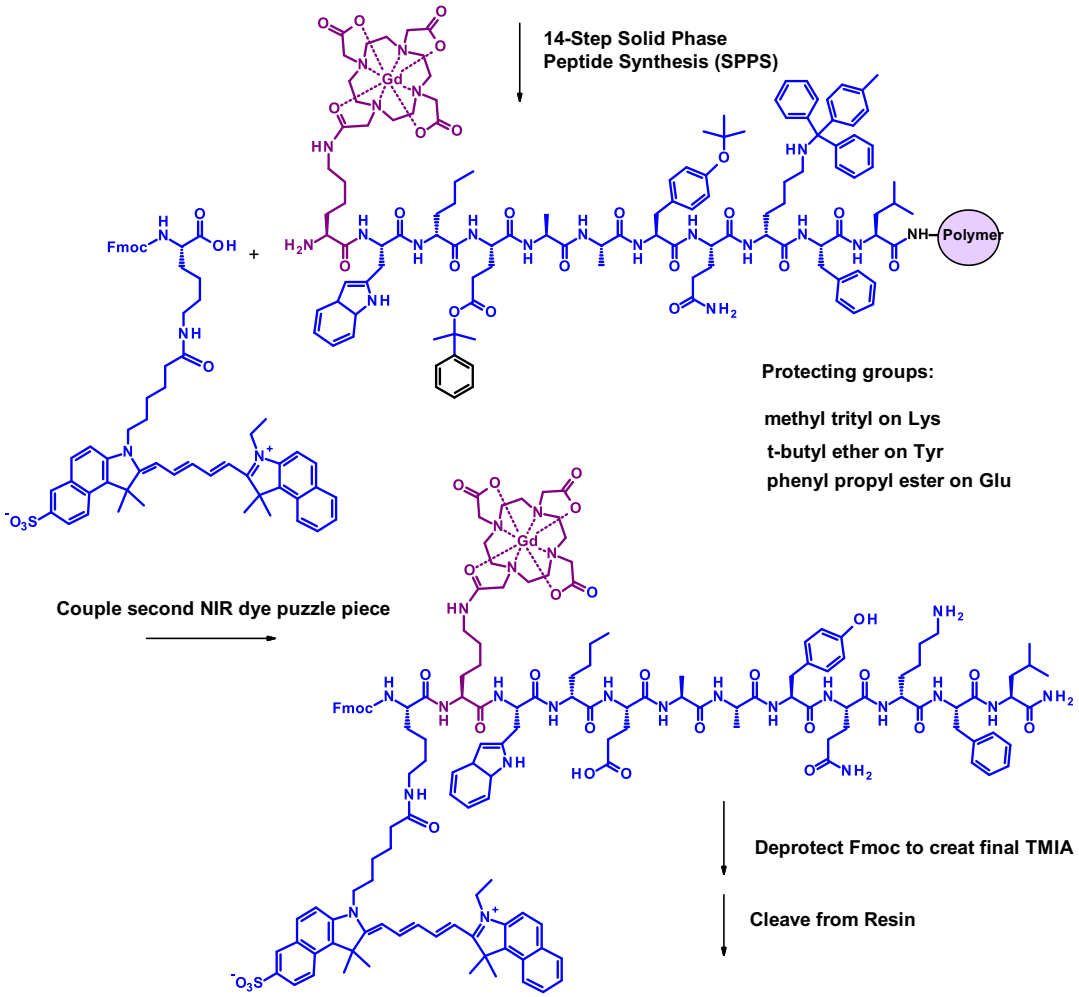

Scheme 11. *Synthesis of Dual-Modal Imaging Module for CFM and MRI, Fmoc-Gd (DOTA)-Cy5.5(1S)*-Trp-d-Nle-Glu-Ala-Ala-Tyr-Gln-d-Lys-Phe-Leu-NH_2 (Dual Modal TMIA Product)

7. 8 Fmoc Protected Gd (DOTA) and Cy5.5(1S) labelled breast cancer peptide 18-4 TMIA Product (Dual-Modal TMIA)

All the optimization methods for SPPS were used to synthesize the dual-modal TMIA product for NIR fluorescence and MIR, which was successfully achieved and was assayed with LC-MS. To test the Fmoc protected Gd-DOTA and Cy5.5(1S) labelled breast cancer 18-4 TMIA agent was cleaved with 1% TFA. The final product, Fmoc-Gd (DOTA)-Cy5.5(1S)-Trp-d-Nle-Glu-Ala-Ala-

Tyr(tBu)-Gln-d-Lys-Phe-Leu-NH_2 is shown below, (LC-MS Results: 1473.97 m/z ($M+2H^+$)/2 and 982.05 m/z ($M+3H^+$)/3).

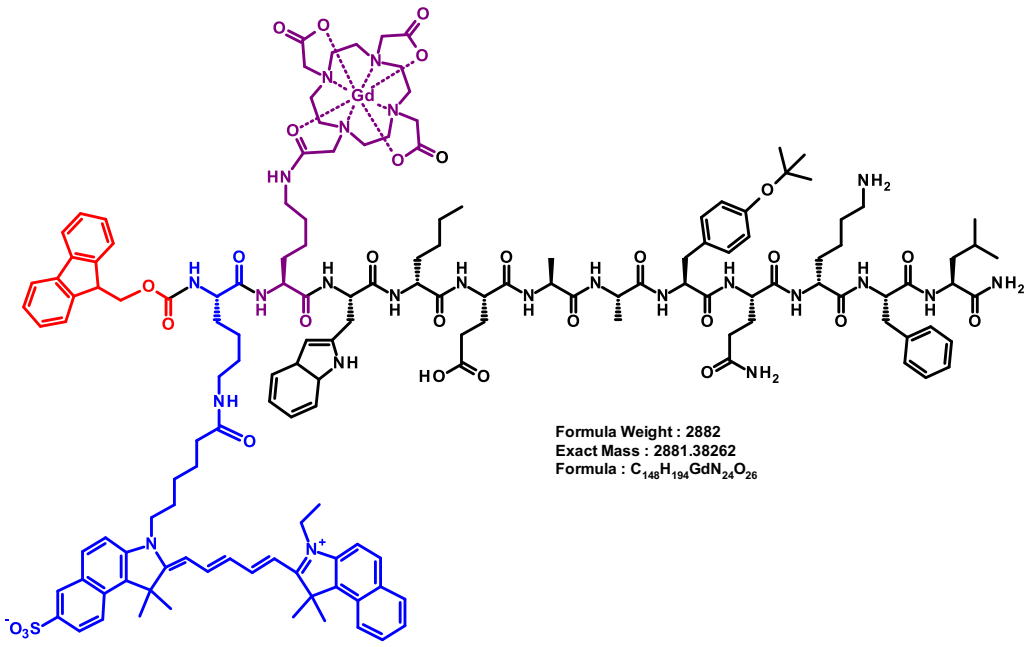

Figure 25. *Stucture of the Fmoc protected Gd(DOTA) and Cy5.5(1S) lablled Breast Cancer Peptide 18-4 Single-Modal TMIA Agent*

Table 8. *Molecular Weight of Fmoc protected Fmoc-Gd (DOTA)-Cy5.5(1S)-18-4-NH_2 Products*

Compounds	**Molecular Weight (g/mol)**	**Half Mass (g/mol)**
Fmoc-d-Lys (Cy5.5)-d-Lys (Gd-DOTA)-Trp-d-Nle-Glu-Ala-Ala-Tyr-Gln-d-Lys-Phe-Leu-NH_2	2881.38	1441.69
Fmoc-d-Lys (Cy5.5)-d-Lys (Gd-DOTA)-Trp-d-Nle-Glu-Ala-Ala-Tyr(tBu)-Gln-d-Lys-Phe-Leu-NH_2	2944.01	1473.00
Fmoc-d-Lys (Cy5.5)- d-Lys (Gd-DOTA)-Trp-d-Nle-Glu (PhiPr)-Ala-Ala-Tyr-Gln-d-Lys-Phe-Leu-NH_2	2999.45	1500.72
Fmoc-d-Lys (Cy5.5)- d-Lys (Gd-DOTA)-Trp-d-Nle-Glu (PhiPr)-Ala-Ala-Tyr(tBu)-Gln-d-Lys-Phe-Leu-NH_2	3055.52	1528.76

Chapter 8. Conclusion

The modular method developed in our lab was found to be a useful method to synthesize single-modal and dual-modal peptide-based TMIAs. The solid phase peptide synthesis (SPPS) developed previously by Xinyu Xu using the Sieber resin was further modified to facilitate coupling of dyes. The first goal of this research, which was to synthesize a BrCa targeting peptide 18-4, reported by Dr. Kaur (who used Rink amide resin) was successfully achieved. The TMIA's that were synthesized will thus be selective for breast cancer cells.

The next goal of this research was to use the modular method and imaging puzzle pieces to synthesize single-modal TMIA's for NIR dye (Cy5.5(1S)) and MRI contrast agent (Gd), which was successfully achieved. The Sieber resin proved to be an effective solution for the use of cyanine dyes such as Cy5.5, which would otherwise decompose in the presence of pure TFA which is necessary to cleave a peptide from Rink resin by allowing cleavage in dilute, 1 % TFA in DCM in which these dyes are stable.

In the first synthesis, the puzzle piece containing Gd-DOTA, attached to a lysine side chain, was used to couple to the Fmoc-deprotected BrCa targeting peptide 18-4, which was followed by the same 1 % TFA cleavage method to provide a Gd-based single modal TMIA agent for MRI. This validates the approach of utilizing SPPS to couple a chelated metal to a growing peptide chain using SPPS.

In the next campaign, the dye Cy5.5 dye on the side chain of lysine was assembled by the modular method into a new TMIA for BrCa known as M3. The synthesis of M3 required critical optimization of the SPPS methods on the resin. The deprotection of the Fmoc was optimized, where a new Fmoc deprotection method was used that did not degrade the Cy5.5 (1S) dye. The

activation step of the NIR dye puzzle piece for coupling was optimized, where the equivalents of DIPEA was increased. Lastly, the cleavage step of the SPPS method was optimized. A new method known as the continuous flow of TFA cleavage method was developed, which solved the binding of the dye to the resin and resulted in higher yield. The TMIA M3was delivered to biologists for evaluation in cell binding and CFM experiments.

The ultimate goal of this research was to use the modular method to synthesize a dual-modal imaging agent for NIR fluorescence and MRI contrast agent. This was successfully achieved and represents the first time that two imaging moieties were brought in to a peptide using SPPS methodology. These critical improvements in the SPPS methods will be vital for future dye TMIA synthesis in our group. Our lab's future goal is to synthesize a single PDT and dual modal NIR-PDT agents that will be useful for breast cancer therapy. The hope is that these methods used to synthesize selective TMIAs for breast cancer will not only detect cancer at an early stage but also kill the cancer.

Chapter 9. Experimental Procedures

9.1 Materials and Methods

Chemicals were purchased from VWR (Radnor, PA), Sigma Aldrich (St. Louis, MO), Alfa Aesar (Ward Hill, MA), TCI (Tokyo, Japan), and Acros Organics (Morris Plains, NY), and were used as received unless otherwise stated. All were HPLC or American Chemical Society grade. Amino acid starting materials and Xanthenyl linker resin were purchased from Bachem (Bubendorf, Switzerland), and Chem-Impex Int'l Inc. (Wood Dale, IL). DOTA was purchased from Macrocyclics (Houston, TX).

The HPLC instrument used was an Agilent 1100 with Diode Array Detector and for LC-MS a Waters 2695 Alliance HPLC with a Waters 2998 Diode Array Detector and a Waters 3100 SQ Mass Spectrometer was used. For HPLC the columns used were: an Agilent XDB C18 column, with dimensions of 3 mm x 100 mm or a Waters XBridge C18 column 50 mm x 3 mm and 3μ particle size. Mass spectra from this instrument were recorded at unit resolution with positive and negative switching mode at 35 or 50 V cone voltages. The flow rate for HPLC-MS was 0.5 mL/min. All aqueous mobile phases for HPLC are 0.1M ammonium acetate unless otherwise noted.

Preparative HPLC (prep-HPLC) was carried out with a Waters 600E system controller, and Waters 600 multi-solvent delivery system using a 30 mL/min flow rate. For SPE purification, a 20 g C-18 Sep-pack Varian Mega Bond Elut (20CC/5GRM) SPE cartridge was utilized for DCL (7).

Aqueous mobile phases for prep-HPLC are 0.1M ammonium acetate unless otherwise noted. Aqueous mobile phases for SPE are not buffered unless otherwise noted. The SPE cartridges were conditioned with their respective organic solvent, then pure DI H2O, then equilibrated with the initial gradient concentration. Gradients were performed in 5% increments with 3-10 mL fractions each unless otherwise noted.

High resolution mass spectra (HRMS) were obtained on a Waters Synapt G2Si (School of Chemical Sciences, University of Illinois at Urbana-Champaign) using the following parameters: Flow injection at flow rate of 0.1 ml/min, H2O/ACN/0.1% Formic Acid, positive and negative mode ESI, Cone voltage =25 V, capillary voltage = 3.0, ion source temperature = 100°C, desolvation temperature =180 °C, nebulizing gas (N2) flow = 200 L/h, cone gas (N2) flow = 5L/h.

9.2 Experimental Procedures

Fmoc-Leu-NH2 (1) Xanthenyl linker resin (850 mg, 247.35 μmol) was pre-swelled in DMF (16.5 mL). This reaction was stirred for 20 minutes and was drained using air pressure. After draining, to the reaction vial the Fmoc deprotection solution (8.5 mL of 5% Piperazine, 2% DBU, 93% DMF) was added and was stirred for 5 minutes. To the resin the deprotection step was repeated three times. The reaction vail was washed three times with DMF (16.5 mL). To a 20 mL scintillation vial the amino acid, Fmoc-Leu-OH (174.8 mg, 494.7 μmol) was dissolved in DMF (16.5), followed by the addition of DIEA (569 μL, 2473.5 μmol). To a separate 20 mL scintillation vial, HATU (178.6

mg, 469.9 μmol) was dissolved in DMF (16.5 mL) and was added to the amino acid mixture and stirred for 5 minutes. Then the mixture was added to the reaction vial and was allowed to stir for 45 minutes at room temperature. After 45 minutes of coupling, the solution was drained and the reaction was washed with DMF (16.5 mL) three times and was followed up by DCM (16.5 mL) three times. A small amount of the resultant resin (1R) (10 μg), was removed from the reaction vial and was cleaved with 1% TFA in DCM (1 mL) for 30 minutes. The product was filtered through glass wool and washed with DCM (1 mL). The eluent was concentrated with a rotovap, dissolved in 0.5 mL of methanol and assayed by LC-MS. LC-MS (LR, ESI) = Calcd. For $C_{21}H_{24}N_2O_3$: 352.178 m/z, found: 353.10 [M+H]+.

Fmoc-Phe-Leu-NH2 (2). Resin 1R was treated by the same procedure as for (1) about using the amino acid, Fmoc-Phe-OH (191.64 mg, 494.7 μmol), followed by cleavage of a small amount of the resultant resin (2R) also by the same procedure as above to yield Fmoc-Phe-Leu-NH_2 (2). LC-MS. LC-MS (LR, ESI) = Calcd. For $C_{30}H_{33}N_3O_4$: 499. 247 m/z, found: 500.11 [M+H]+.

Fmoc-d-Lys-Phe-Leu-NH2 (3). Resin 2R was treated by the same procedure as for (1) about using the amino acid, Fmoc-d-Lys (MTT)-OH (249.45 mg, 494.7 μmol), followed by cleavage of a small amount of the resultant resin (3R) also by the same procedure as above to yield Fmoc-d-Lys-Phe-Leu-NH_2 (3). LC-MS. LC-MS (LR, ESI) = Calcd. For $C_{36}H_{45}N_5O_5$: 627.34 m/z, found: 628.22 [M+H]+.

Fmoc-Gln-d-Lys-Phe-Leu-NH2 (4). Resin 3R was treated by the same procedure as for (1) about using the amino acid, Fmoc-Gln-OH (191.14 mg, 494.7 μmol), followed by cleavage of a small amount of the resultant resin (4R) also by the same procedure as above to yield Fmoc-Gln-d-Lys-Phe-Leu-NH_2 (4). LC-MS. LC-MS (LR, ESI) = Calcd. For $C_{41}H_{53}N_7O_7$: 755.40 m/z, found: 756.20 [M+H]+.

Fmoc-Tyr(tBu)-Gln-d-Lys-Phe-Leu-NH2 (5). Resin 4R was treated by the same procedure as for (1) about using the amino acid, Fmoc-Tyr(tBu)-OH (227.36 mg, 494.7 μmol), followed by cleavage of a small amount of the resultant resin (5R) also by the same procedure as above to yield Fmoc-Tyr(tBu)-Gln-d-Lys-Phe-Leu-NH2 (5). LC-MS. LC-MS (LR, ESI) = Calcd. For $C_{54}H_{70}N_8O_9$: 974.52 m/z, found: 975.16 [M+H]+.

Fmoc-Ala-Tyr(tBu)-Gln-d-Lys-Phe-Leu-NH2 (6). Resin 5R was treated by the same procedure as for (1) about using the amino acid, Fmoc-Ala-OH (154.0 mg, 494.7 μmol), followed by cleavage of a small amount of the resultant resin (6R) also by the same procedure as above to yield Fmoc-Ala-Tyr(tBu)-Gln-d-Lys-Phe-Leu-NH2 (6). LC-MS. LC-MS (LR, ESI) = Calcd. For $C_{57}H_{75}N_9O_{10}$: 1045.56 m/z, found: 1046.23 [M+H]+.

Fmoc-Ala-Ala-Tyr(tBu)-Gln-d-Lys-Phe-Leu-NH2 (7). Resin 6R was treated by the same procedure as for (1) about using the amino acid, Fmoc-Ala-OH (154.0 mg, 494.7 μmol), followed by cleavage of a small amount of the resultant resin (7R) also by the same procedure as above to yield Fmoc-Ala-Ala-Tyr(tBu)-Gln-d-Lys-Phe-Leu-NH2 (7). LC-MS. LC-MS (LR, ESI) = Calcd. For $C_{60}H_{80}N_{10}O_{11}$: 1116.60 m/z, found: 1117.20 [M+H]+.

Fmoc-Glu-Ala-Ala-Tyr(tBu)-Gln-d-Lys-Phe-Leu-NH2 (8). Resin 7R was treated by the same procedure as for (1) about using the amino acid, Fmoc-Glu (PhiPr)-OH (210.48 mg, 494.7 μmol), followed by cleavage of a small amount of the resultant resin (8R) also by the same procedure as above to yield Fmoc-Glu-Ala-Ala-Tyr(tBu)-Gln-d-Lys-Phe-Leu-NH2 (8). LC-MS. LC-MS (LR, ESI) = Calcd. For $C_{65}H_{87}N_{11}O_{14}$: 1245.64 m/z, found: 1246.22 [M+H]+.

Fmoc-d-Nle-Glu-Ala-Ala-Tyr(tBu)-Gln-d-Lys-Phe-Leu-NH2 (9). Resin 8R was treated by the same procedure as for (1) about using the amino acid, Fmoc-d-Nle-OH (174.82 mg, 494.7 μmol), followed by cleavage of a small amount of the resultant resin (9R) also by the same procedure as above to yield Fmoc-d-Nle-Glu-Ala-Ala-Tyr(tBu)-Gln-d-Lys-Phe-Leu-NH2 (9). LC-MS. LC-MS (LR, ESI) = Calcd. For $C_{71}H_{96}N_{12}O_{15}$: 1358.72 m/z, found: 1359.38 [M+H]+.

Fmoc-Trp-d-Nle-Glu-Ala-Ala-Tyr-Gln-d-Lys-Phe-Leu-NH2 (10). Resin 9R was treated by the same procedure as for (1) about using the amino acid, Fmoc-Trp-OH (260.5 mg, 494.7 μmol), followed by cleavage of a small amount of the resultant resin (10R) also by the same procedure as above to yield Fmoc-Trp-d-Nle-Glu-Ala-Ala-Tyr-Gln-d-Lys-Phe-Leu-NH2 (10). LC-MS (LR, ESI) = Calcd. For $C_{78}H_{100}N_{14}O_{16}$: 1488.74 m/z, found: 1489.71 [M+H]+.

Fmoc-Trp-d-Nle-Glu-Ala-Ala-Tyr(tBu)-Gln-d-Lys-Phe-Leu-NH2 (11). Resin 9R was treated by the same procedure as for (1) about using the amino acid, Fmoc-Trp-OH (260.5 mg, 494.7 μmol), followed by cleavage of a small amount of the resultant resin (11R) also by the same procedure as above to yield Fmoc-Trp-d-Nle-Glu-Ala-Ala-Tyr(tBu)-Gln-d-Lys-Phe-Leu-NH2 (10). LC-MS (LR, ESI) = Calcd. For $C_{82}H_{108}N_{14}O_{16}$: 1544.80 m/z, found: 1545.44 [M+H]+.

NH_2-Trp-d-Nle-Glu-Ala-Ala-Tyr(tBu)-Gln-d-Lys-Phe-Leu-NH2 (12). Resin 11R was treated with Fmoc deprotection method, which was followed by cleavage of the resultant resin (12R) also by the same procedure as above to yield NH_2-Trp-d-Nle-Glu-Ala-Ala-Tyr(tBu)-Gln-d-Lys-Phe-Leu-NH2 (12). LC-MS (LR, ESI) = Calcd. For $C_{67}H_{98}N_{14}O_{14}$: 1322.73 m/z, found: 1323.55 [M+H]+, found: 662.51 ($M+2H^+$)/2. HRMS: Calcd. MW 1322.73869, (M+1): 1323.74663, [(M+2)/2]: 662.37729, Found 662.3759 (- 2.09 ppm).

Fmoc-Gd (DOTA)-Trp-d-Nle-Glu-Ala-Ala-Tyr-Gln-d-Lys-Phe-Leu-NH_2 (13). Small amount of resin 12R (30 mg) was treated by the same procedure as for (1) about using the puzzle piece, Fmoc-d-Lys (Gd-DOTA)-NH_2 (15.21 mg, 87.3 μmol), followed by cleavage of the resultant resin (13R) also by the same procedure as above to yield Fmoc-Gd (DOTA)-Trp-d-Nle-Glu-Ala-Ala-Tyr-Gln-d-Lys-Phe-Leu-NH2 (13). LC-MS (LR, ESI) = Calcd. for $C_{100}H_{135}GdN_{20}O_{24}$: MW 2157.9199, (M+1): 2158.93; [(M+2)/2]: 1079.97; found: 1080.30 m/z ($M+2H^+$)/2. HRMS: Calcd. MW 2157.9199, (M+1): 2158.92786; [(M+2)/2]: 1079.96790, Found 1079.96950 (- 1.48 ppm).

NH_2-Gd (DOTA)-Trp-d-Nle-Glu-Ala-Ala-Tyr-Gln-d-Lys-Phe-Leu-NH_2 (14). Resin 13R was treated by Fmoc deprotection method, followed by cleavage of the resultant resin (14R) also by the same procedure as above to yield NH_2-Gd (DOTA)-Trp-d-Nle-Glu-Ala-Ala-Tyr-Gln-d-Lys-Phe-Leu-NH2

(14). LC-MS (LR, ESI) = Calcd. For $C_{85}H_{125}GdN_{20}O_{22}$: 996 m/z, ½ mass 1080.5, found: 996.26 m/z $(M+2H^+)/2$.

Fmoc-D-Lys(Cy5.5-1S)-OH (Cy5.51S Puzzle Piece) (15). This imaging module was prepared by a method published by our group.[57] LC-MS (LR, ESI) = Calcd. For $C_{62}H_{66}N_4O_8S_1$: $(M+1)^+$: 1027.47 m/z, ½ mass, found: 1027.60 m/z. HRMS: Calcd. MW 1026.46014, (M+1): 1027.46808, Found 1027.4653 (- 2.71 ppm).

Fmoc-D-Lys(Cy5.5-1S)-NHS (Activated Cy5.51S Puzzle Pieces NHS ester) (16). The activation of imaging module **Fmoc-D-Lys(Cy5.5-1S)-OH** was carried out using TSTU by a method published by our group.[57] In order to test the activation, a small aliquot of the product was quenched by dissolved in a solution of 0.1 % butyl amine to yield the butyl amide which was assayed by LC-MS. The conversion to activated ester was over 99 % complete. LC-MS (LR, ESI) = Calcd. For $C_{66}H_{75}N_5O_7S_1$: $(M+1)^+$: 1082.54 m/z, ½ mass , found: 1082.33 m/z.

NH_2-Cy5.5(1S)-Trp-d-Nle-Glu-Ala-Ala-Tyr-Gln-d-Lys-Phe-Leu-NH_2 (17). Small amount of resin 12R (30 mg) was treated by the same procedure as for (1) about using the puzzle piece, Fmoc-d-Lys (Cy5.5(1S))-NH_2 (14.5 mg, 13.09 μmol), followed by cleavage of the resultant resin also by the same procedure as above to yield Fmoc-Cy5.5(1S)-Trp-d-Nle-Glu-Ala-Ala-Tyr-Gln-d-Lys-Phe-Leu-NH2. The resultant resin was treated by Fmoc deprotection method, followed by cleavage of the resultant resin (15R) also by the same procedure as above to yield NH_2-Cy5.5(1S)-Trp-d-Nle-Glu-Ala-Ala-Tyr-Gln-d-Lys-Phe-Leu-NH_2 (17). LC-MS (LR, ESI) = Calcd. For $C_{110}H_{144}N_{18}O_{19}S_1$: 2158.92 m/z, ½ mass 1027.53, found: 1027.60 m/z $(M+2H^+)/2$. HRMS: Calcd. MW 2053.05759, (M+1): 2054.06553, [(M+2)/2]: 1027.53674, Found 1027.5366 (- 1.31 ppm).

Fmoc-Gd (DOTA)--Cy5.5(1S)-Trp-d-Nle-Glu-Ala-Ala-Tyr(tBu)-Gln-d-Lys-Phe-Leu-NH_2 (18). Resin 15R was treated by the same procedure as for (1) about using the puzzle piece Fmoc-d-Lys (Gd-DOTA)-NH_2 (15.21 mg, 87.3 μmol), followed by cleavage of the resultant resin (16R) also by the same procedure as above to yield Fmoc-Gd (DOTA)--Cy5.5(1S)-Trp-d-Nle-Glu-Ala-Ala-Tyr(tBu)-Gln-d-Lys-Phe-Leu-NH_2 (18). LC-MS (LR, ESI) = Calcd. For $C_{110}H_{145}N_{18}O_{19}S$: 3053.50 m/z, ½ mass 1472, ⅓ mass 981, found: 1473.97 m/z $(M+2H^+)/2$, 982.05 m/z $(M+3H^+)/3$.

References

(1) Sankaranarayanan, R.; Ferlay, J. Burden of Breast and Gynecological Cancers in Low-Resource Countries. In *Breast and Gynecological Cancers*; Springer New York: New York, NY, 2013; pp 1–17. https://doi.org/10.1007/978-1-4614-1876-4_1.

(2) Jacobs, M. A.; Wolff, A. C.; Macura, K. J.; Stearns, V.; Ouwerkerk, R.; El Khouli, R.; Bluemke, D. A.; Wahl, R. Multiparametric and Multimodality Functional Radiological Imaging for Breast Cancer Diagnosis and Early Treatment Response Assessment. *J. Natl. Cancer Inst. Monogr.* **2015**, *2015* (51), 40.

(3) Sharma, G. N.; Dave, R.; Sanadya, J.; Sharma, P.; Sharma, K. K. Various Types and Management of Breast Cancer: An Overview. *J. Adv. Pharm. Technol. Res.* **2010**, *1* (2), 109–126.

(4) Kamińska, M.; Ciszewski, T.; Łopacka-Szatan, K.; Miotła, P.; Starosławska, E. Breast Cancer Risk Factors. *Menopausal Rev.* **2015**, *3*, 196–202. https://doi.org/10.5114/pm.2015.54346.

(5) What Is Breast Cancer? | Breastcancer.org https://www.breastcancer.org/symptoms/understand_bc/what_is_bc (accessed 2021 -06 -21).

(6) Breast Cancer: Stages | Cancer.Net https://www.cancer.net/cancer-types/breast-cancer/stages (accessed 2021 -06 -21).

(7) Metastatic Breast Cancer - National Breast Cancer Foundation https://www.nationalbreastcancer.org/metastatic-breast-cancer (accessed 2021 -06 -21).

(8) Stages of Breast Cancer | Memorial Sloan Kettering Cancer Center https://www.mskcc.org/cancer-care/types/breast/diagnosis/stages-breast (accessed 2021 -06 -21).

(9) Magnetic Resonance Imaging (MRI) Breast https://www.radiologyinfo.org/en/info/breastmr (accessed 2021 -06 -21).

(10) Gundry, K. R. The Application of Breast MRI in Staging and Screening for Breast Cancer. *Oncol. Williston Park N* **2005**, *19* (2), 159.

(11) Radiation Risks of X-rays and Scans http://www.imagingpathways.health.wa.gov.au/index.php/consumer-info/general-information-about-diagnostic-imaging/radiation-risks-of-x-rays-and-scans (accessed 2021 -06 -21).

(12) Choe, R.; Konecky, S. D.; Corlu, A.; Lee, K.; Durduran, T.; Busch, D. R.; Pathak, S.; Czerniecki, B. J.; Tchou, J.; Fraker, D. L.; Demichele, A.; Chance, B.; Arridge, S. R.; Schweiger, M.; Culver, J. P.; Schnall, M. D.; Putt, M. E.; Rosen, M. A.; Yodh, A. G. Differentiation of Benign and Malignant Breast Tumors by In-Vivo Three-Dimensional Parallel-Plate Diffuse Optical Tomography. *J. Biomed. Opt.* **2009**, *14* (2), 024020–024020. https://doi.org/10.1117/1.3103325.

(13) Using MRI to Detect Breast Cancer https://www.webmd.com/breast-cancer/breast-cancer-mri#1 (accessed 2021 -06 -21).

(14) Sheth, R. A.; Mahmood, U. Optical Molecular Imaging and Its Emerging Role in Colorectal Cancer. *Am. J. Physiol. Gastrointest. Liver Physiol.* **2010**, *299* (4), G807.

(15) Chen, K.; Chen, X. Design and Development of Molecular Imaging Probes. *Curr. Top. Med. Chem.* **2010**, *10* (12), 1227.
(16) Muller, M.; Society of Photo-optical Instrumentation Engineers. *Introduction to Confocal Fluorescence Microscopy*, 2nd ed.; SPIE: Bellingham, Wash. (1000 20th St. Bellingham WA 98225-6705 USA), 2006; Vol. v. TT 69.;TT69.;
(17) Pierce, M. C.; Javier, D. J.; Richards-Kortum, R. Optical Contrast Agents and Imaging Systems for Detection and Diagnosis of Cancer. *Int. J. Cancer* **2008**, *123* (9), 1979–1990. https://doi.org/10.1002/ijc.23858.
(18) Luo, S.; Zhang, E.; Su, Y.; Cheng, T.; Shi, C. A Review of NIR Dyes in Cancer Targeting and Imaging. *Biomaterials* **2011**, *32* (29), 7127–7138. https://doi.org/10.1016/j.biomaterials.2011.06.024.
(19) In Vivo Imaging | Biotium https://biotium.com/products/in-vivo-imaging/ (accessed 2021 -06 -21).
(20) Cyanine dyes https://www.lumiprobe.com/tech/cyanine-dyes (accessed 2021 -06 -22).
(21) J.P. Hornak. *The Basics of MRI*; Interactive Learning Software, Henietta, NY, 2012.
(22) Grover, V. P. B.; Tognarelli, J. M.; Crossey, M. M. E.; Cox, I. J.; Taylor-Robinson, S. D.; McPhail, M. J. W. Magnetic Resonance Imaging: Principles and Techniques: Lessons for Clinicians. *J. Clin. Exp. Hepatol.* **2015**, *5* (3), 246–255. https://doi.org/10.1016/j.jceh.2015.08.001.
(23) Who Invented the MRI? | AffordableMRI.com https://affordablemri.com/who-invented-the-mri/ (accessed 2021 -06 -22).
(24) Forshult, S. E.; Karlstads universitet; Avdelningen för fysik. *Magnetic Resonance Imaging: MRI : An Overview*; Faculty of Technology and Science, Physics, Karlstad University: Karlstad, 2007.
(25) Jones, K. Modular Synthesis of Targeted Molecular Imaging Agents for MRI, PET, and PET-MRI of Cancer. 109.
(26) Grover, V. P. B.; Tognarelli, J. M.; Crossey, M. M. E.; Cox, I. J.; Taylor-Robinson, S. D.; McPhail, M. J. W. Magnetic Resonance Imaging: Principles and Techniques: Lessons for Clinicians. *J. Clin. Exp. Hepatol.* **2015**, *5* (3), 246–255. https://doi.org/10.1016/j.jceh.2015.08.001.
(27) Schmitthenner, H. F.; Weidman, C.; Barrett, T. Modular Imaging Agents Containing Amino Acids and Peptides, 2020.
(28) Xu, X. Solid Phase Synthesis of Modular Peptide-Based Targeted Molecular Imaging Agents, Rochester Institute of Technology, Rochester, NY, 2019.
(29) Deng, Y.; Xu, A.; Yu, Y.; Fu, C.; Liang, G. Biomedical Applications of Fluorescent and Magnetic Resonance Imaging Dual-Modality Probes. *Chembiochem Eur. J. Chem. Biol.* **2019**, *20* (4), 499–510. https://doi.org/10.1002/cbic.201800450.
(30) Bondell, S. Fluorescent Imaging Could be 'Game Changer' in Breast Cancer Surgery | Moffitt https://moffitt.org/endeavor/archive/fluorescent-imaging-could-be-game-changer-in-breast-cancer-surgery/ (accessed 2021 -06 -23).
(31) Zhao, J.; Chen, J.; Ma, S.; Liu, Q.; Huang, L.; Chen, X.; Lou, K.; Wang, W. Recent Developments in Multimodality Fluorescence Imaging Probes. *Acta Pharm. Sin. B* **2018**, *8* (3), 320–338. https://doi.org/10.1016/j.apsb.2018.03.010.

(32) Soudy, R.; Gill, A.; Sprules, T.; Lavasanifar, A.; Kaur, K. Proteolytically Stable Cancer Targeting Peptides with High Affinity for Breast Cancer Cells. *J. Med. Chem.* **2011**, *54* (21), 7523–7534. https://doi.org/10.1021/jm200750x.
(33) Chemotherapy Side Effects https://www.cancer.org/treatment/treatments-and-side-effects/treatment-types/chemotherapy/chemotherapy-side-effects.html (accessed 2021 -06 -23).
(34) The 10 most common chemotherapy side effects https://www.medicalnewstoday.com/articles/323485 (accessed 2021 -06 -23).
(35) Photodynamic Therapy for Cancer - National Cancer Institute https://www.cancer.gov/about-cancer/treatment/types/photodynamic-therapy (accessed 2021 -06 -23).
(36) Definition of photosensitizing agent - NCI Dictionary of Cancer Terms - National Cancer Institute https://www.cancer.gov/publications/dictionaries/cancer-terms/def/photosensitizing-agent (accessed 2021 -06 -23).
(37) Skoog, D. A.; Holler, F. J.; Crouch, S. R. *Principles of Instrumental Analysis*, Seventh edition.; Cengage Learning: Australia, 2018.
(38) Abrahamse, H.; Hamblin, M. R. New Photosensitizers for Photodynamic Therapy. *Biochem. J.* **2016**, *473* (4), 347.
(39) Hans, S. Proposal: Targeted Probes for Photodynamic Therapy of Breast Cancer.
(40) Wu, H.; Huang, J. Optimization of Protein and Peptide Drugs Based on the Mechanisms of Kidney Clearance. *Protein Pept. Lett.* **2018**, *25* (6), 514.
(41) Endocytosis and Exocytosis | Biology for Majors I https://courses.lumenlearning.com/suny-wmopen-biology1/chapter/endocytosis-and-exocytosis/ (accessed 2021 -06 -23).
(42) Soudy, R.; Etayash, H.; Bahadorani, K.; Lavasanifar, A.; Kaur, K. Breast Cancer Targeting Peptide Binds Keratin 1: A New Molecular Marker for Targeted Drug Delivery to Breast Cancer. *Mol. Pharm.* **2017**, *14* (3), 593–604. https://doi.org/10.1021/acs.molpharmaceut.6b00652.
(43) MSOE Center for BioMolecular Modeling -Protein Structure Jmol Tutorials https://cbm.msoe.edu/includes/modules/jmolProteinStructure/primarystructure.html (accessed 2021 -06 -24).
(44) Palomo, J. M. Solid-Phase Peptide Synthesis: An Overview Focused on the Preparation of Biologically Relevant Peptides. *RSC Adv.* **2014**, *4* (62), 32658–32672. https://doi.org/10.1039/C4RA02458C.
(45) Bioavailability - an overview | ScienceDirect Topics https://www.sciencedirect.com/topics/medicine-and-dentistry/bioavailability (accessed 2021 -06 -24).
(46) Hormone Therapy for Breast Cancer Fact Sheet - National Cancer Institute https://www.cancer.gov/types/breast/breast-hormone-therapy-fact-sheet (accessed 2021 -06 -24).
(47) Triple-Negative Breast Cancer: Overview, Treatment, and More https://www.breastcancer.org/symptoms/types/triple-negative (accessed 2021 -06 -24).
(48) Peptide Synthesis | Thermo Fisher Scientific - US https://www.thermofisher.com/us/en/home/life-science/protein-biology/protein-

biology-learning-center/protein-biology-resource-library/pierce-protein-methods/peptide-synthesis.html (accessed 2021 -06 -24).
(49) Carlson, S. Manual and Automated Solid Phase Synthesis of Peptides for Breast Cancer Cell Targeting. 2.
(50) solid phase peptide synthesis https://www.biosyn.com/tew/solid-phase-peptide-synthesis.aspx (accessed 2021 -06 -24).
(51) HPLC Separation Modes | Waters https://www.waters.com/waters/en_US/HPLC-Separation-Modes/nav.htm?cid=10049076&locale=en_US (accessed 2021 -06 -24).
(52) How to choose the right resin functionality for solid phase peptide synthesis https://selekt.biotage.com/peptideblogs/how-to-choose-the-right-resin-functionality-for-solid-phase-peptide-synthesis (accessed 2021 -06 -24).
(53) Fmoc Deprotection in Peptide Synthesis – Peptide Chemistry Portal https://peptidechemistryportal.com/fmoc-deprotection-in-peptide-synthesis/ (accessed 2021 -06 -24).
(54) Schmitthenner, H. F.; Barrett, T. M.; Beach, S. A.; Heese, L. E.; Weidman, C.; Dobson, D. E.; Mahoney, E. R.; Schug, N. C.; Jones, K. G.; Durmaz, C.; Otasowie, O.; Aronow, S.; Lee, Y. P.; Ophardt, H. D.; Becker, A. E.; Hornak, J. P.; Evans, I. M.; Ferran, M. C. Modular Synthesis of Peptide-Based Single- and Multimodal Targeted Molecular Imaging Agents. *ACS Appl. Bio Mater.* **2021**, No. Journal Article. https://doi.org/10.1021/acsabm.1c00157.
(55) Schug, N. C. Modular Synthesis of Dual- and Tri-Modal Targeted Molecular Imaging Agents, Rochester Institute of Technology, Rochester, NY, 2020.
(56) Schmitthenner, H. F.; Dobson, D. E.; Jones, K. G.; Akporji, N.; Soika, D. Q. M.; Nastiuk, K. L.; Hornak, J. P. Modular Synthesis of DOTA-Metal-Based PSMA-Targeted Imaging Agents for MRI and PET of Prostate Cancer. *Chem. Eur. J.* **2019**, *25* (61), 13848–13854. https://doi.org/10.1002/chem.201903390.
(57) Dobson, D. E.; Mahoney, E. R.; Mach, T. P.; LeTourneau, R. J.; Schmitthenner, H. F. Pentamethine Sulfobenzoindocyanine Dyes with Low Net Charge States and High Photostability. *Photochem. Photobiol. Sci.* **2020**, *19* (1), 56–65. https://doi.org/10.1039/C9PP00445A.

Appendix I. HPLC-MS and HRMS Results

Compound 1: Fmoc-Leu-NH_2 (SPPS intermediate monopeptide product of 18-4)

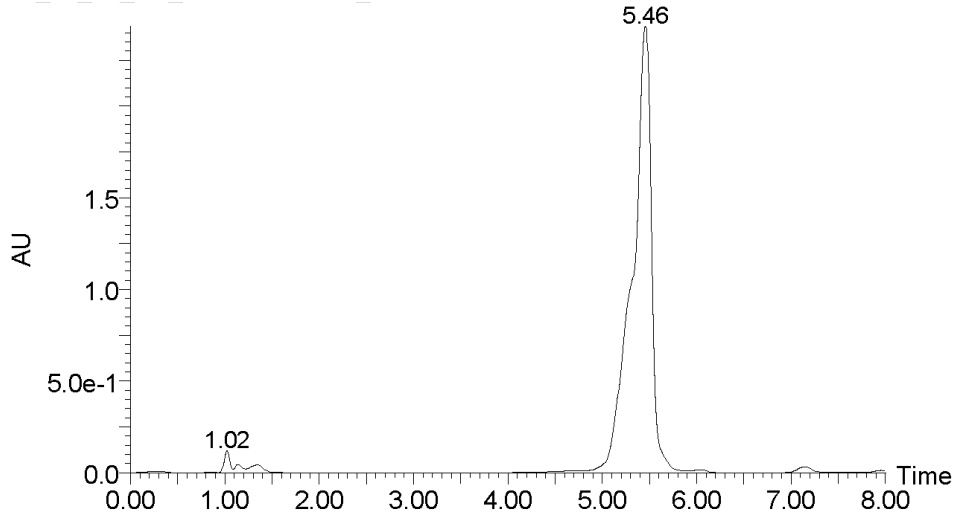

Single Wavelength Chromatogram of **1** at 263 nm of main peak at 5.46 min

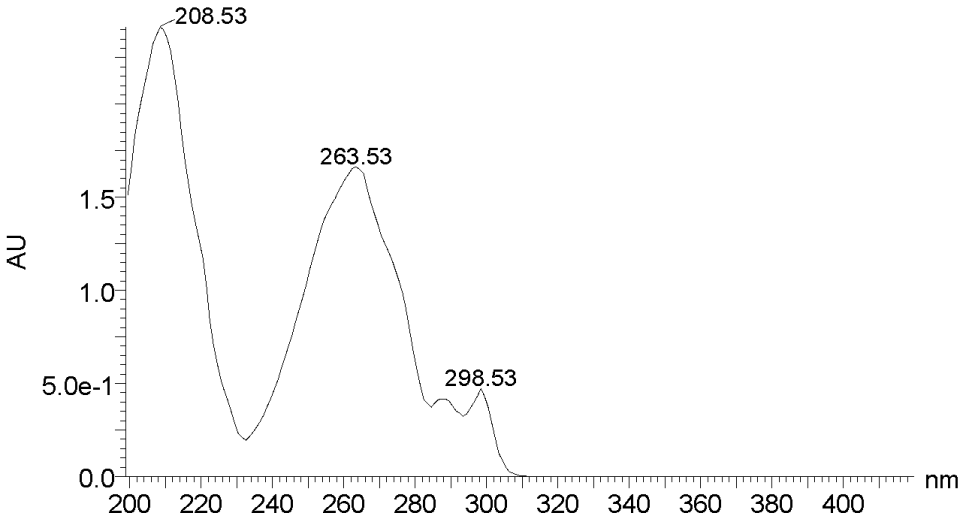

UV-Vis Diode array of **1** spectrum at 5.46 min with characteristic peak at 263 nm for Fmoc protecting group

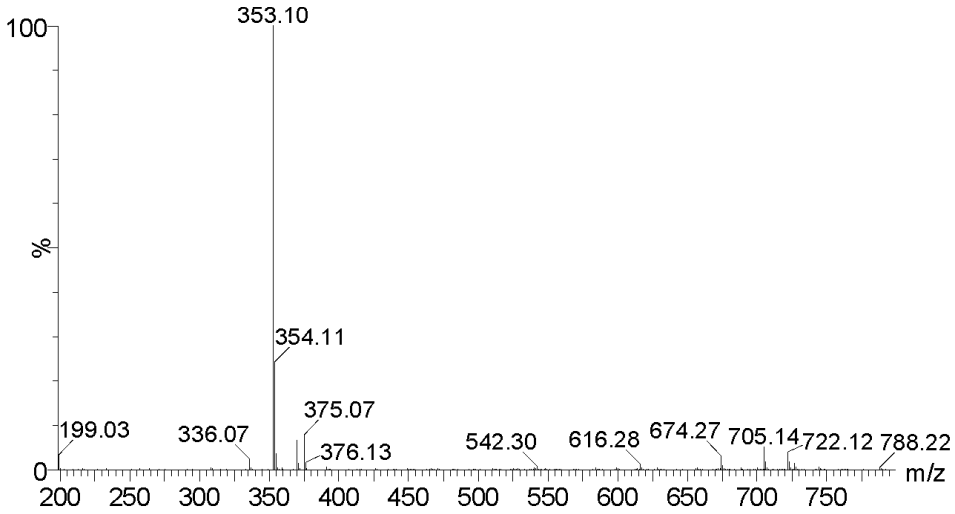

Positive Ion Mass spectrum of **1** at 5.46 min, product 353.10 m/z [M+H]+

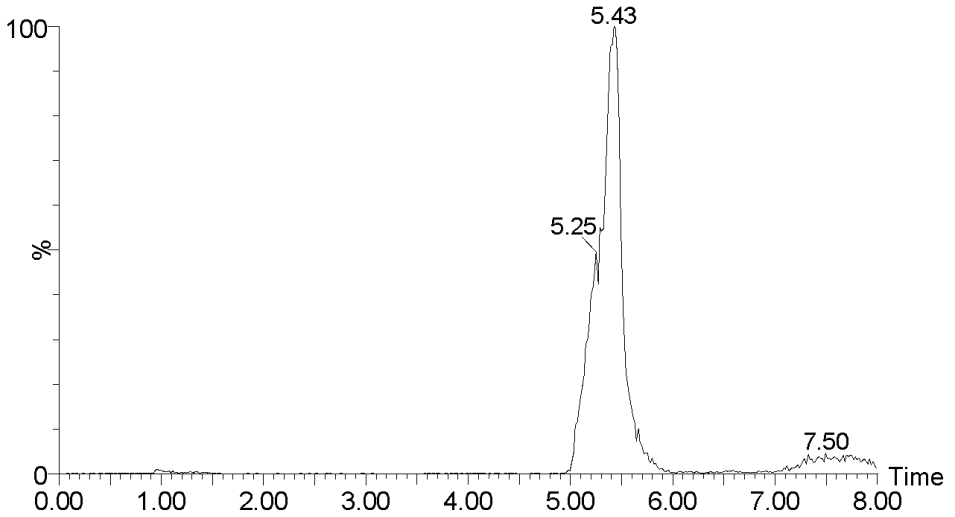

Extracted (Single) Ion Chromatogram (XIC) at 353 amu

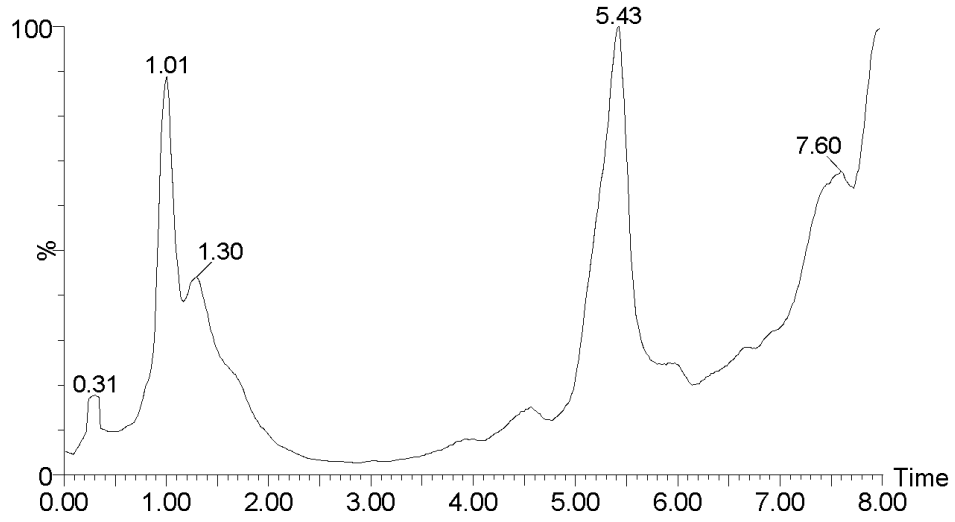

Total Ion Chromatogram (TIC) of **1**

Compound 2: Fmoc-Phe-Leu-NH_2 (SPPS intermediate dipeptide product of 18-4)

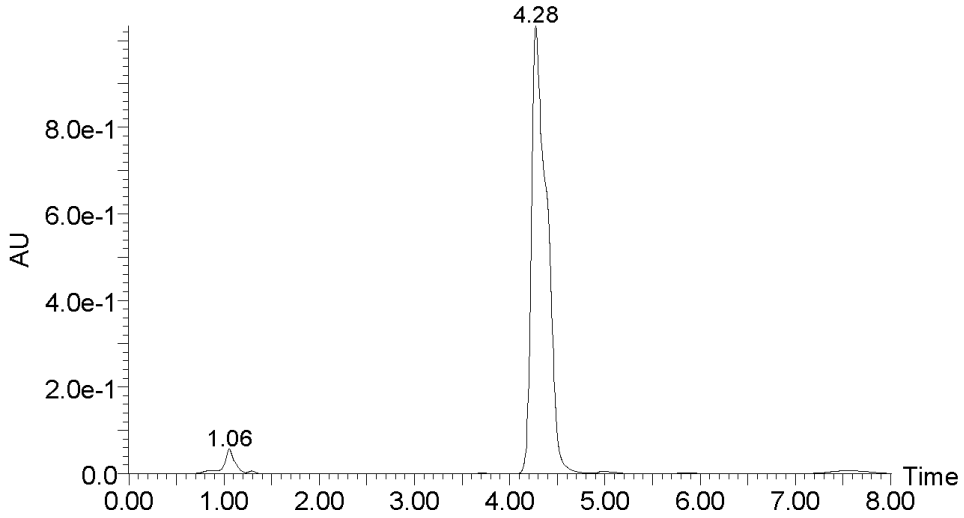

Single Wavelength Chromatogram of **2** at 263 nm of main peak at 4.28 min

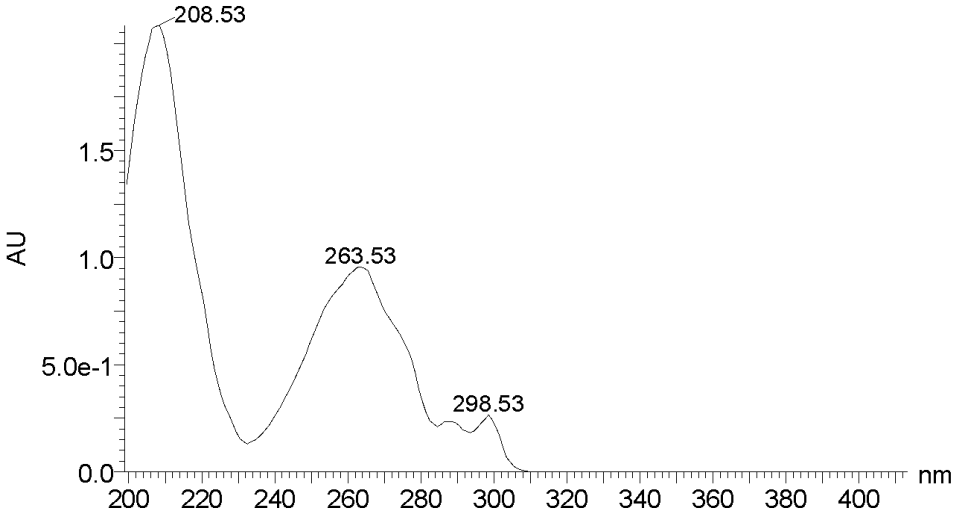

UV-Vis Diode array of **2** spectrum at 4.28 min with characteristic peak at 263 nm for Fmoc protecting group

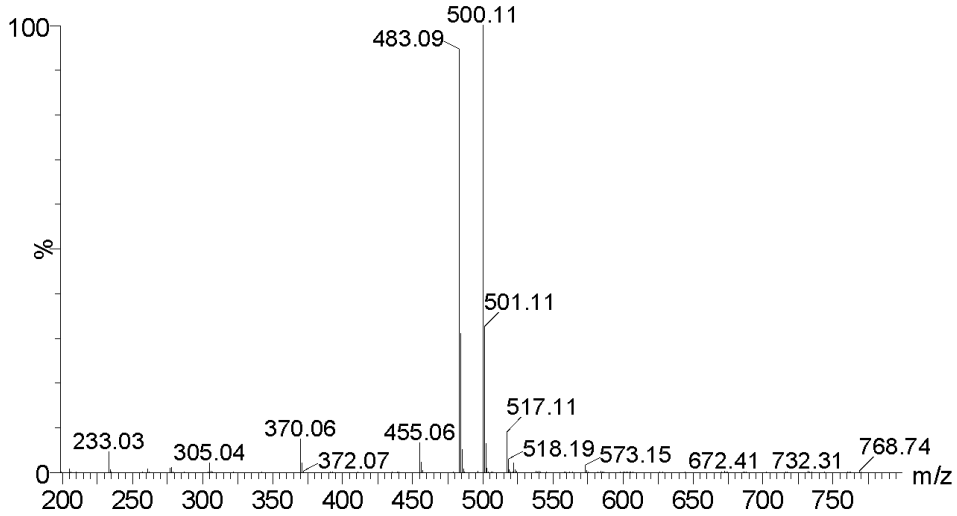

Positive Ion Mass spectrum of **2** at 4.28 min, product 500.11 m/z [M+H]+

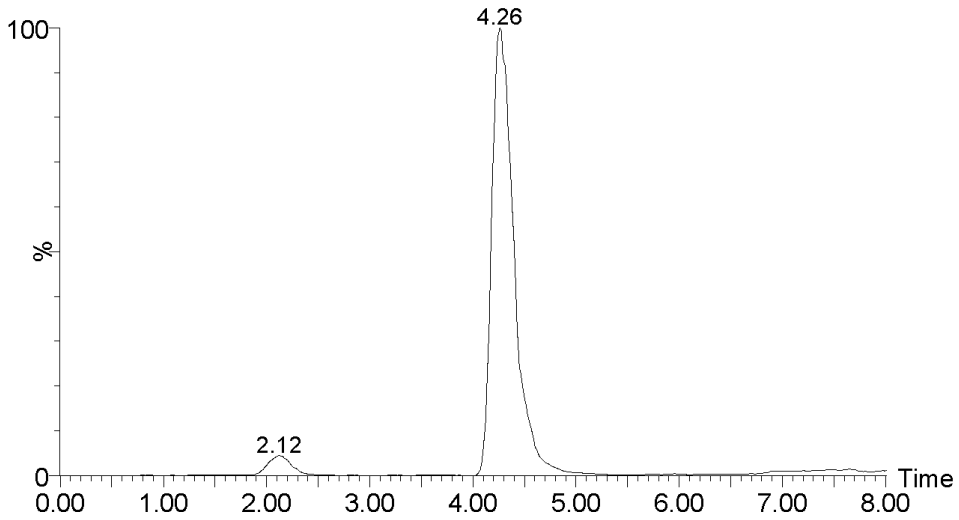

Extracted (Single) Ion Chromatogram (XIC) at 500 amu

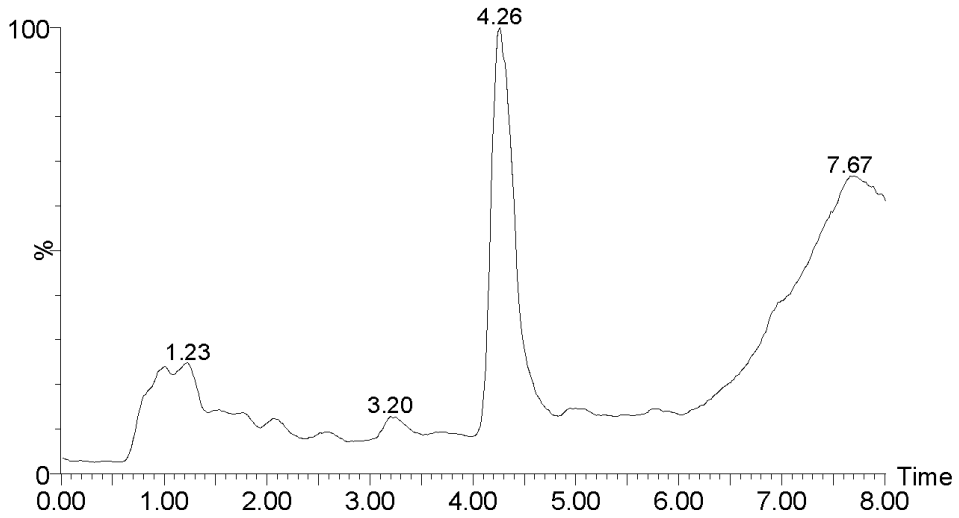

Total Ion Chromatogram (TIC) of **2**

Compound 3: Fmoc-dLys-Phe-Leu-NH_2 (SPPS intermediate tripeptide product of 18-4)

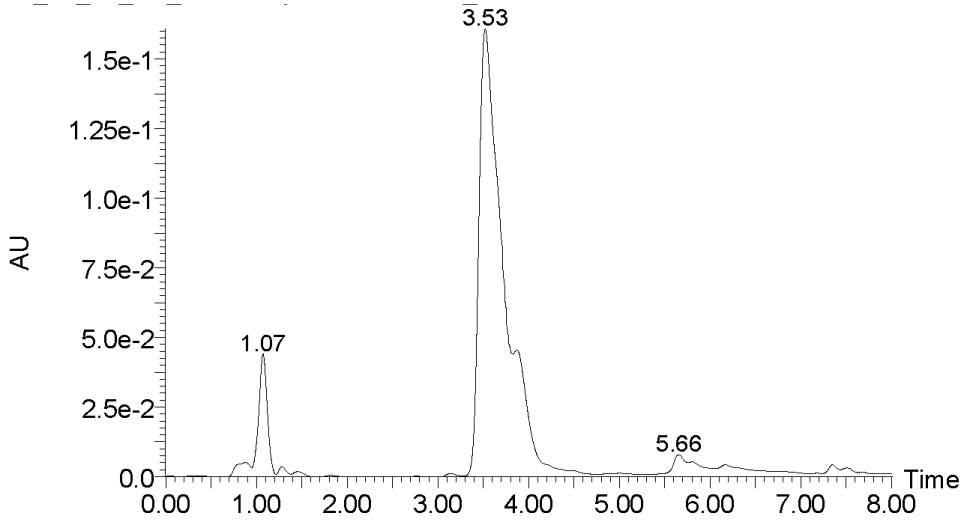

Single Wavelength Chromatogram of **3** at 263 nm of main peak at 3.53 min

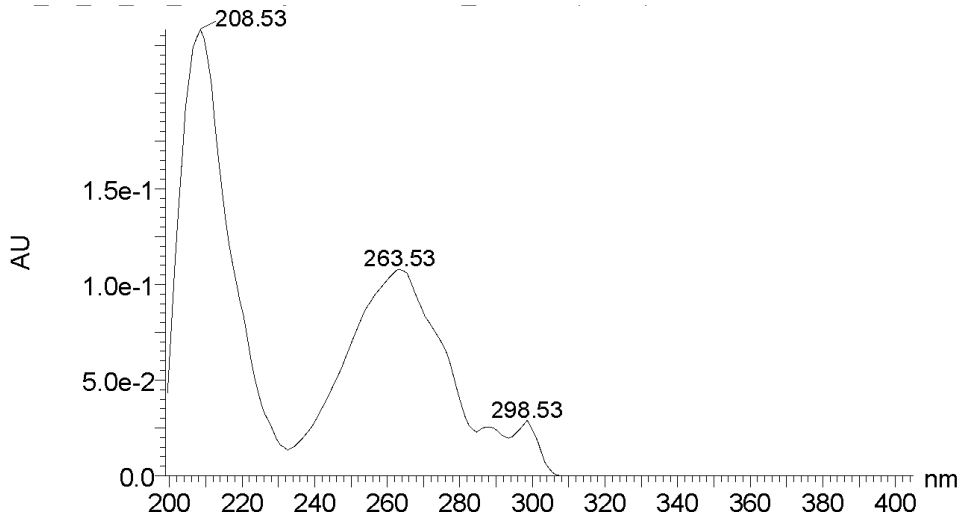

UV-Vis Diode array of **3** spectrum at 3.53 min with characteristic peak at 263 nm for Fmoc protecting group

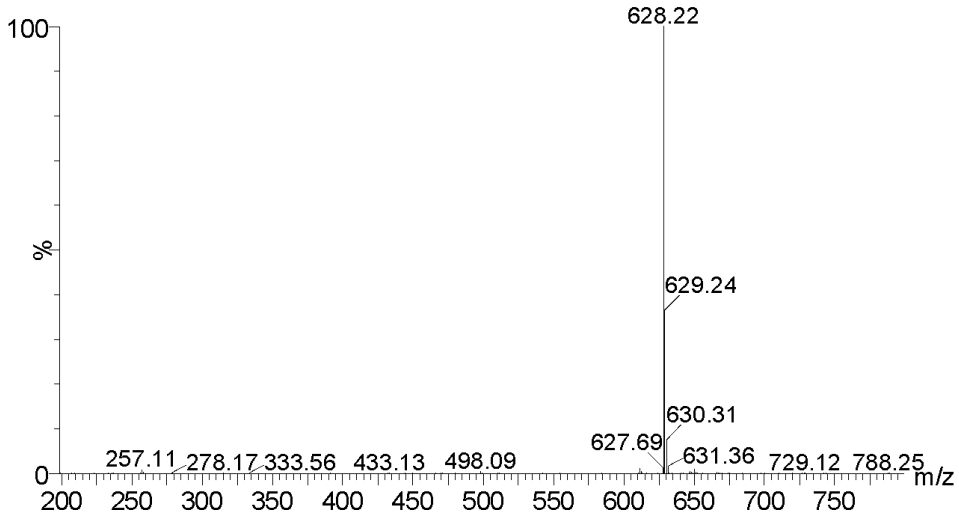

Positive Ion Mass spectrum of **3** at 3.53 min, product 628.22 m/z $[M+H]_+$

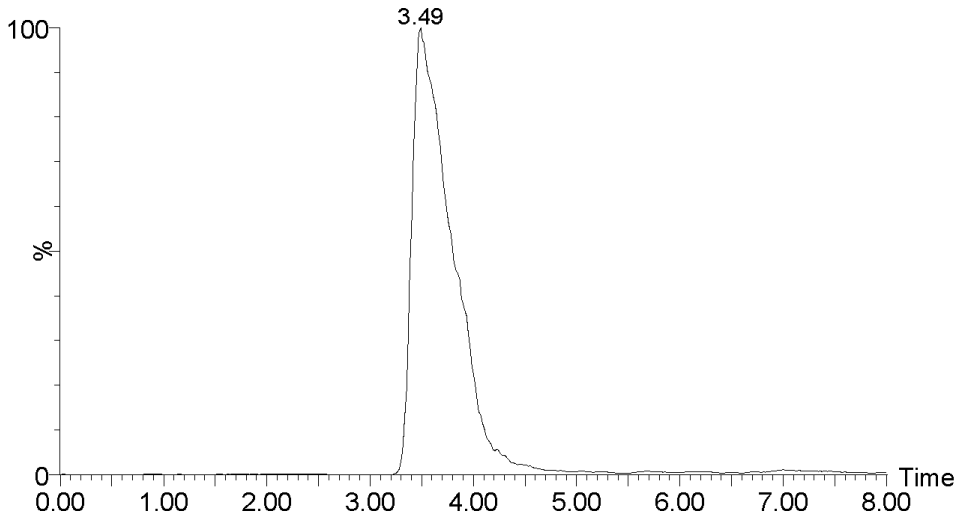

Extracted (Single) Ion Chromatogram (XIC) at 628 amu

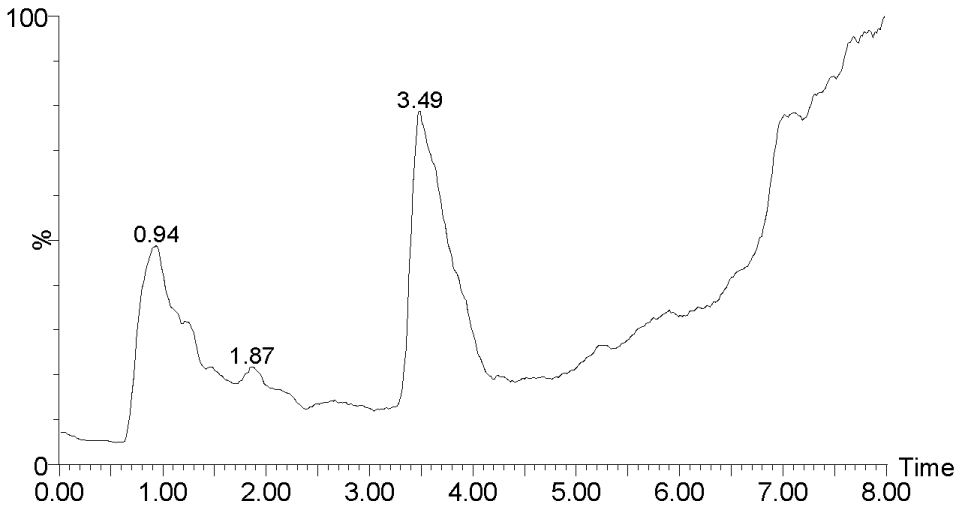

Total Ion Chromatogram (TIC) of **3**

Compound 4: Fmoc-Gln-dLys-Phe-Leu-NH_2 (SPPS intermediate tetrapeptide product of 18-4)

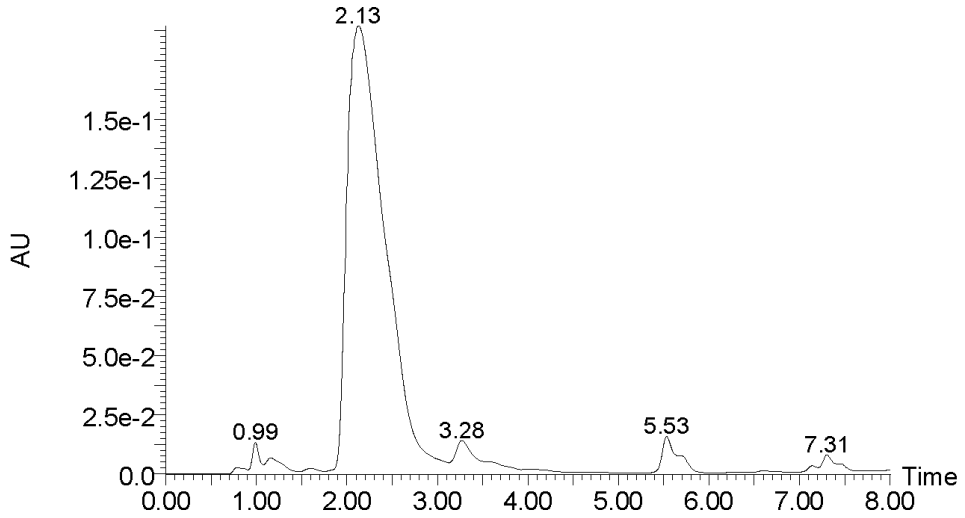

Single Wavelength Chromatogram of **4** at 263 nm of main peak at 2.13 min

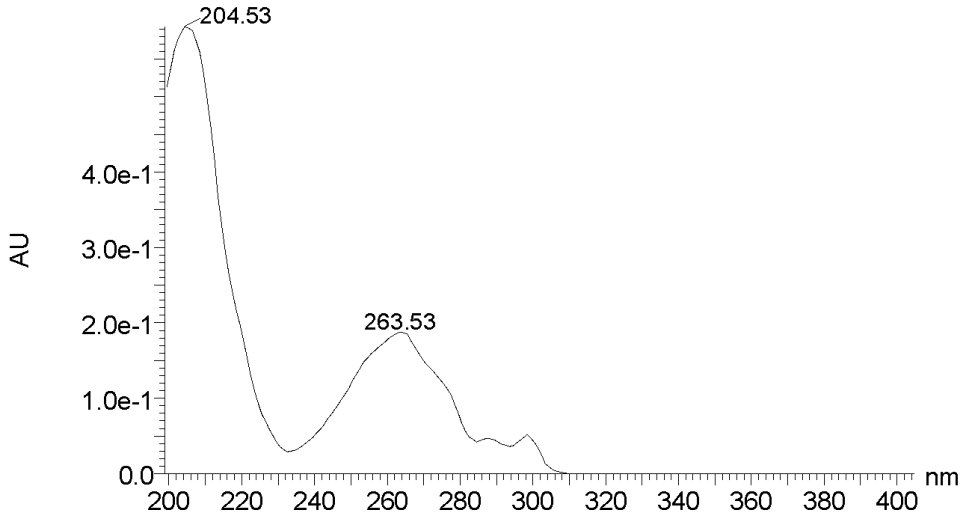

UV-Vis Diode array of **4** spectrum at 2.13 min with characteristic peak at 263 nm for Fmoc protecting group

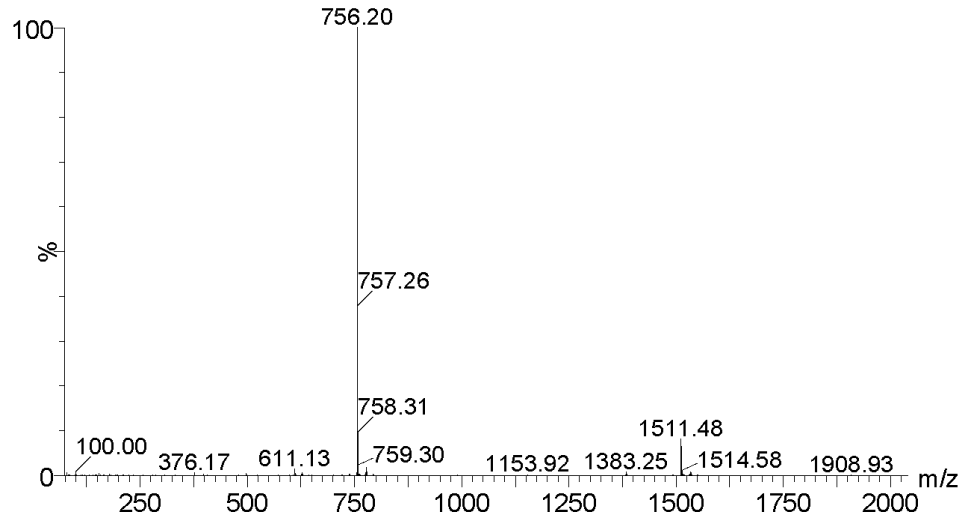

Positive Ion Mass spectrum of **4** at 2.13 min, product 756.20 m/z $[M+H]_+$

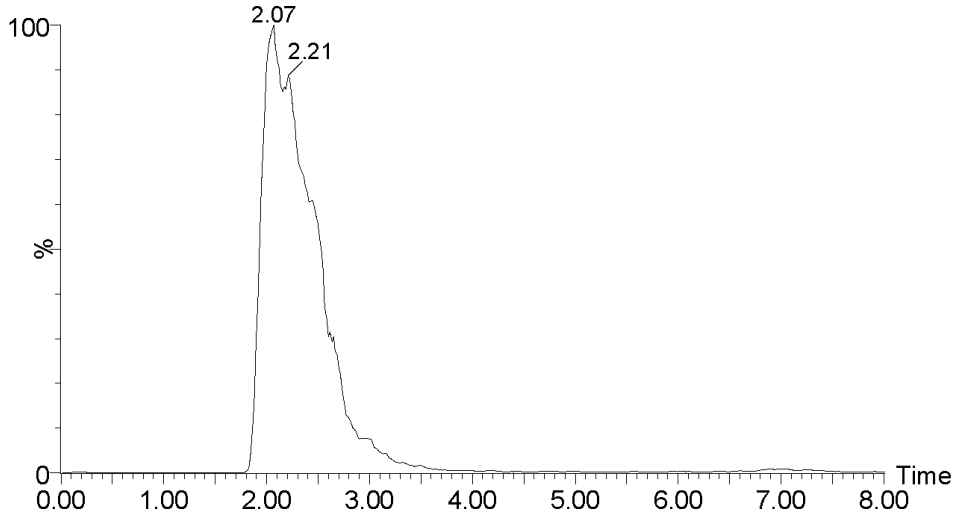

Extracted (Single) Ion Chromatogram (XIC) at 756 amu

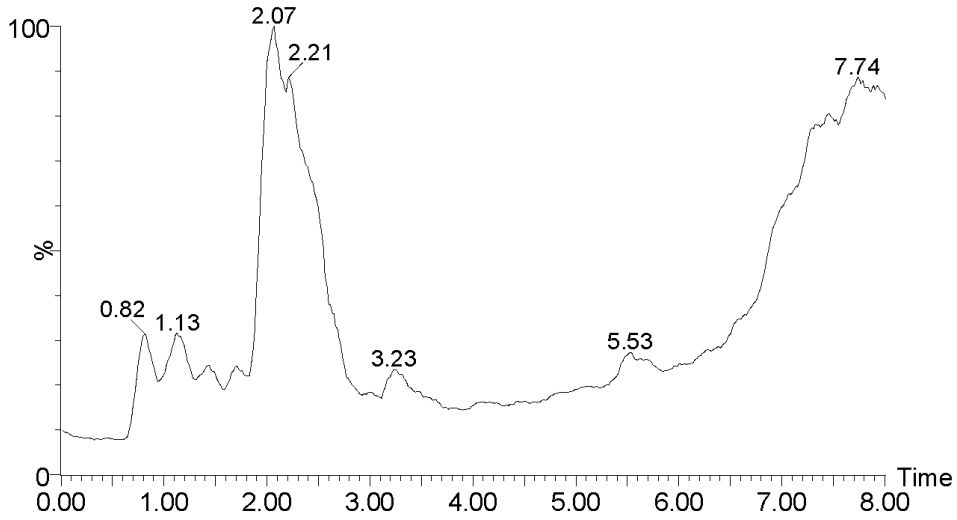

Total Ion Chromatogram (TIC) of **4**

Compound 5: Fmoc-Tyr Gln-dLys-Phe-Leu-NH_2 (SPPS intermediate pentapeptide product of 18-4)

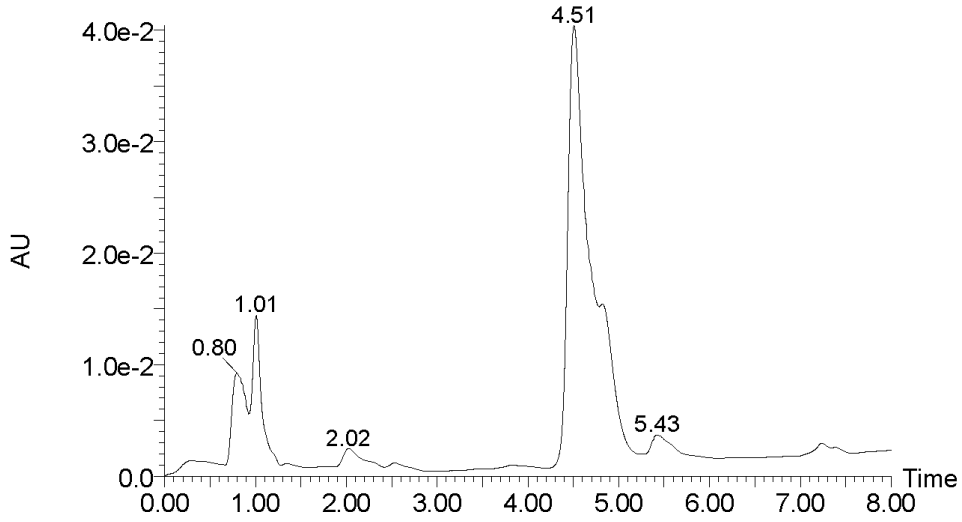

Single Wavelength Chromatogram of **5** at 263 nm of main peak at 4.51 min

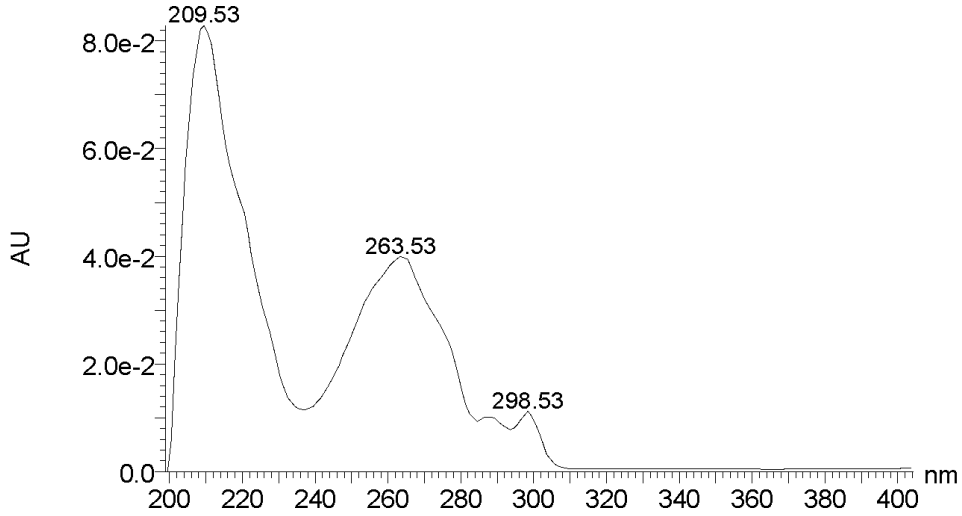

UV-Vis Diode array of **5** spectrum at 4.51 min with characteristic peak at 263 nm for Fmoc protecting group

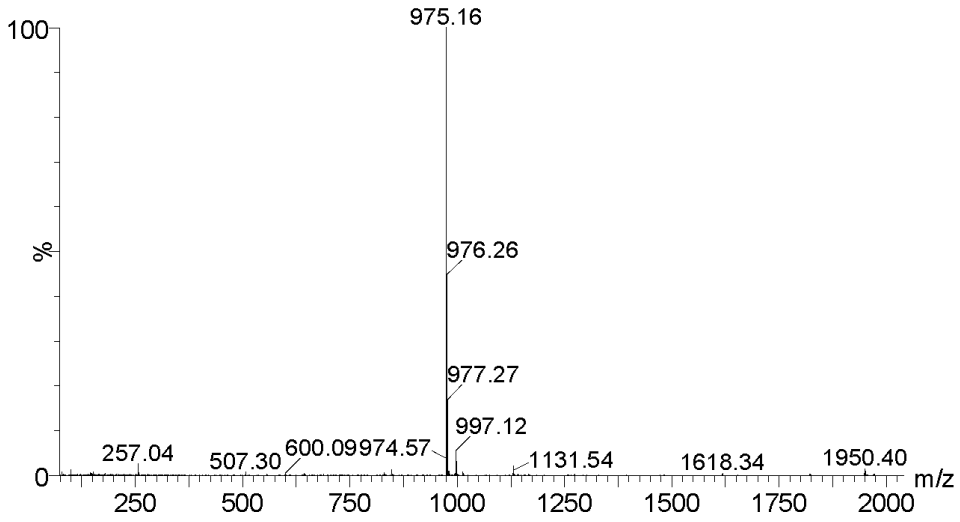

Positive Ion Mass spectrum of **5** at 4.51 min, product 975.16 m/z $[M+H]_+$

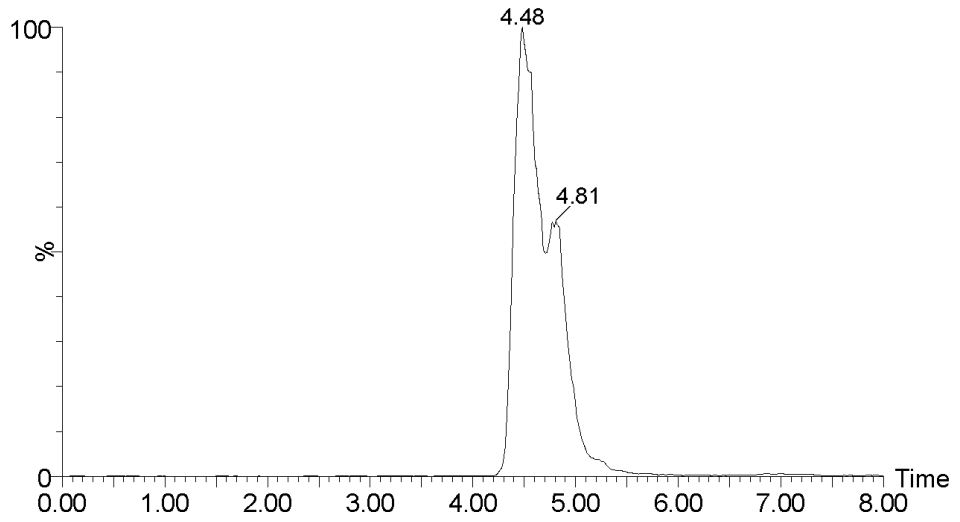

Extracted (Single) Ion Chromatogram (XIC) at 975 amu

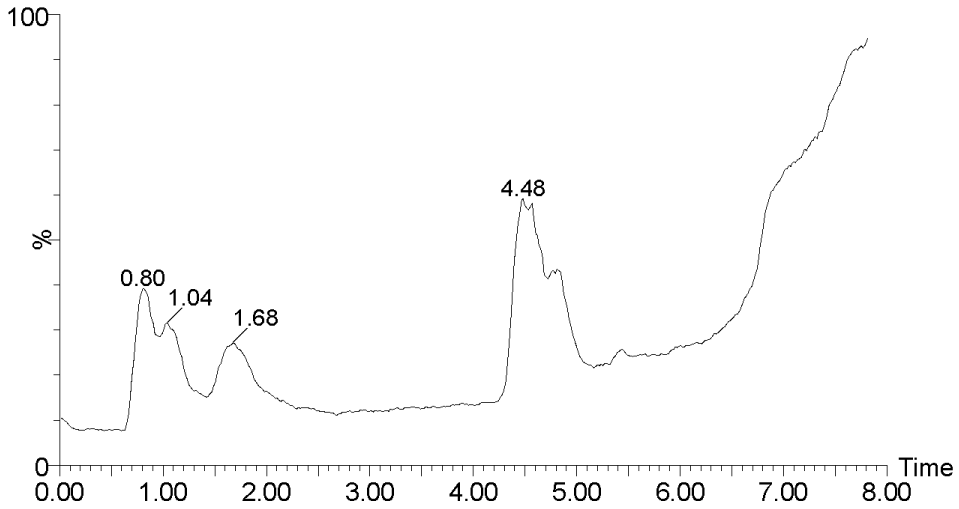

Total Ion Chromatogram (TIC) of **5**

Compound 6: Fmoc-Ala-Tyr Gln-dLys-Phe-Leu-NH_2 (SPPS intermediate hexapeptide product of 18-4)

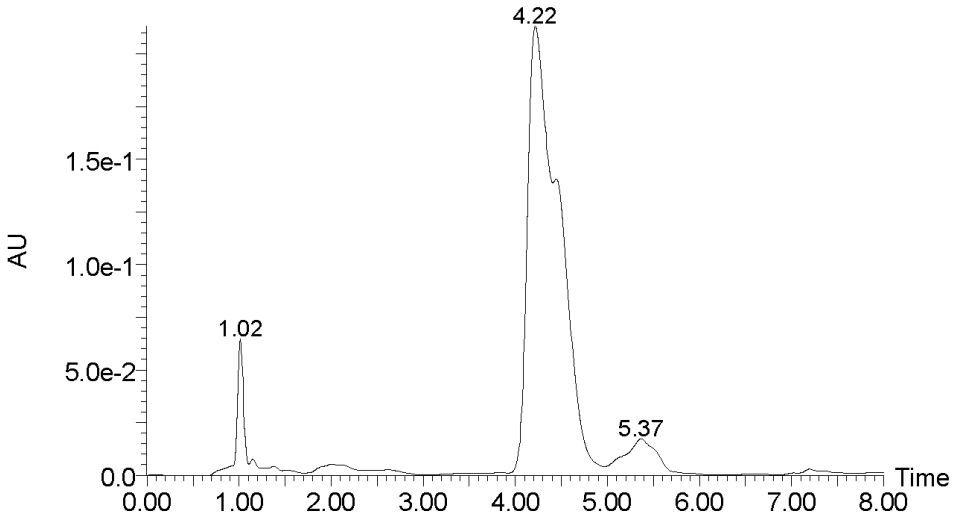

Single Wavelength Chromatogram of **6** at 263 nm of main peak at 4.22 min

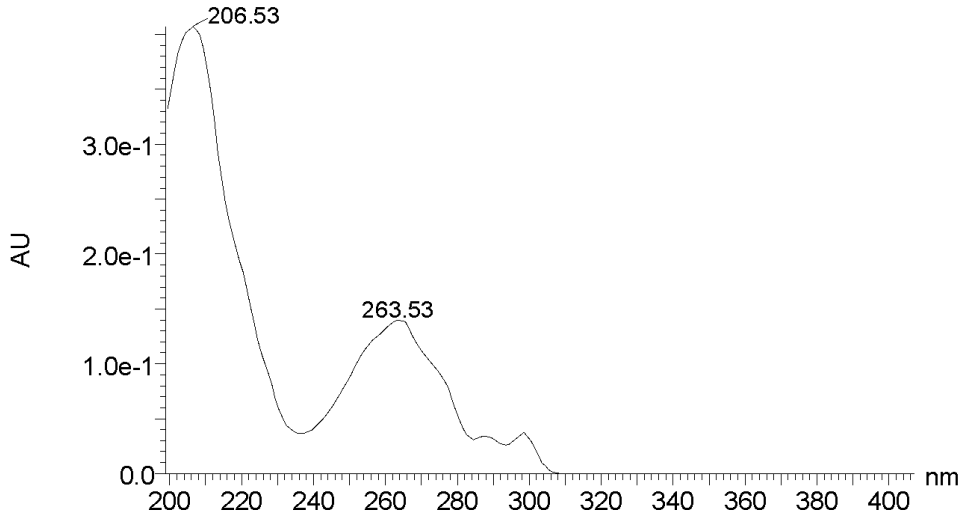

UV-Vis Diode array of **6** spectrum at 4.22 min with characteristic peak at 263 nm for Fmoc protecting group

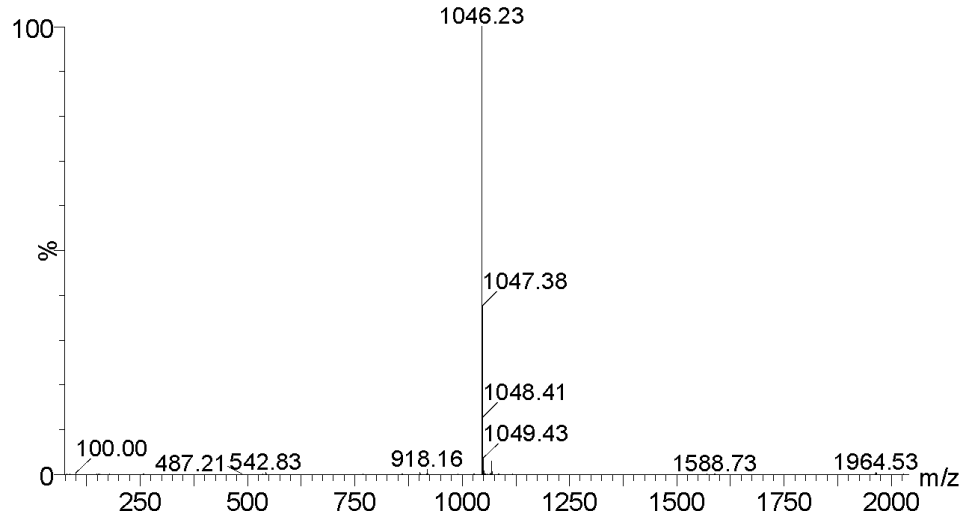

Positive Ion Mass spectrum of **6** at 4.22 min, product 1046.23 m/z $[M+H]_+$

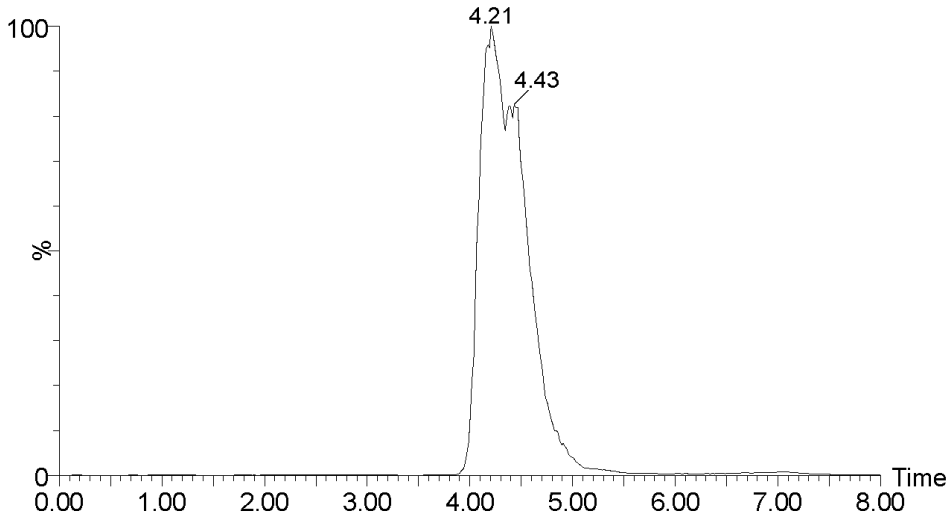

Extracted (Single) Ion Chromatogram (XIC) at 1046.23 amu

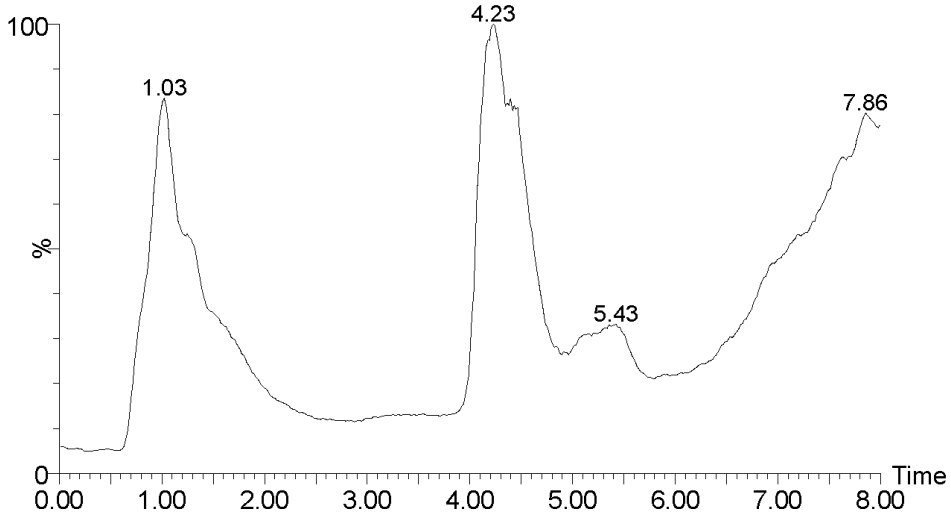

Total Ion Chromatogram (TIC) of **6**

Compound 7: Fmoc- Ala-Ala-Tyr Gln-dLys-Phe-Leu-NH_2 (SPPS intermediate heptapeptide product of 18-4)

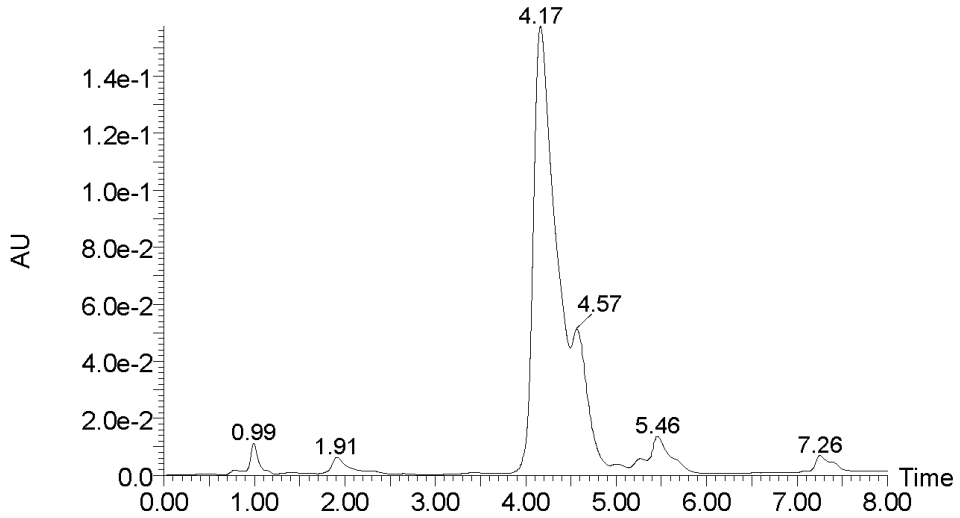

Single Wavelength Chromatogram of **7** at 263 nm of main peak at 4.17 min

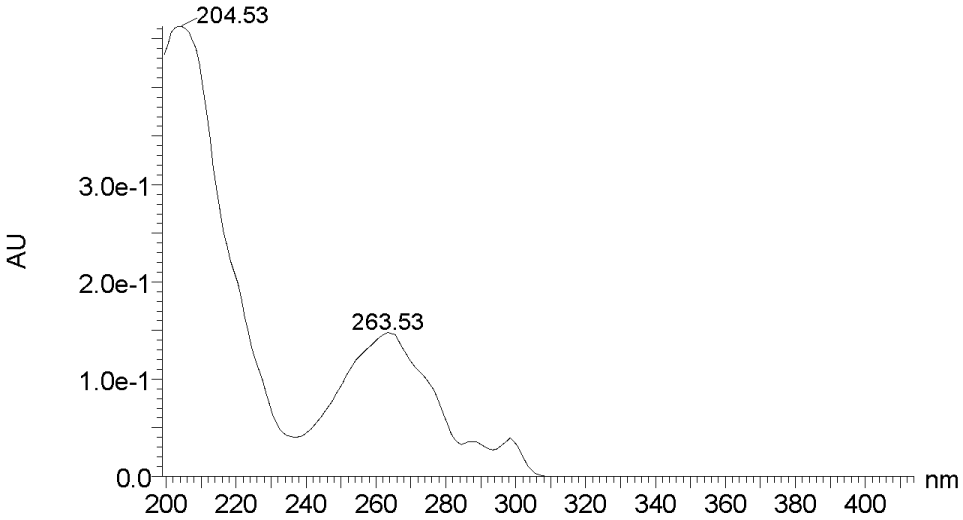

UV-Vis Diode array of **7** spectrum at 4.17 min with characteristic peak at 263 nm for Fmoc protecting group

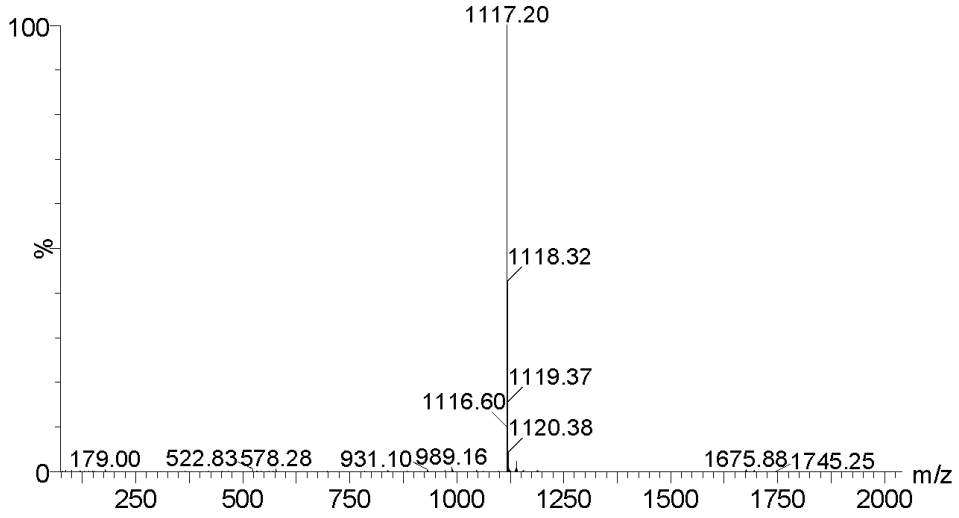

Positive Ion Mass spectrum of **7** at 4.17 min, product 1117.20 m/z $[M+H]_+$

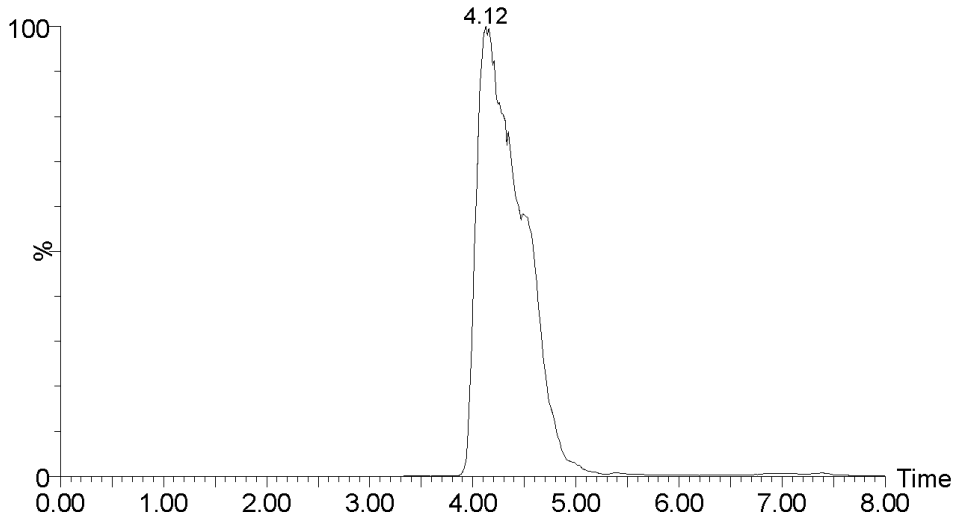

Extracted (Single) Ion Chromatogram (XIC) at 1117.20 amu

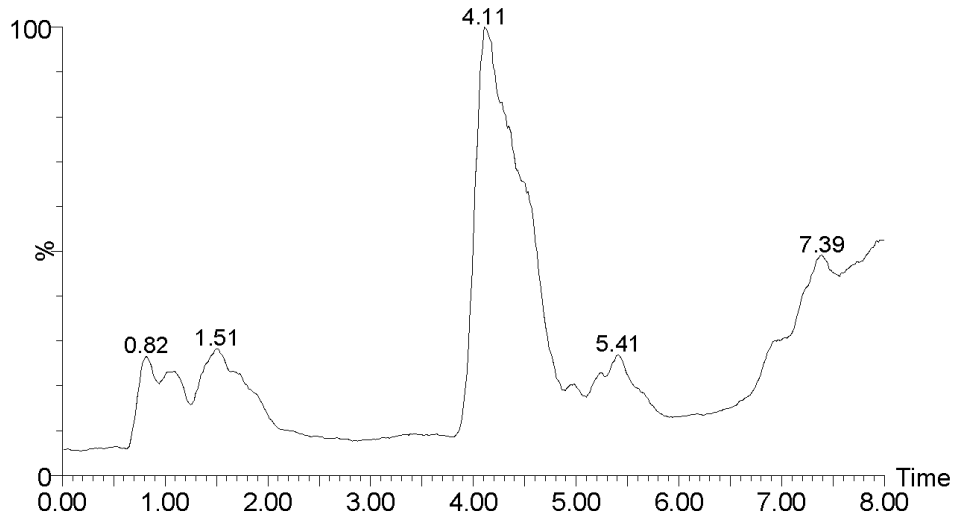

Total Ion Chromatogram (TIC) of **7**

Compound 8: Fmoc- Glu-Ala-Ala-Tyr Gln-dLys-Phe-Leu-NH_2 (SPPS intermediate octapeptide product of 18-4)

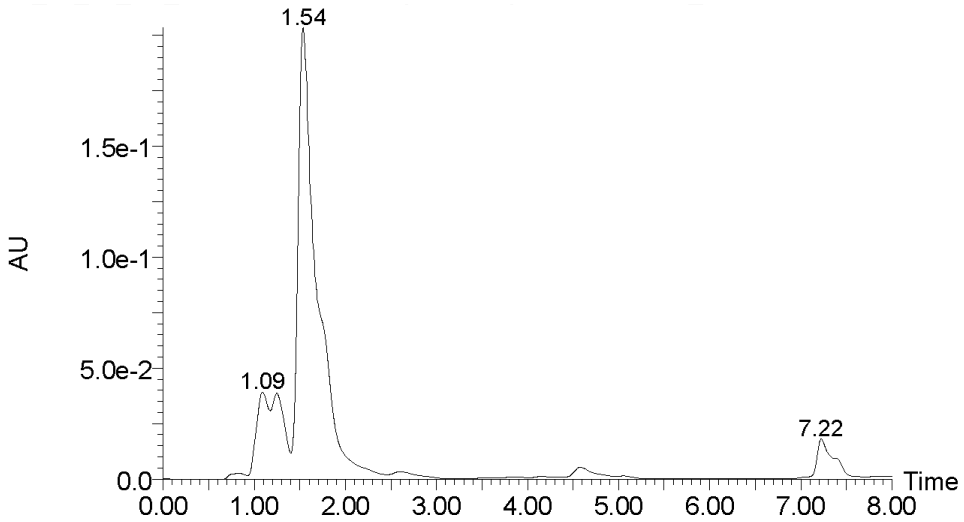

Single Wavelength Chromatogram of **8** at 263 nm of main peak at 1.54 min

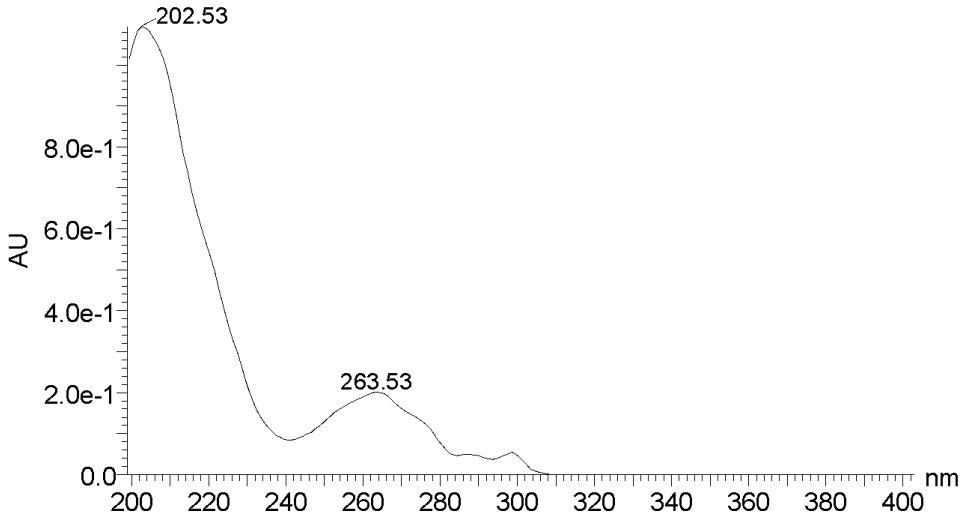

UV-Vis Diode array of **8** spectrum at 1.54 min with characteristic peak at 263 nm for Fmoc protecting group

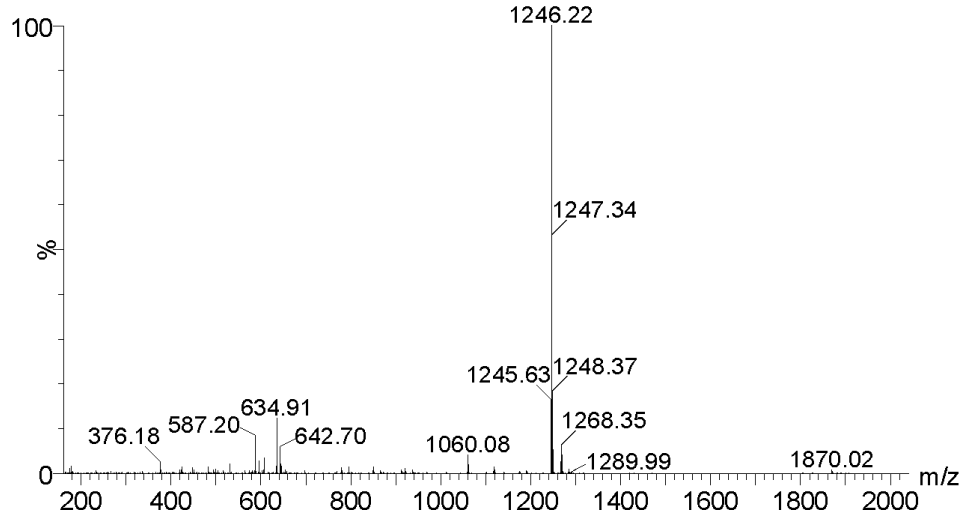

Positive Ion Mass spectrum of **8** at 1.54 min, product 1246.22 m/z $[M+H]_+$

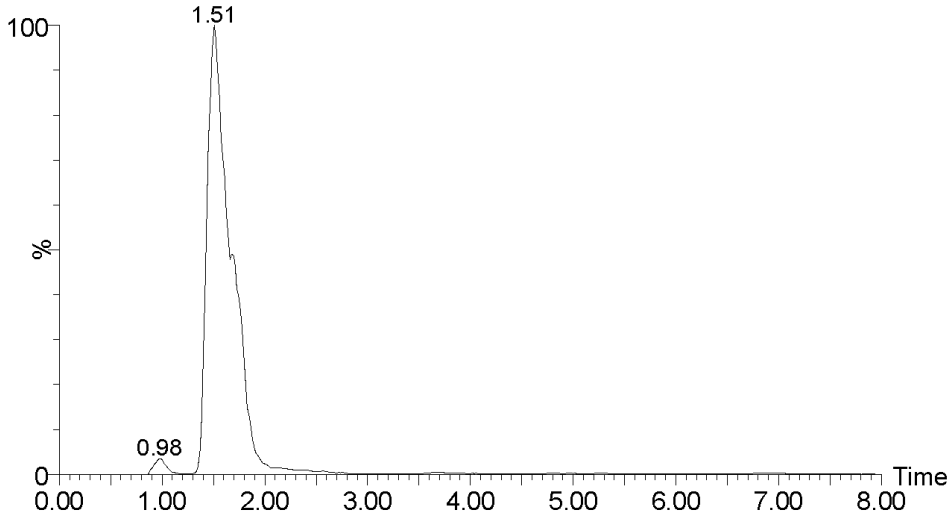

Extracted (Single) Ion Chromatogram (XIC) at 1246.22 amu

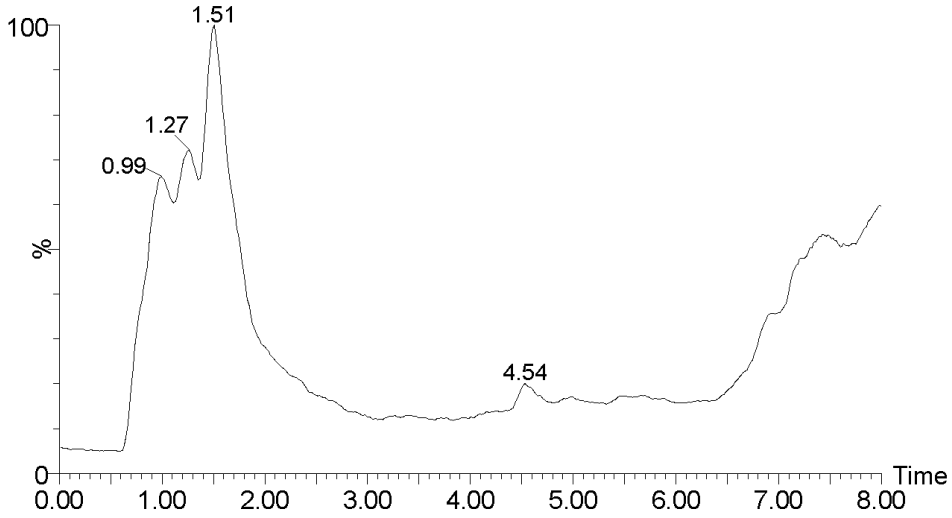

Total Ion Chromatogram (TIC) of **8**

Compound 9: Fmoc-dNle-Glu-Ala-Ala-Tyr Gln-dLys-Phe-Leu-NH_2 (SPPS intermediate nonapeptide product of 18-4)

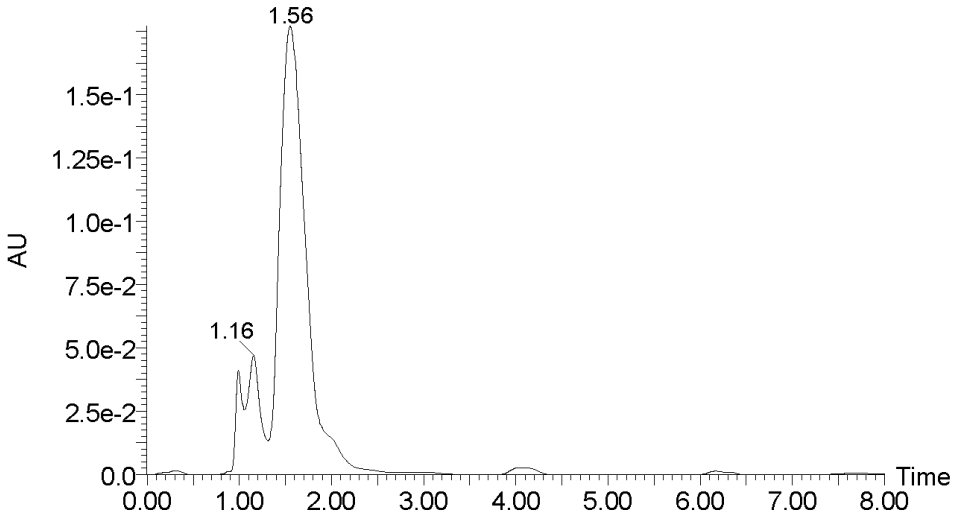

Single Wavelength Chromatogram of **9** at 263 nm of main peak at 1.56 min

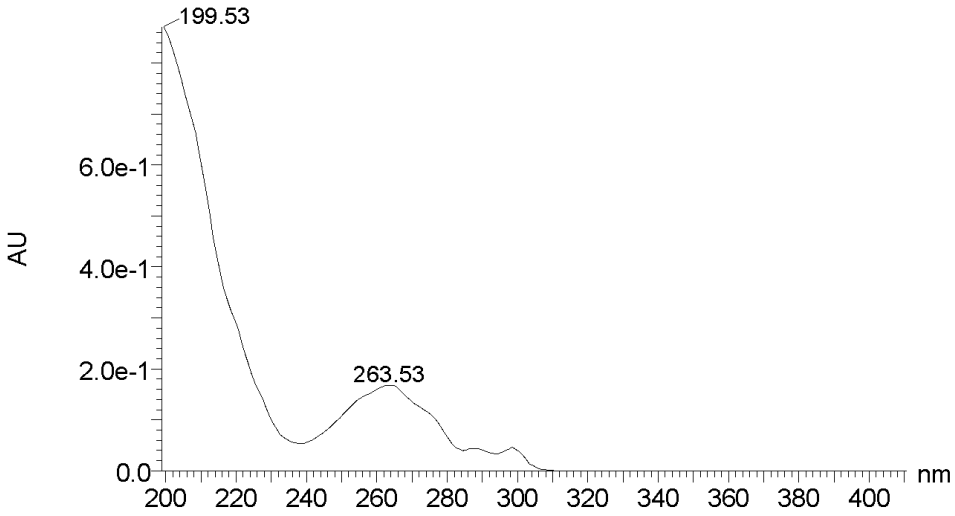

UV-Vis Diode array of **9** spectrum at 1.56 min with characteristic peak at 263 nm for Fmoc protecting group

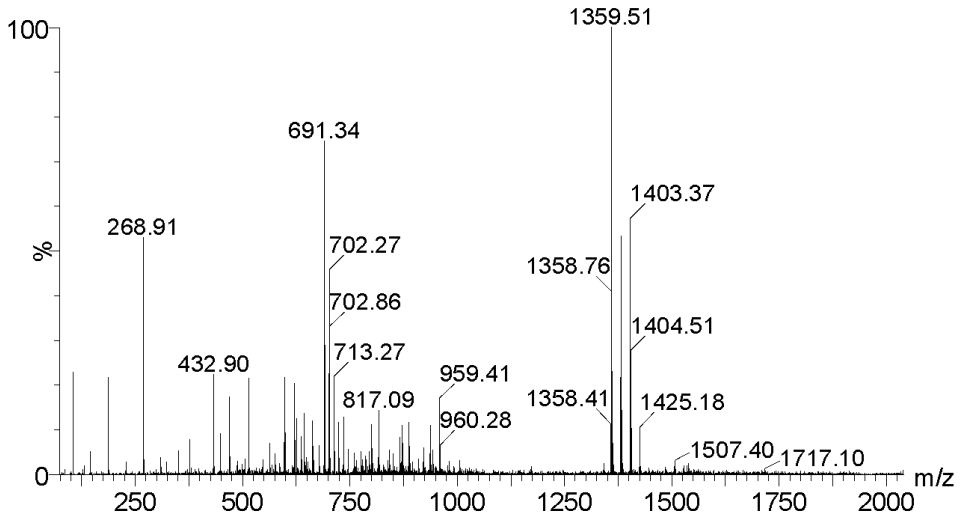

Positive Ion Mass spectrum of **9** at 1.56 min, product 1359.38 m/z $[M+H]_+$

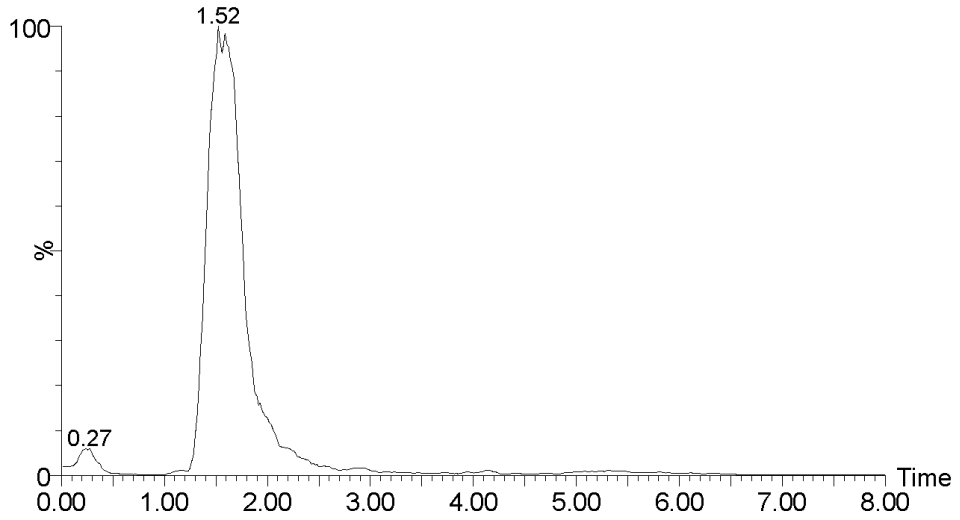

Extracted (Single) Ion Chromatogram (XIC) at 1359.38 amu

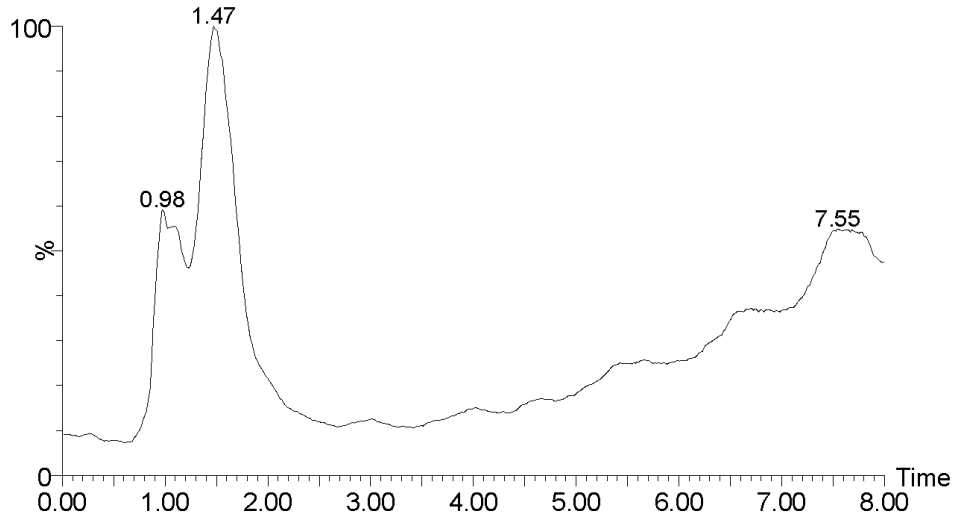

Total Ion Chromatogram (TIC) of **9**

Compound 10: Fmoc-trp-dNle-Glu-Ala-Ala-Tyr Gln-dLys-Phe-Leu-NH_2 (SPPS decapeptide product of 18-4)

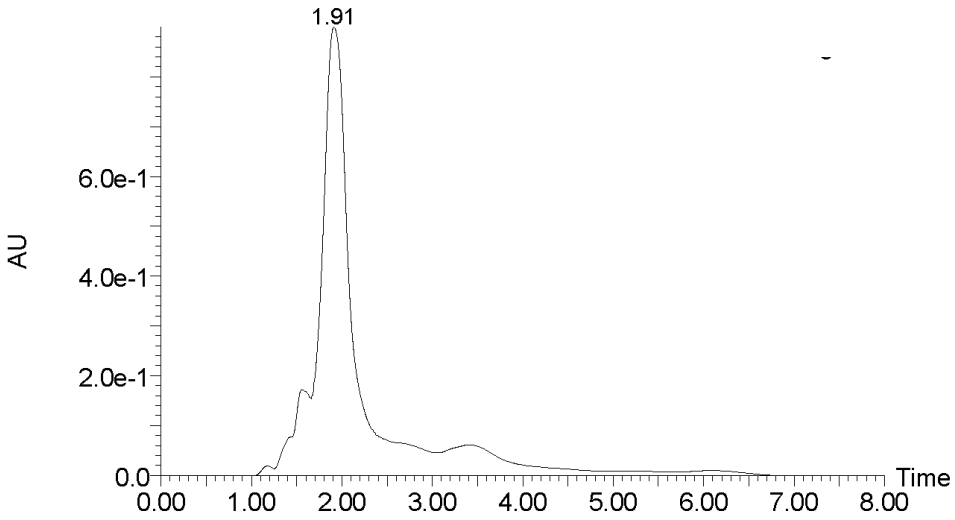

Single Wavelength Chromatogram of **10** at 263 nm of main peak at 1.91 min

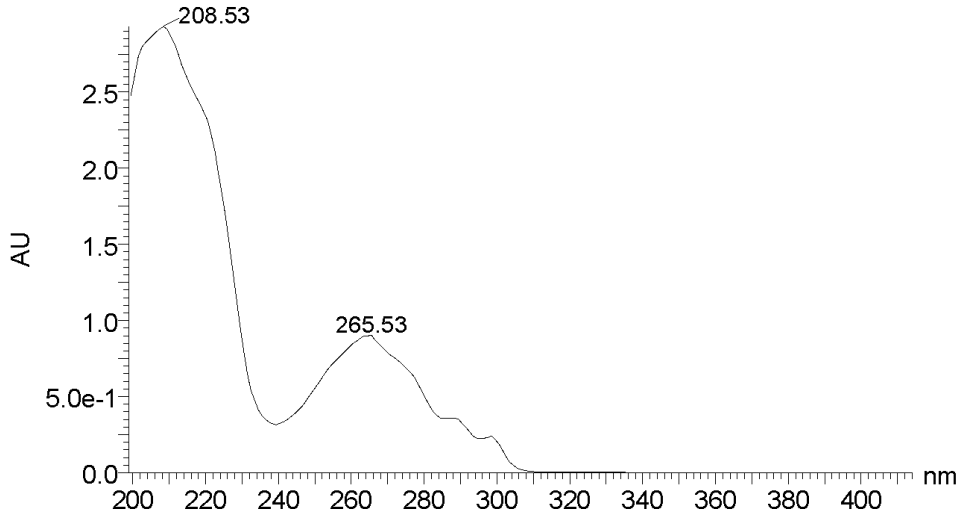

UV-Vis Diode array of **10** spectrum at 1.91 min with characteristic peak at 263 nm for Fmoc protecting group

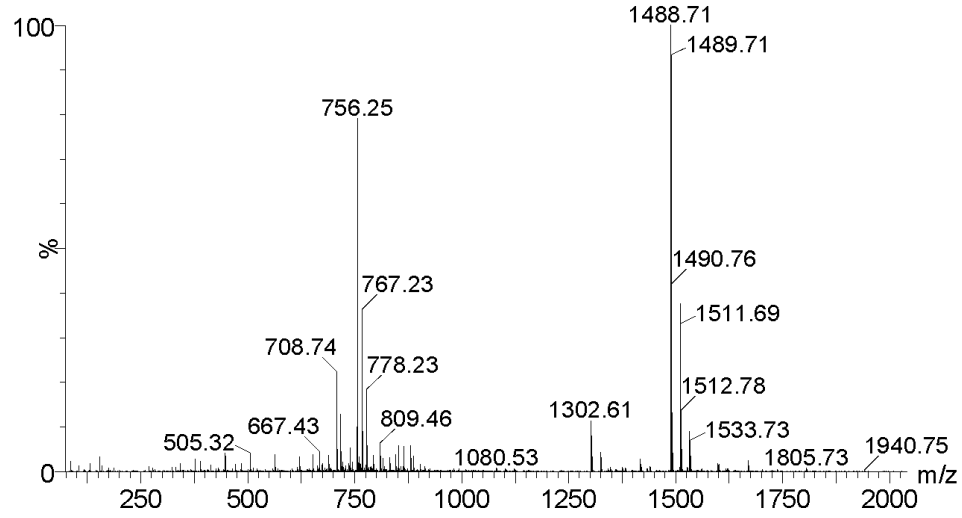

Positive Ion Mass spectrum of **10** at 1.91 min, product 1489.71 m/z $[M+H]_+$, 756.25 m/z $(M+2H^+)/2$, No protecting group on the 18-4

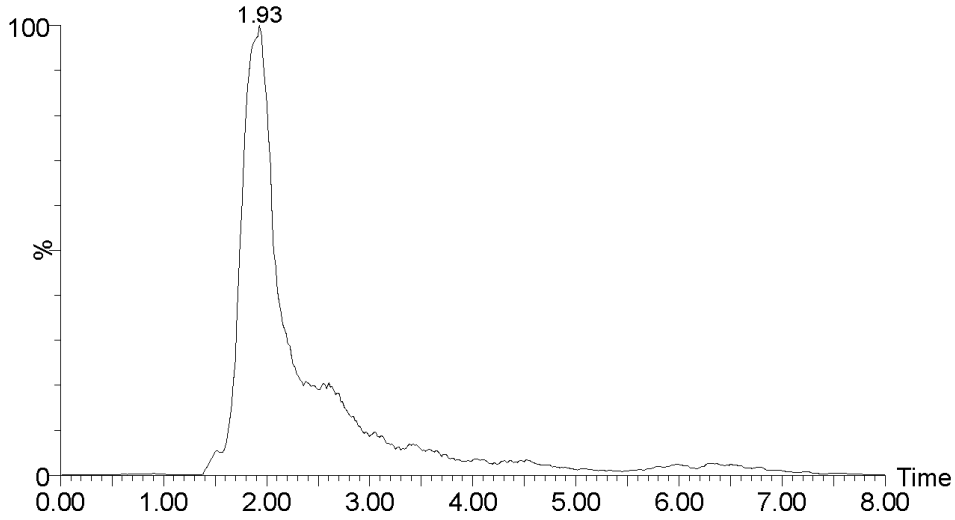

Extracted (Single) Ion Chromatogram (XIC) at 1488.70 amu

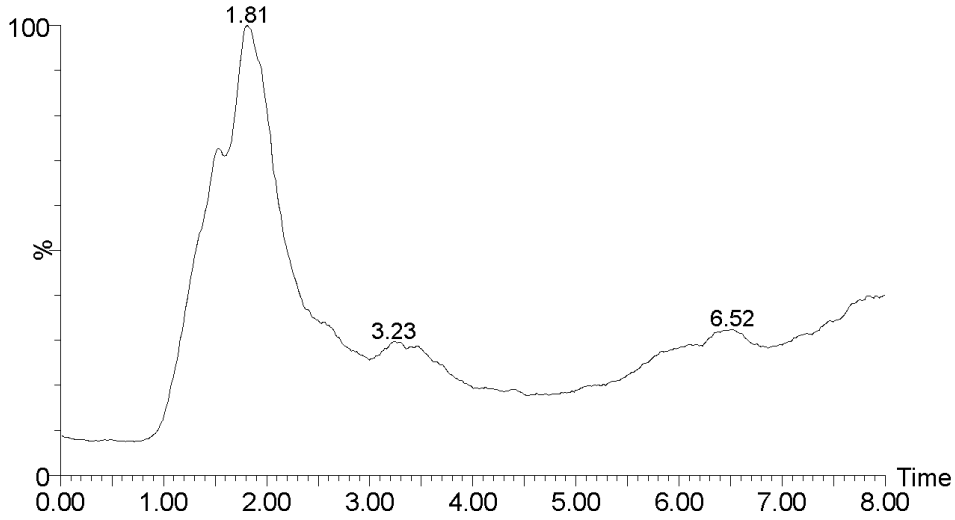

Total Ion Chromatogram (TIC) of **10**

Compound 11: Fmoc-trp-dNle-Glu-Ala-Ala-Tyr(tBu)-Gln-dLys-Phe-Leu-NH_2 (SPPS decapeptide product of 18-4)

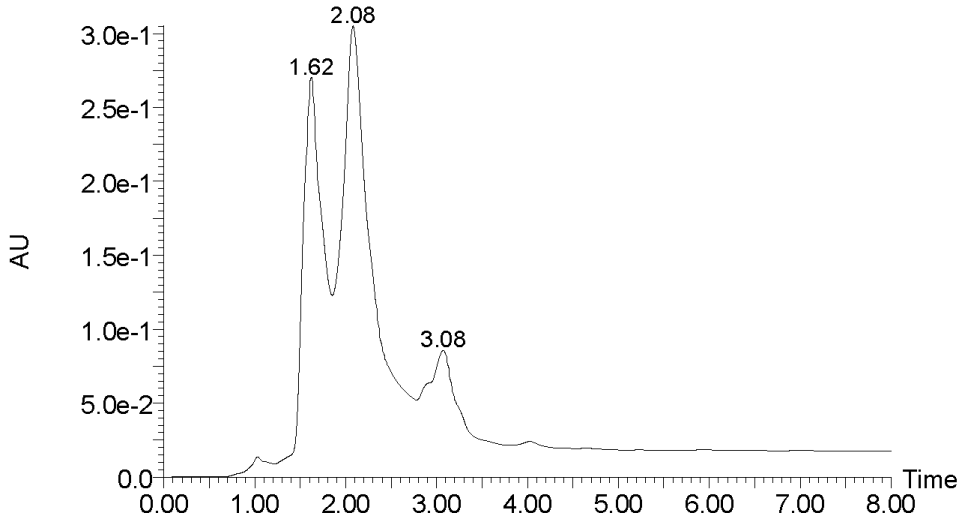

Single Wavelength Chromatogram of **11** at 263 nm of main peak at 2.08 min

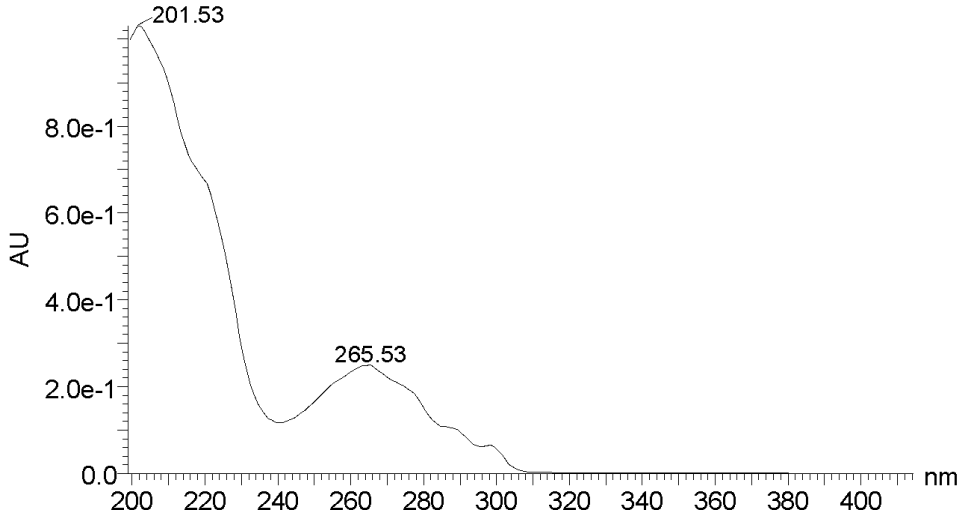

UV-Vis Diode array of **11** spectrum at 2.08 min with characteristic peak at 263 nm for Fmoc protecting group

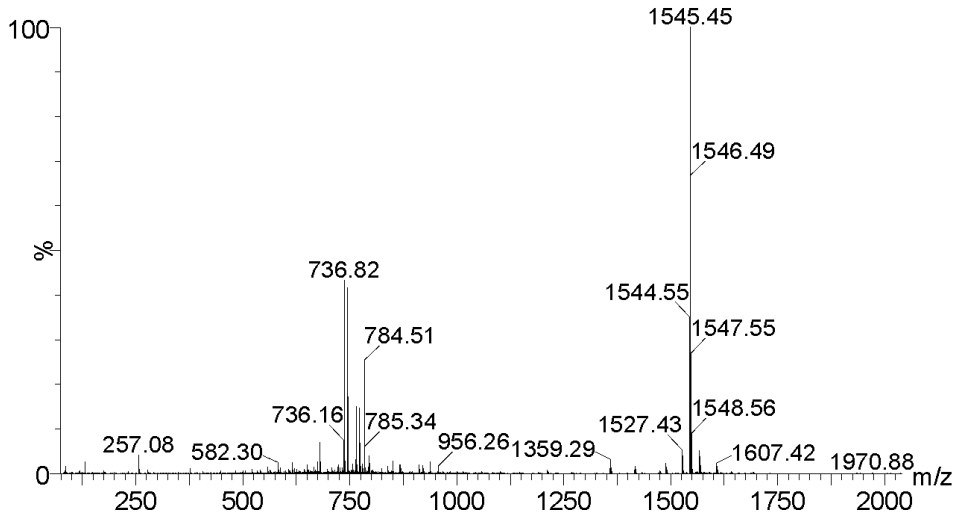

Positive Ion Mass spectrum of **11** at 2.08 min, product 1545.44 m/z $[M+H]_+$, 736.82 m/z $(M+2H^+)/2$, tButyl protecting group on tyrosine

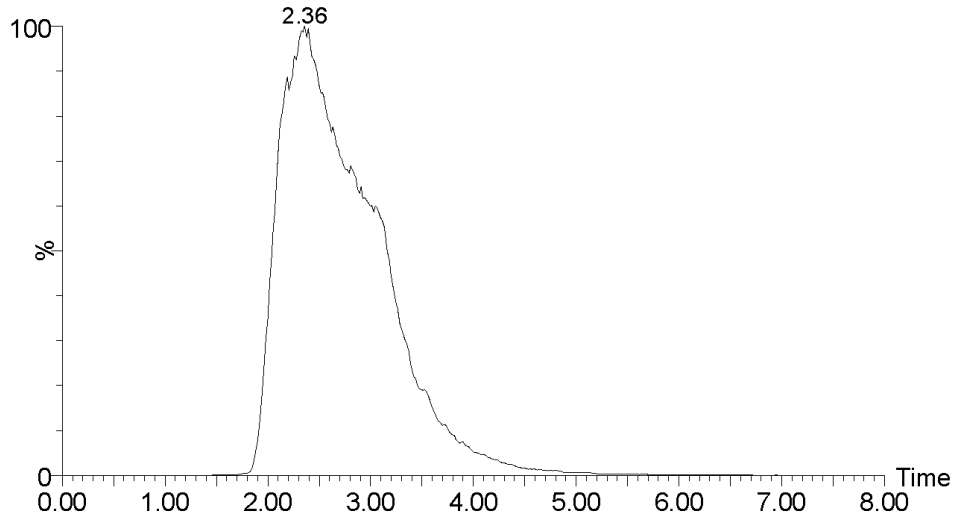

Extracted (Single) Ion Chromatogram (XIC) at 1545.44 amu

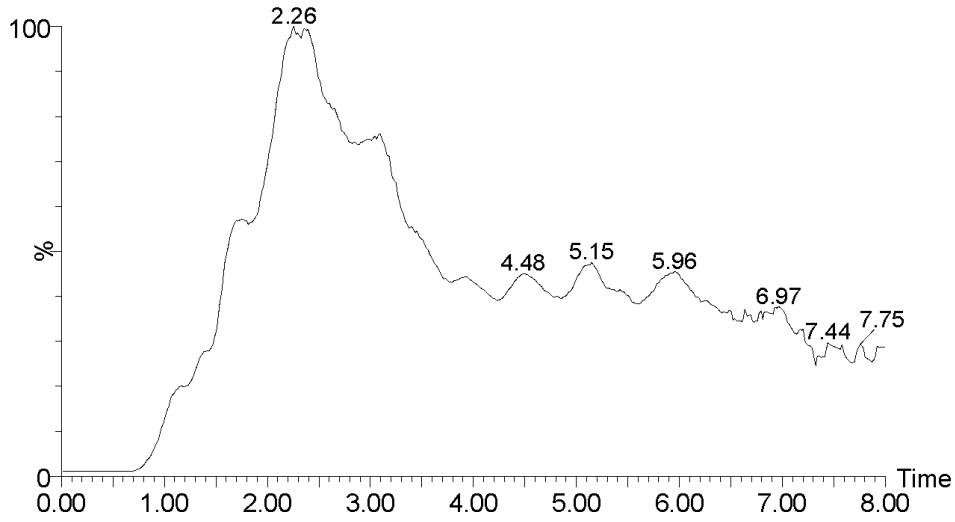

Total Ion Chromatogram (TIC) of **11**

Compound 12: NH_2-trp-dNle-Glu-Ala-Ala-Tyr(tBu)-Gln-dLys-Phe-Leu-NH_2 (SPPS decapeptide product of 18-4)

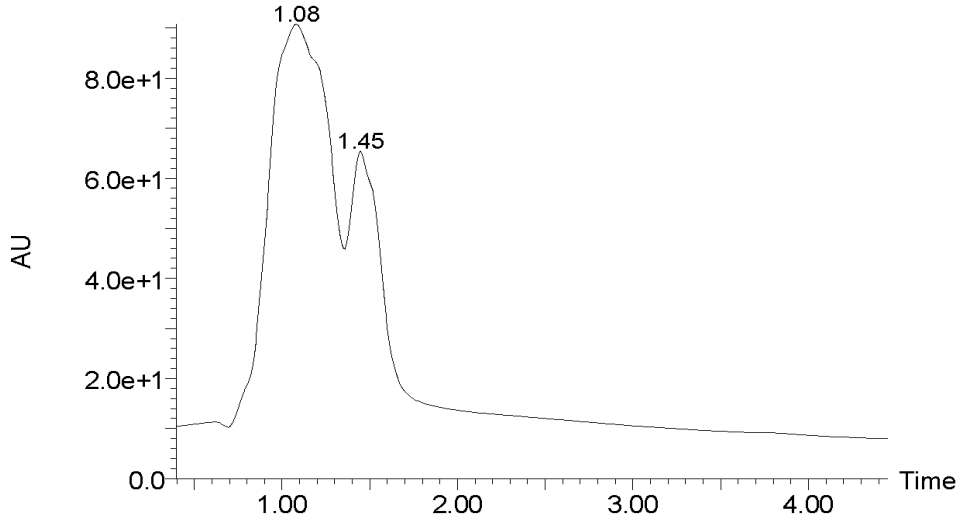

Single Wavelength Chromatogram of **12**, main peak at 1.45 min

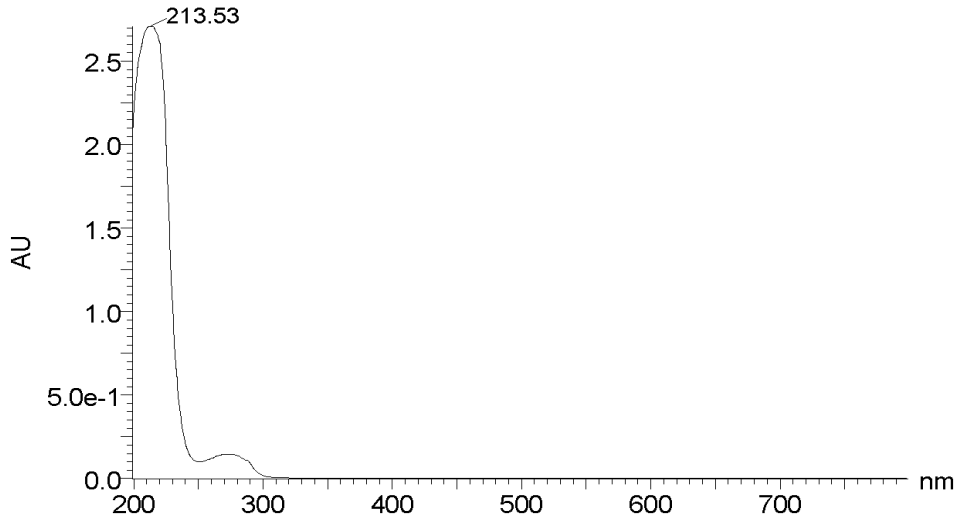

UV-Vis Diode array of **12** spectrum at 1.45 min with no characteristic peak at 263 nm for Fmoc protecting group, Tryptophan and Tyrosine absorb at 270 nm

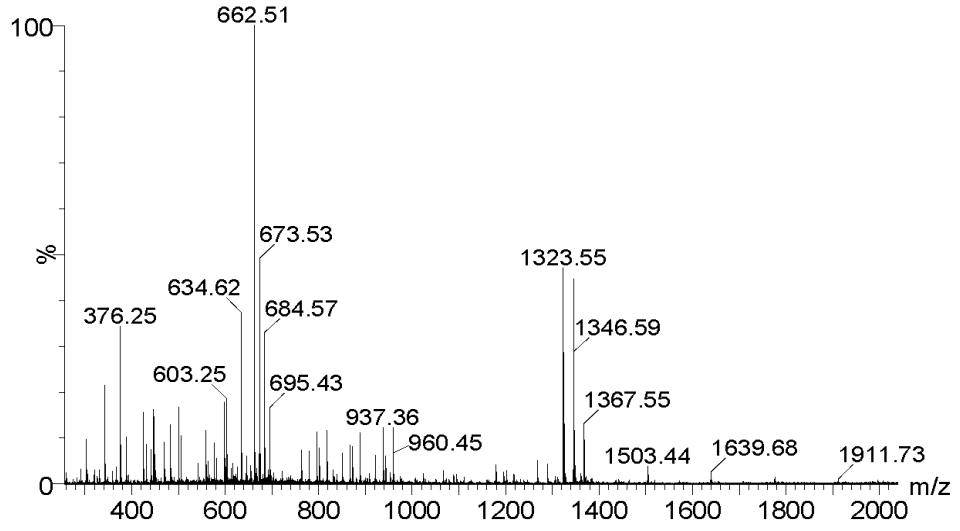

Positive Ion Mass spectrum of **12** at 1.45 min, product 1323.55 m/z $[M+H]_{+}$, 662.51 m/z $(M+2H^{+})/2$, tButyl protecting group on tyrosine

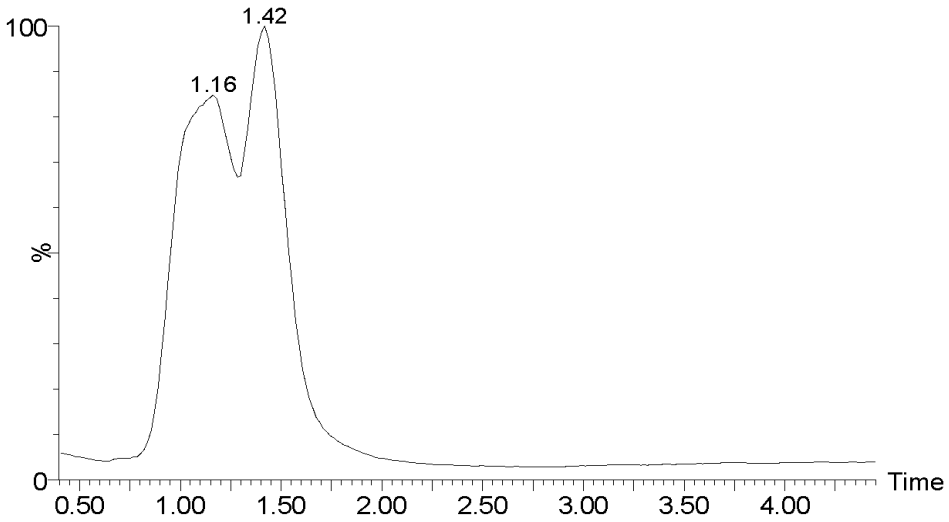

Extracted (Single) Ion Chromatogram (XIC) at 1323.55 amu

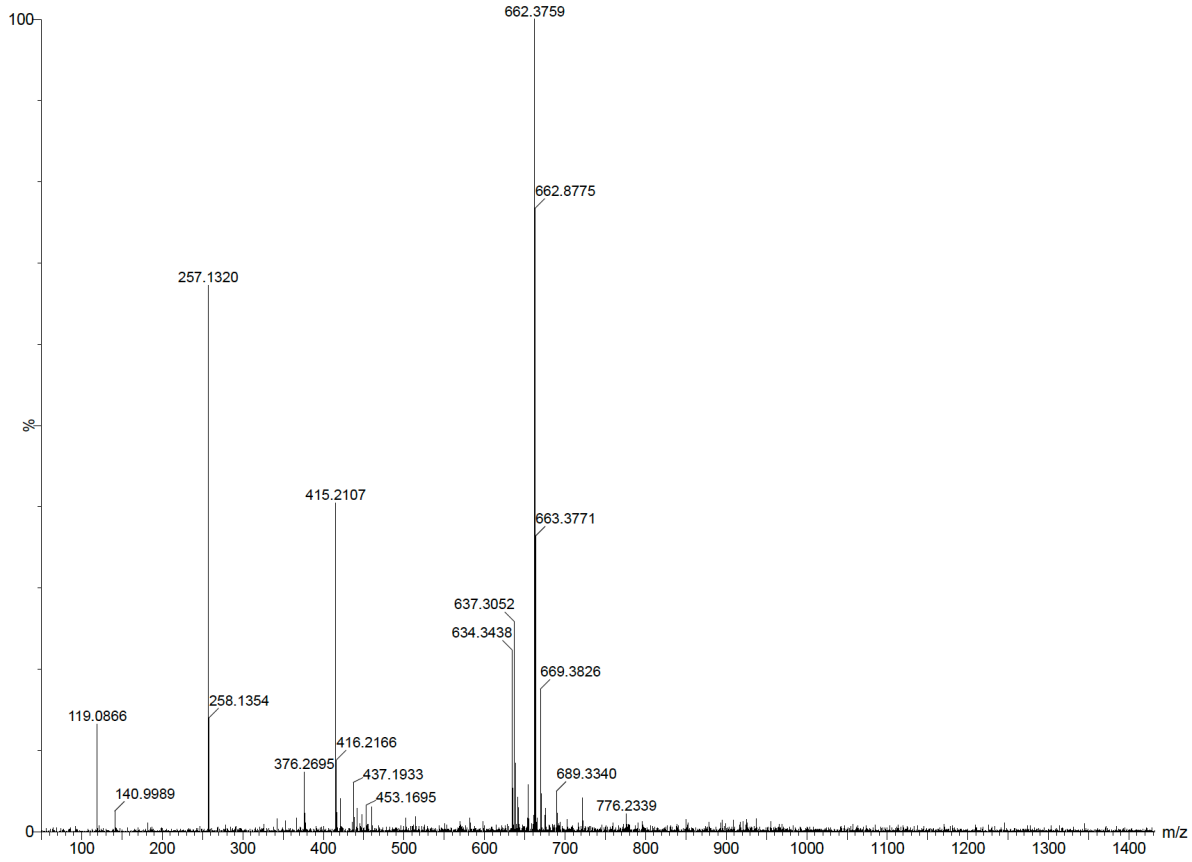

HRMS Positive Ion Mass Spectra of product **12** (Calc. MW 1322.73869, ½ mass 662.37729, Found 662.3759)

Compound 13: Fmoc-Gd(DOTA)-trp-dNle-Glu-Ala-Ala-Tyr(tBu)-Gln-dLys-Phe-Leu-NH_2 (Single Modal TMIA for MRI)

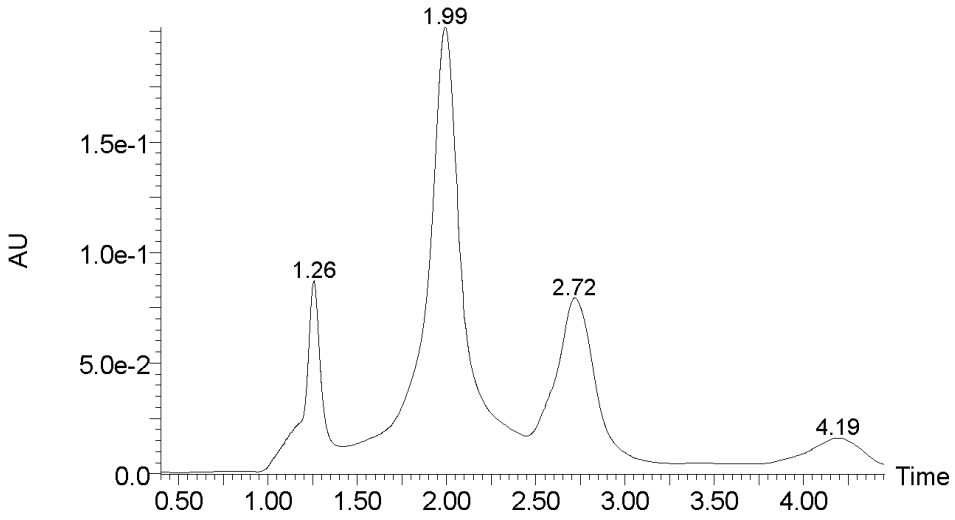

Single Wavelength Chromatogram of **13**, main peak at 1.99 min

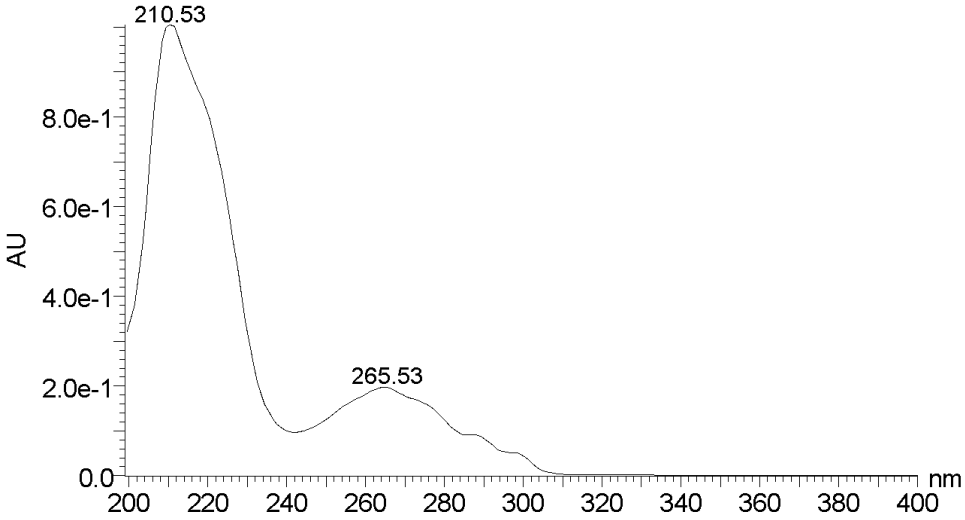

UV-Vis Diode array of **13** spectrum at 1.99 min with characteristic peak at 265 nm for Fmoc protecting group

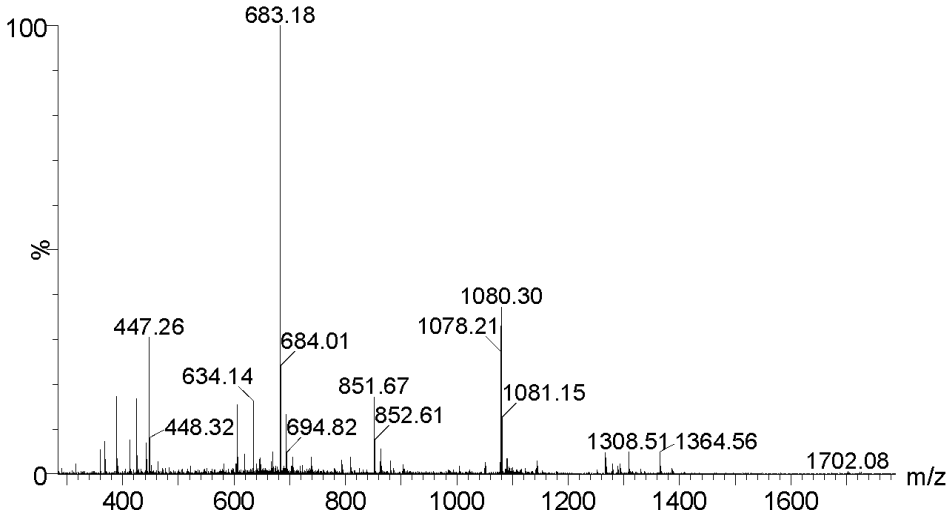

Positive Ion Mass spectrum of **13** at 1.99 min, product 1080.30 m/z $(M+2H^+)/2$

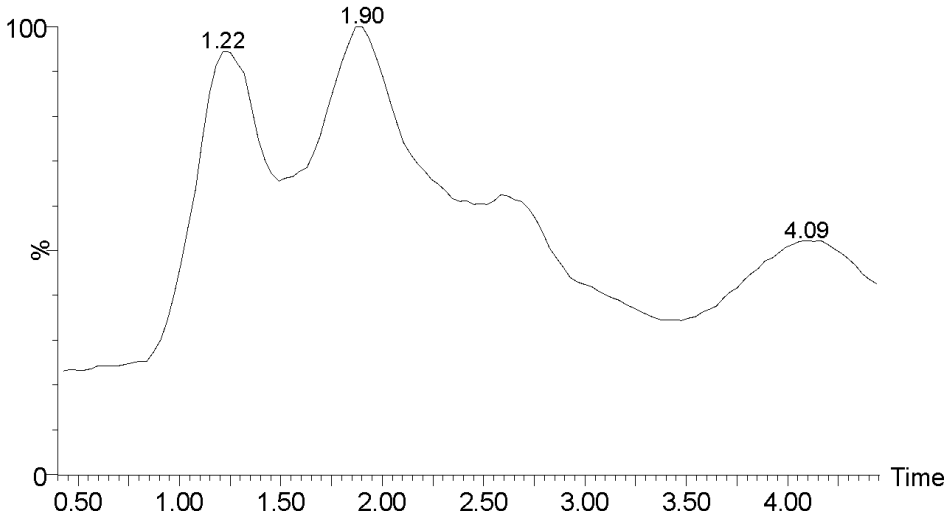

Extracted (Single) Ion Chromatogram (XIC) at 1080 amu

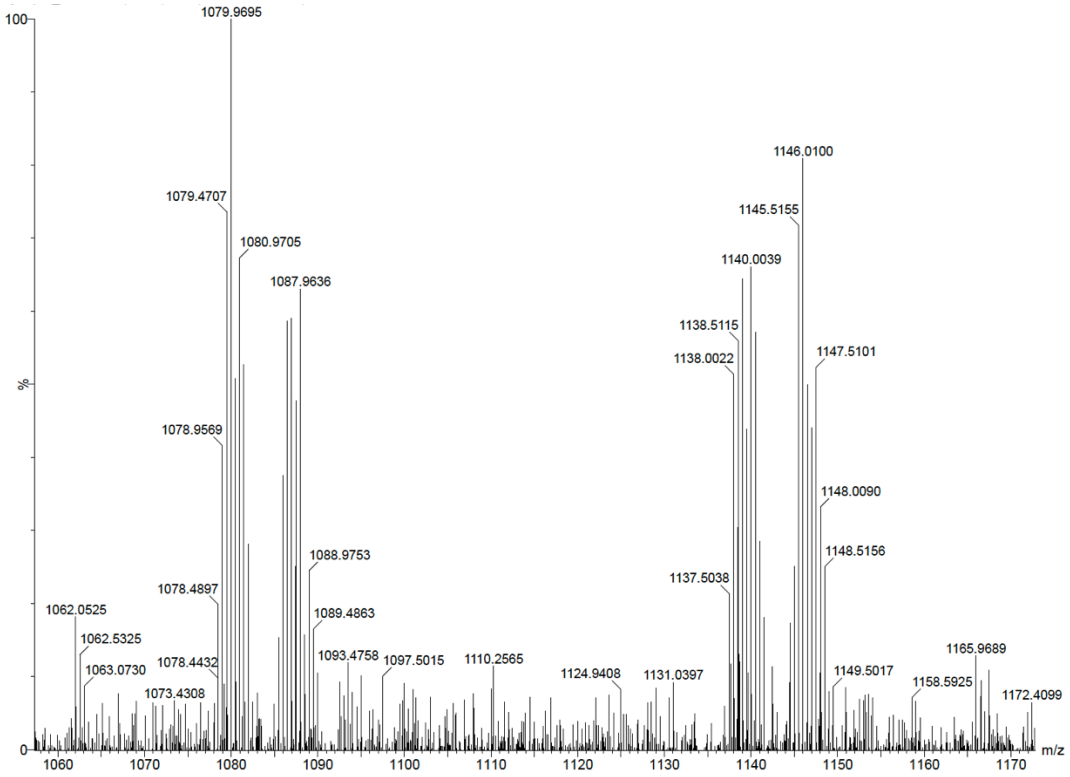

HRMS Positive Ion Mass Spectra of product **13** (Calc. MW 2157.91992, ½ mass 1079.96790, Found 1079.9695 m/z $(M+2H^+)/2$), water adduct also seen at 1087.9636 m/z)

Compound 14: NH_2-Gd (DOTA)-trp-dNle-Glu-Ala-Ala-Tyr(tBu)-Gln-dLys-Phe-Leu-NH_2 (Single Modal TMIA for MRI)

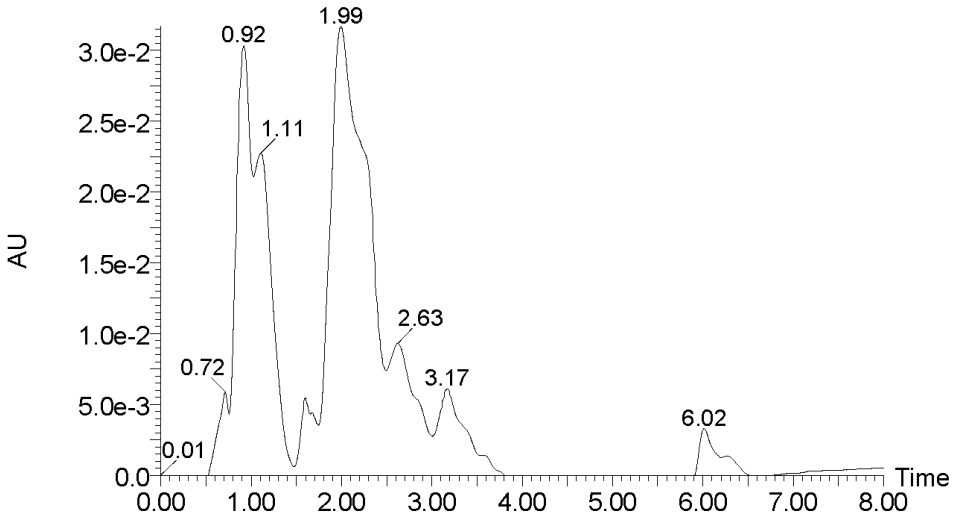

Single Wavelength Chromatogram of **14**, main peak at 1.99 min

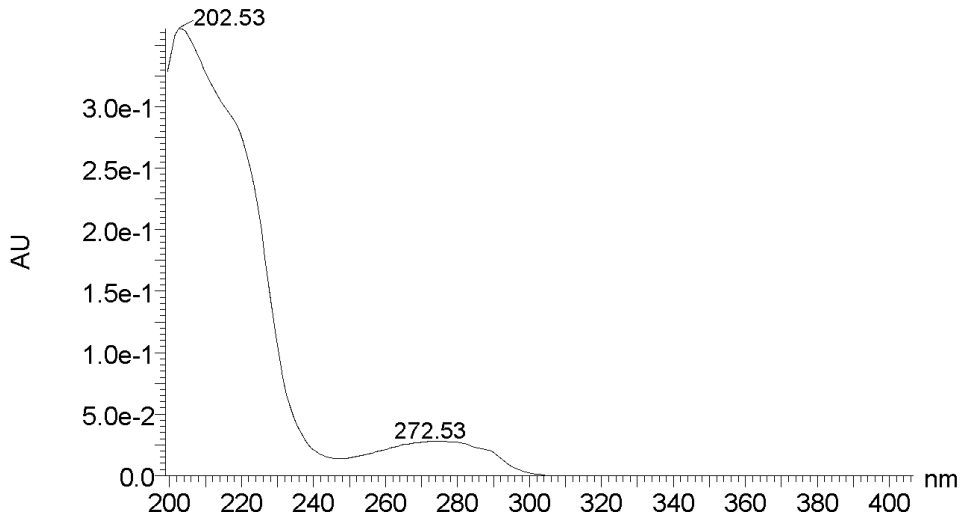

UV-Vis Diode array of **14** spectrum at 1.99 min with no characteristic peak at 263 nm for Fmoc protecting group, Tryptophan and Tyrosine absorb at 270 nm

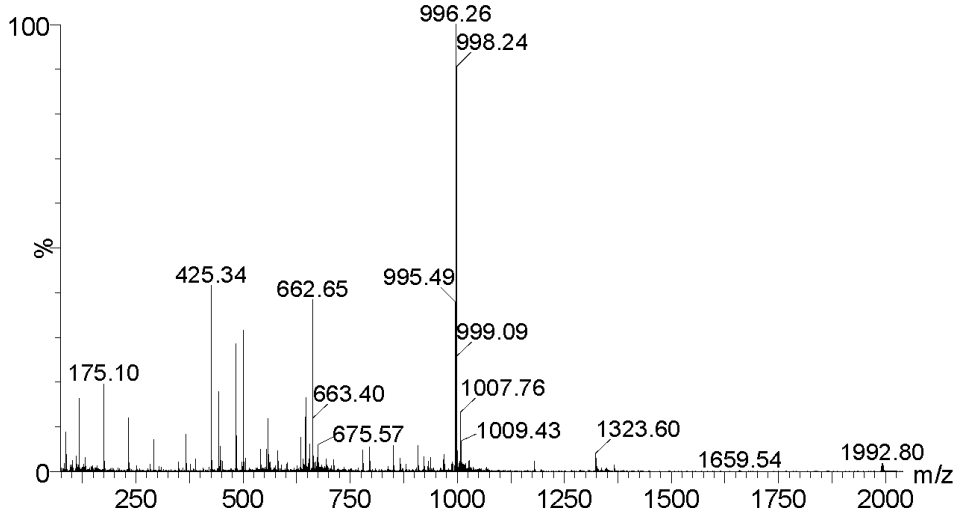

Positive Ion Mass spectrum of **14** at 1.99 min, product 996.26 m/z $(M+2H^+)/2$

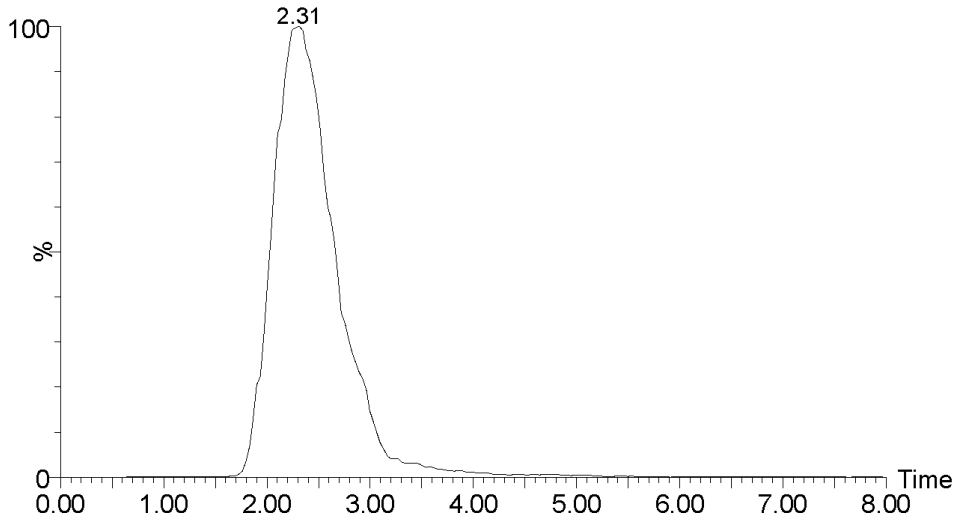

Extracted (Single) Ion Chromatogram (XIC) at 996.26 amu

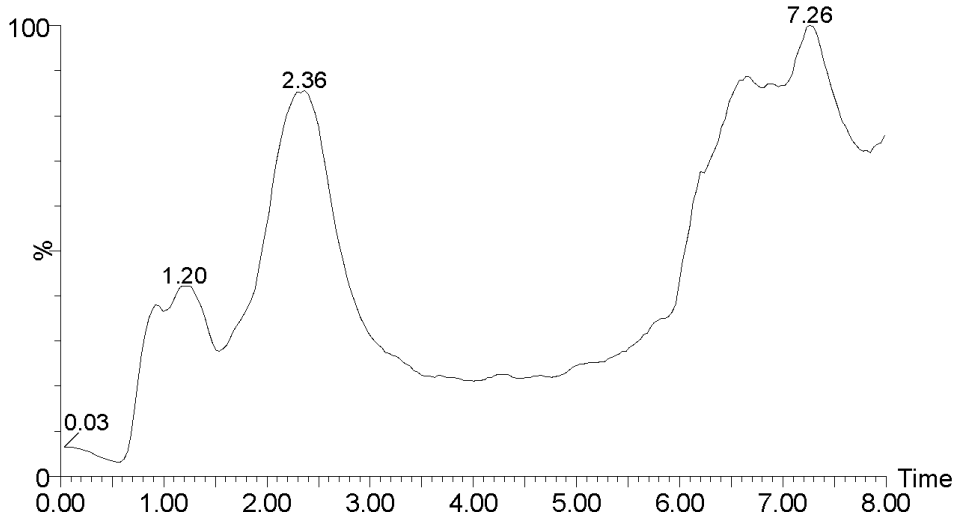

Total Ion Chromatogram (TIC) of **14**

Compound 15: Cy5.5(1S) Puzzle piece

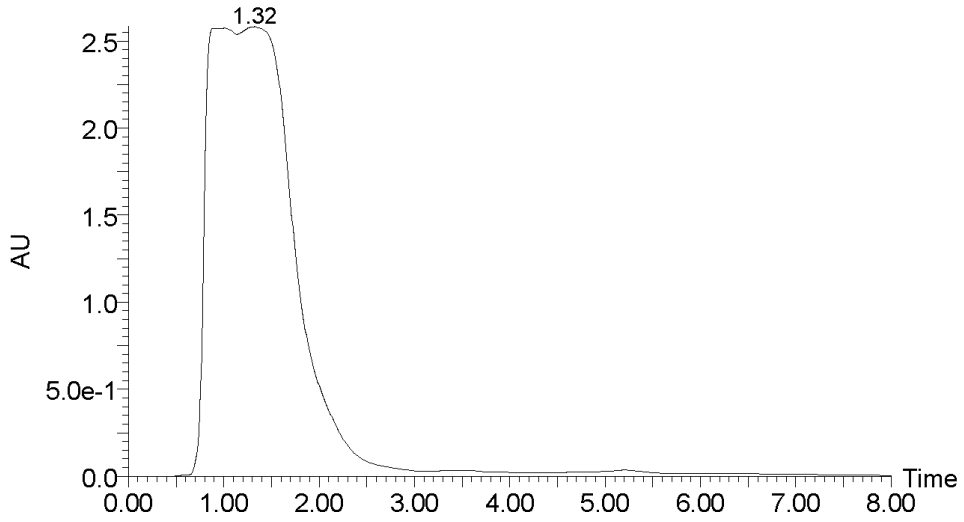

Single Wavelength Chromatogram of **15**, main peak at 1.32 min

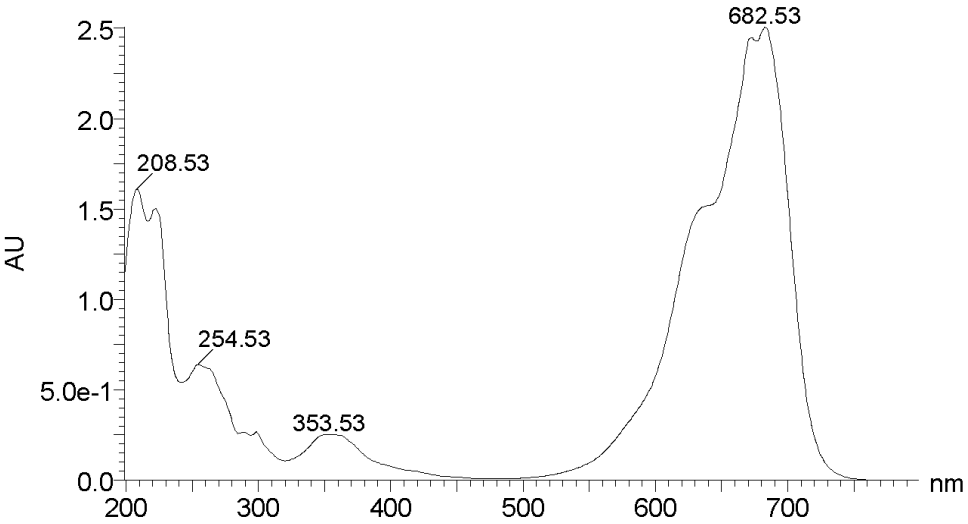

UV-Vis Diode array of **15** spectrum at 1.32 min with characteristic peak at 682 nm for Cy5.5(1S) dye

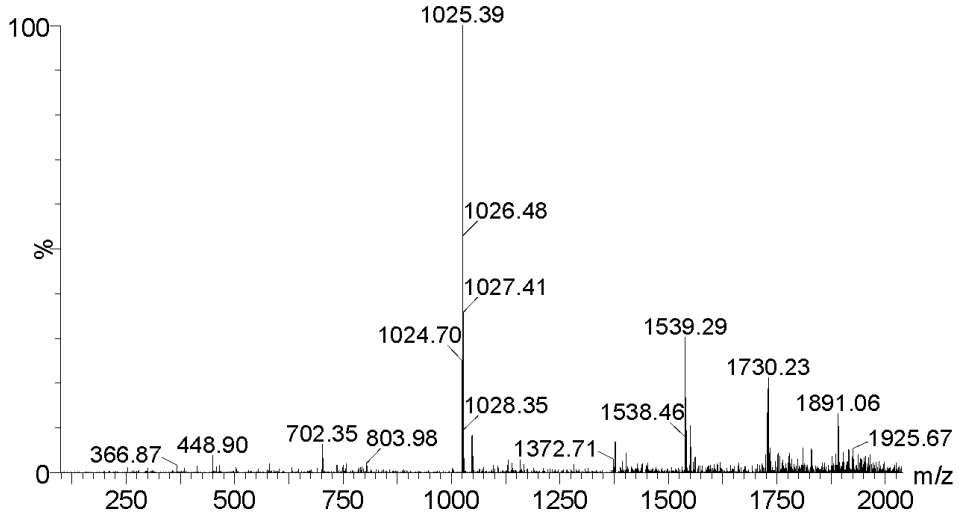

Negative Ion Mass spectrum of **15** at 1.32 min, product 1025.39 m/z $(M+2H^+)/2$

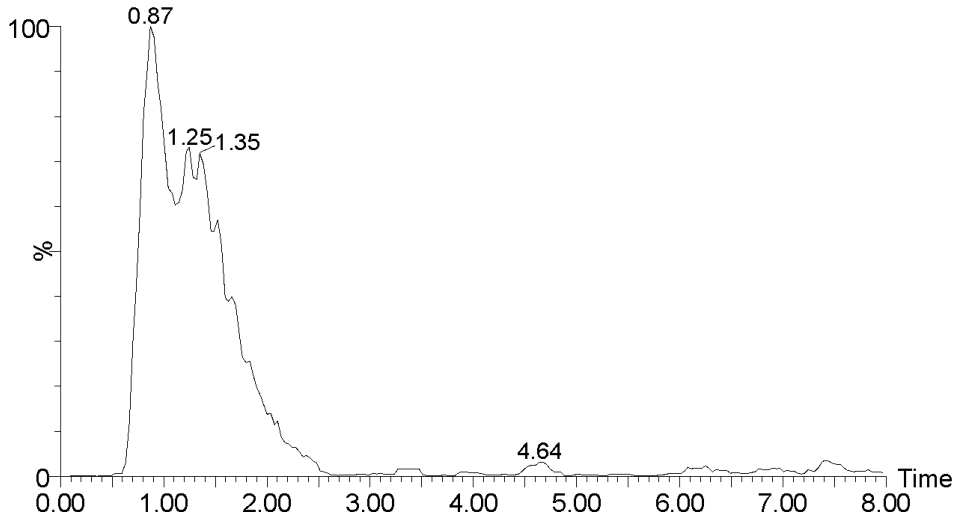

Extracted (Single) Ion Chromatogram (XIC) for Negative Ion at 1025 amu

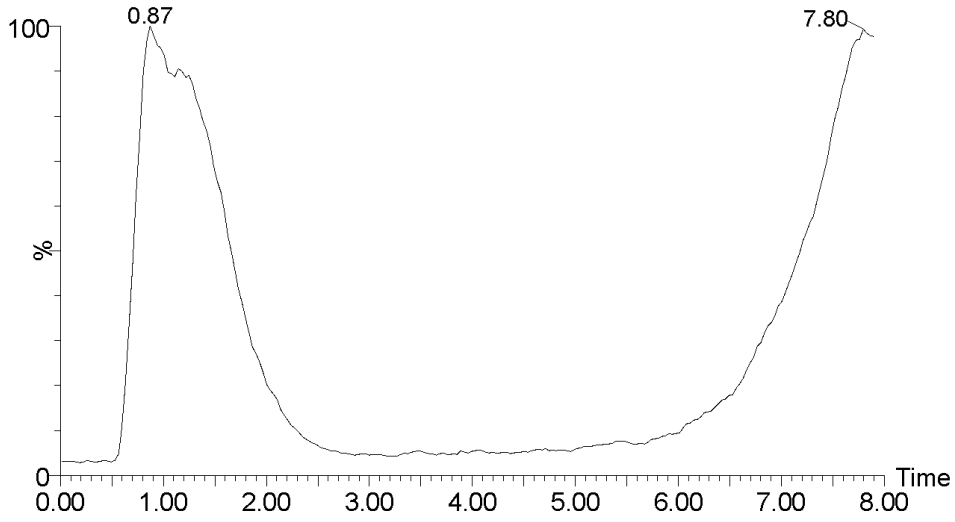

Negative Ion Total Ion Chromatogram (TIC) of **15**

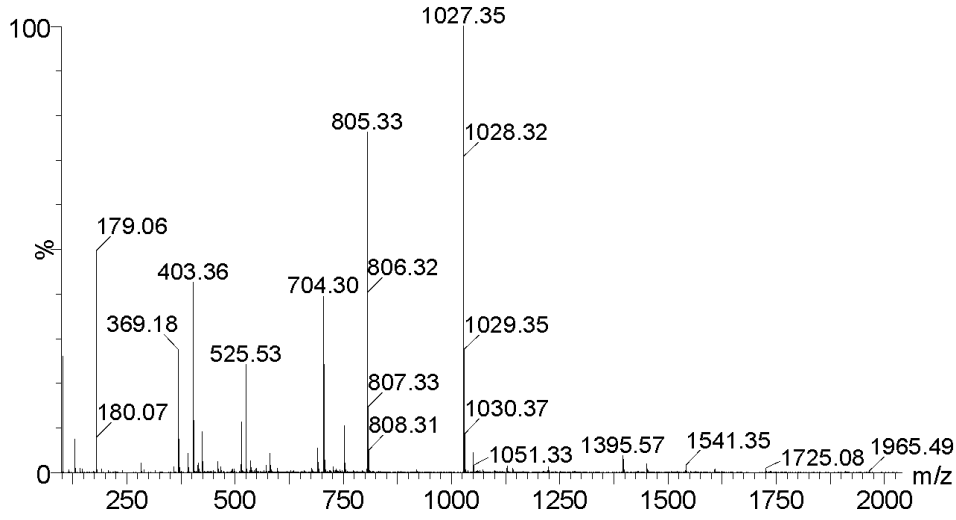

Positive Ion Mass spectrum of **15** at 1.32 min, product 1027.35 m/z $(M+2H^+)/2$

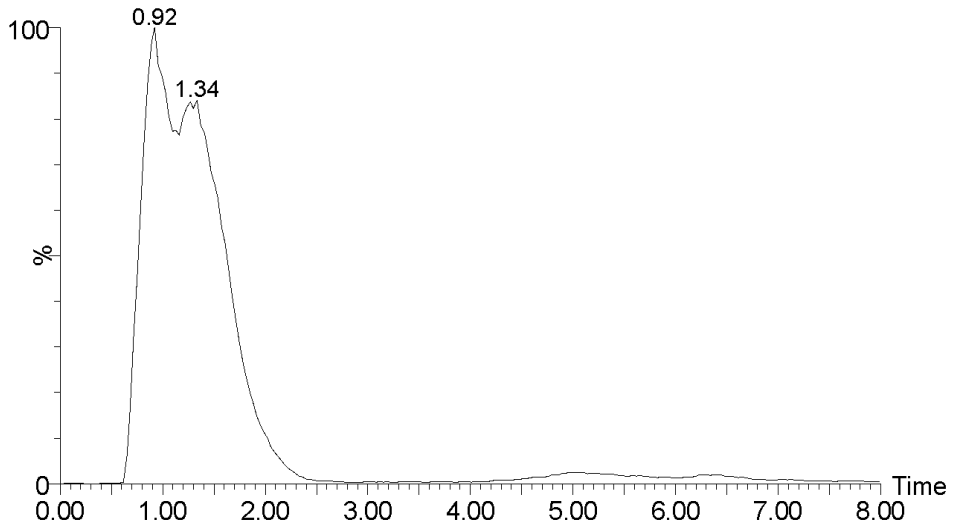

Extracted (Single) Ion Chromatogram (XIC) for Positive Ion at 1027.35 amu

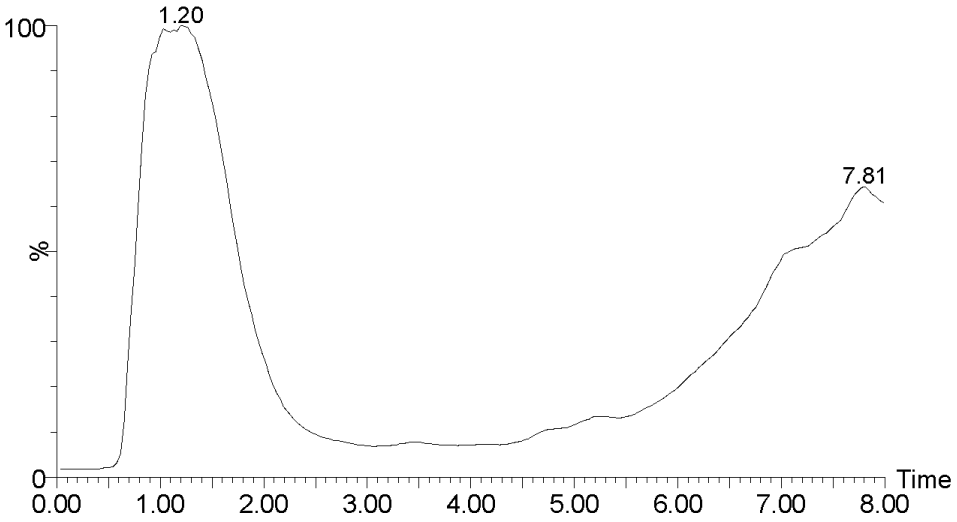

Positive Ion Total Ion Chromatogram (TIC) of **15**

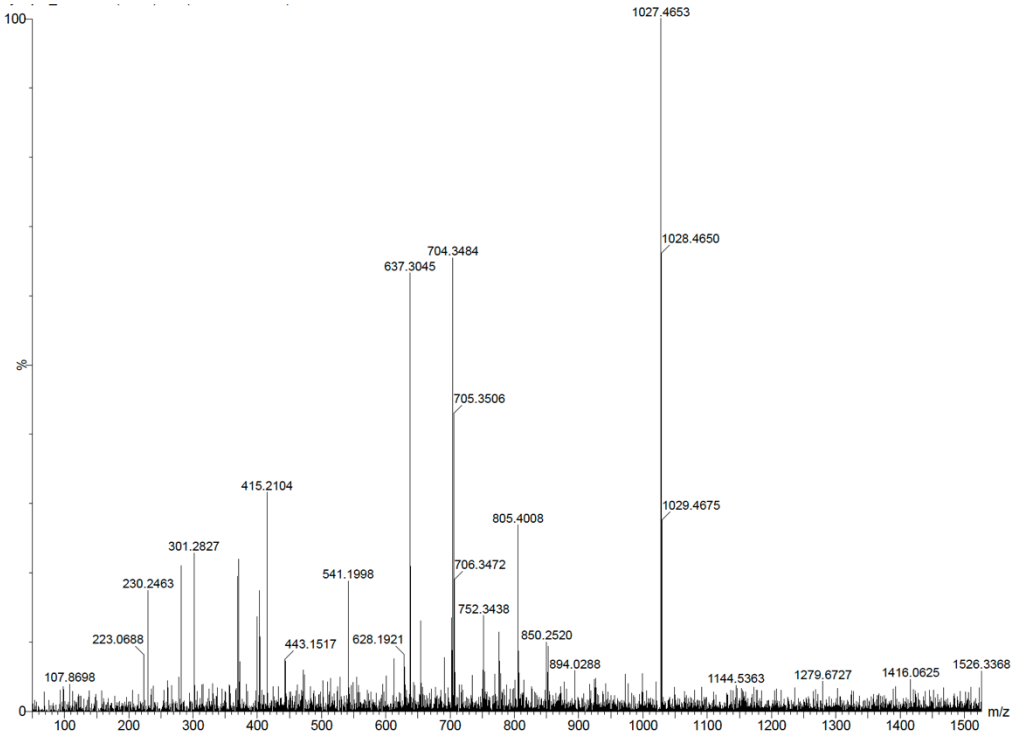

HRMS Positive Ion Mass Spectra of product **15** (Calc. MW 1027.46808,Found 1027.4653 m/z)

Compound 16: Butyl Amine Quench

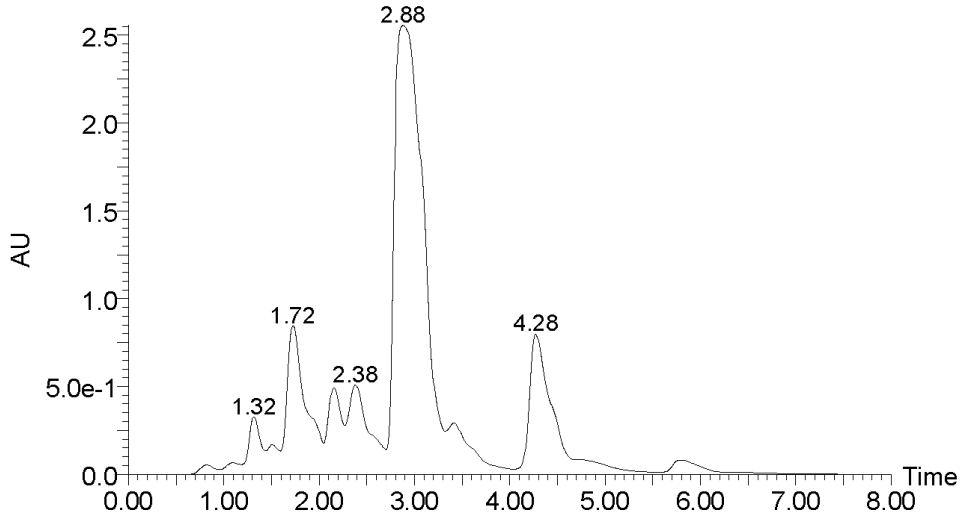

Single Wavelength Chromatogram of **16**, main peak at 2.88 min

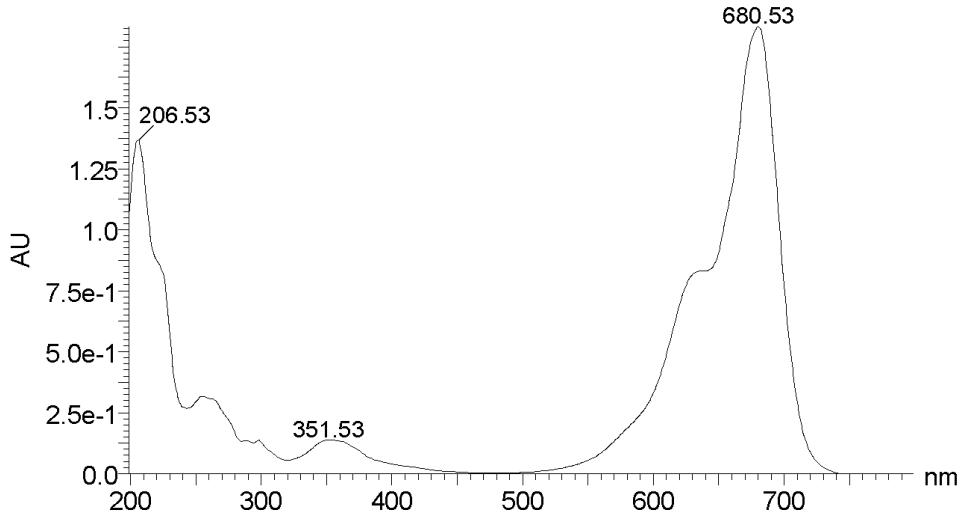

UV-Vis Diode array of **15** spectrum at 2.88 min with characteristic peak at 680 nm for Cy5.5(1S) Dye

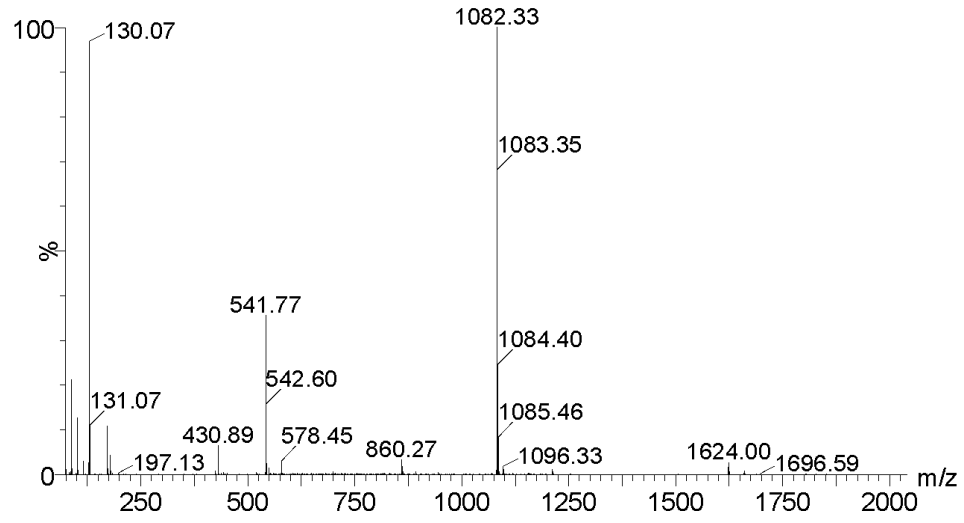

Positive Ion Mass spectrum of **16** at 2.88 min, product 1082.33 m/z $[M+H]_+$

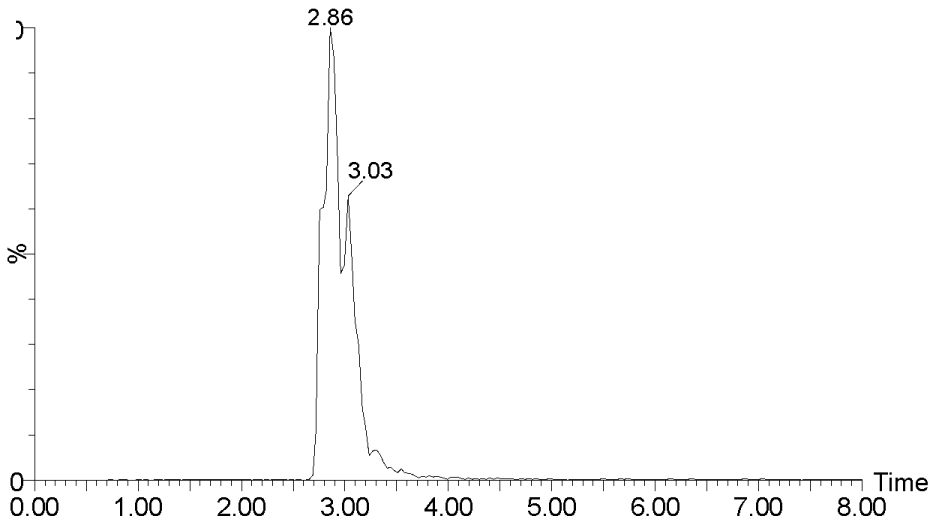

Extracted (Single) Ion Chromatogram (XIC) for Positive Ion at 1082.33 amu

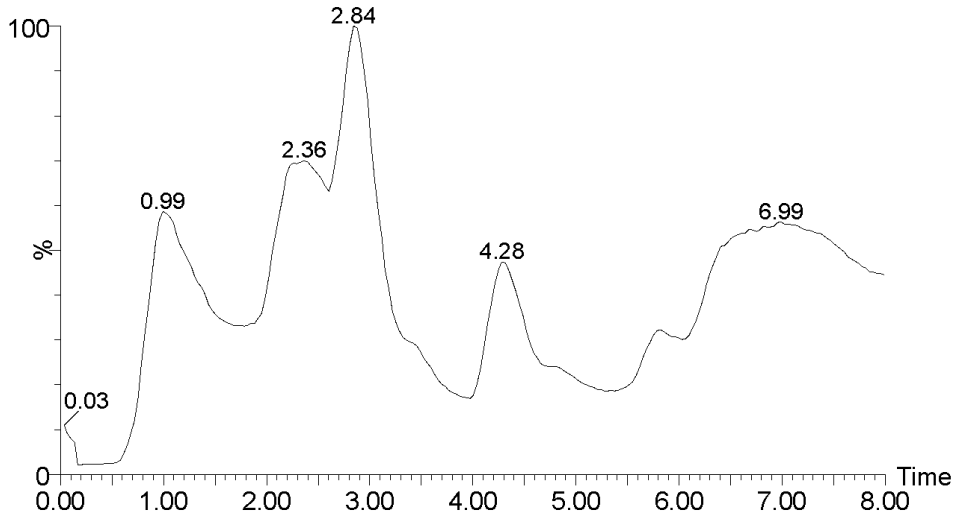

Positive Ion Total Ion Chromatogram (TIC) of **16**

Compound 17: NH_2-Cy5.5(1S)-Trp-d-Nle-Glu-Ala-Ala-Tyr-Gln-d-Lys-Phe-Leu-NH_2 (M3-TMIA Product)

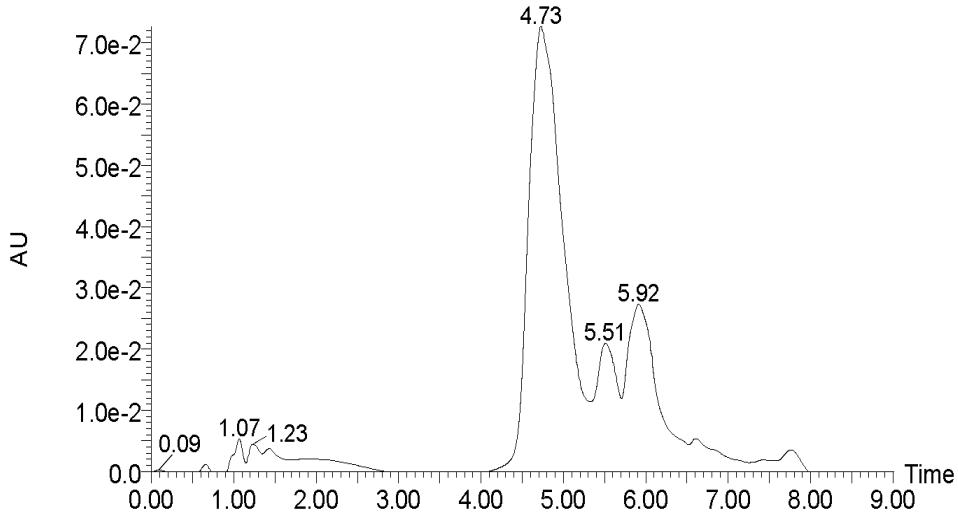

Single Wavelength Chromatogram of **17** at 680 nm, main peak at 4.73 min

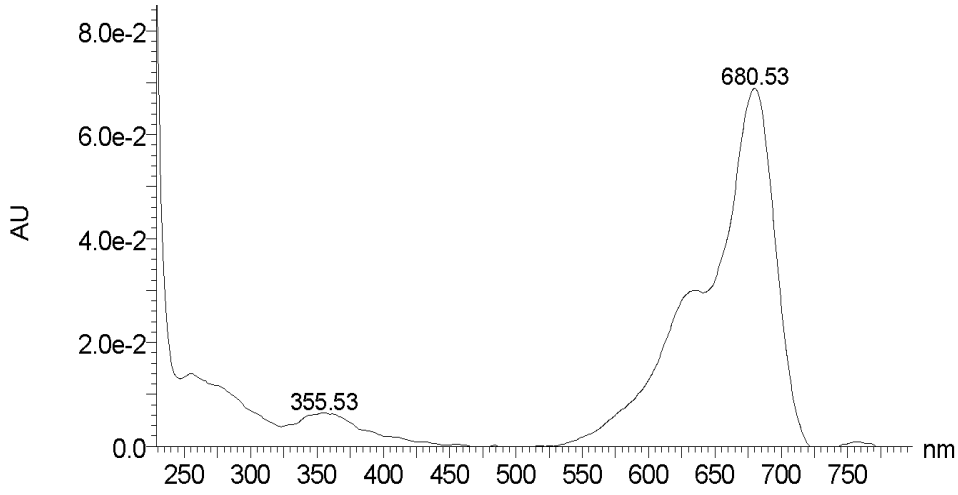

UV-Vis Diode array of **17** spectrum at 4.73 min with characteristic peak at 680 nm for Cy5.5(1S) dye

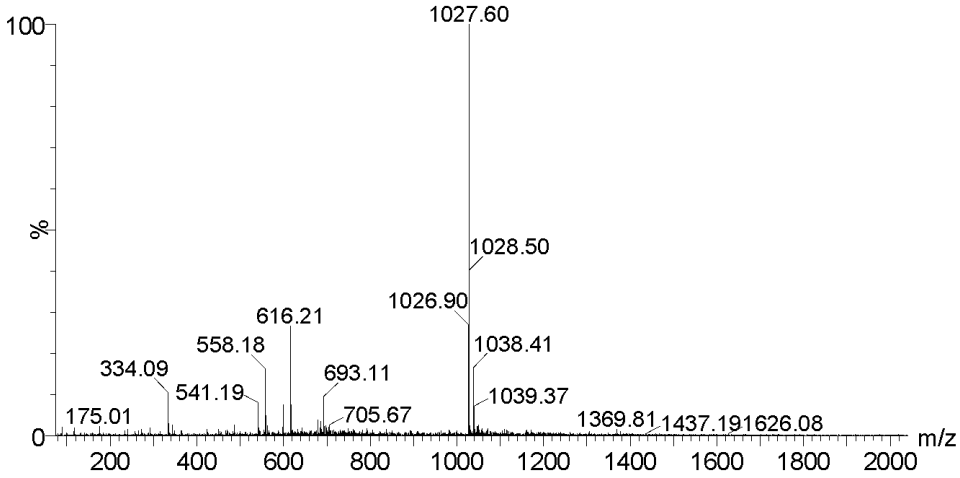

Positive Ion Mass spectrum of **17** at 4.73 min, product 1027.60 m/z $(M+2H^+)/2$

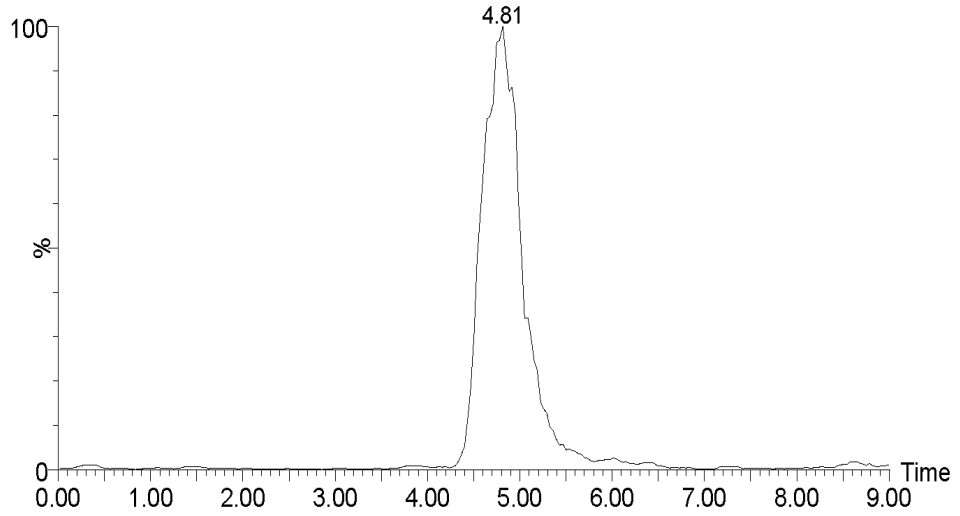

Extracted (Single) Ion Chromatogram (XIC) for Positive Ion at 1027.60 amu

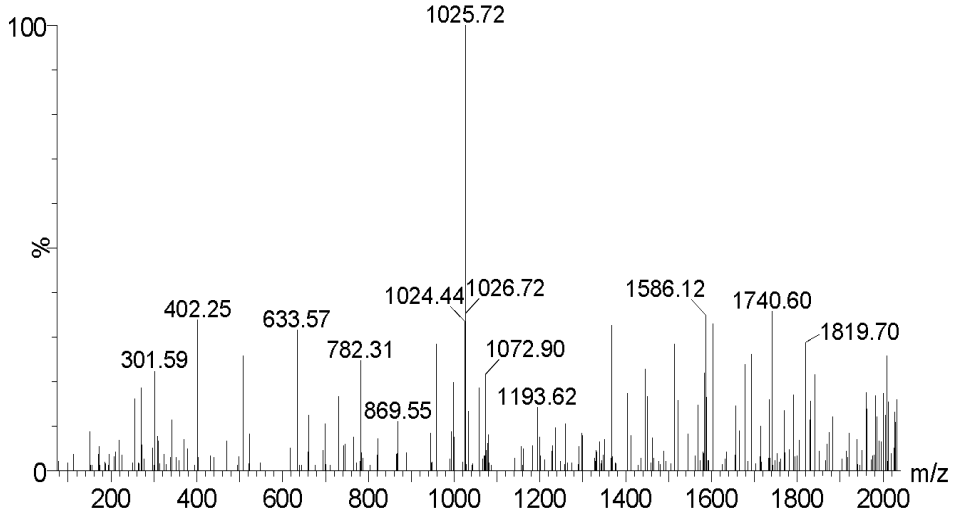

Negative Ion Mass spectrum of **17** at 4.73 min, product 1025.72 m/z $(M+2H^+)/2$

Compound 17: NH_2-Cy5.5(1S)-Trp-d-Nle-Glu-Ala-Ala-Tyr-Gln-d-Lys-Phe-Leu-NH_2 (M3-TMIA Product for Continuous TFA Cleavage Method)

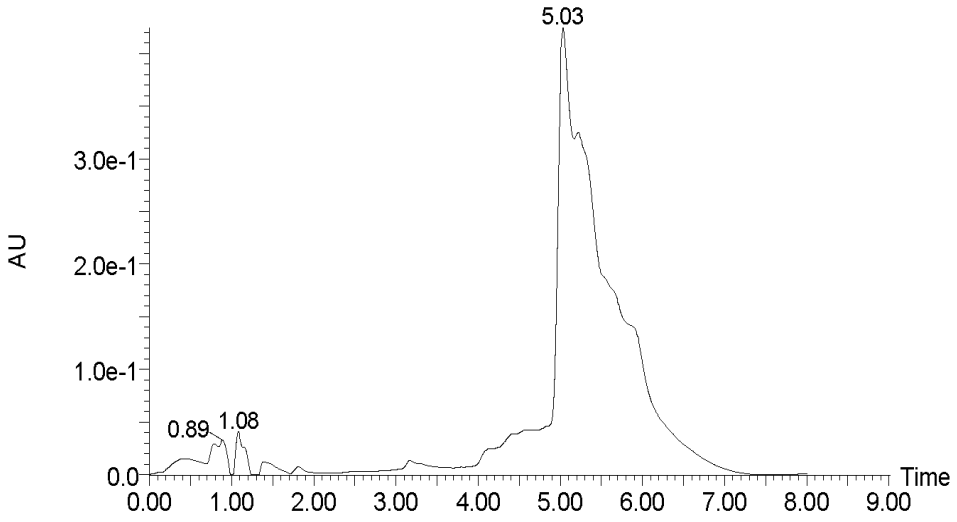

Single Wavelength Chromatogram of **17**, main peak at 5.03 min

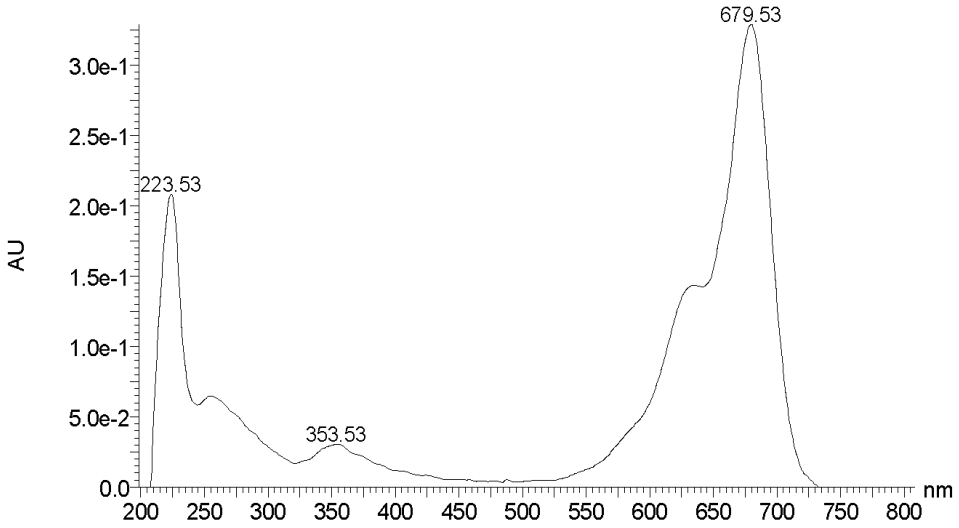

UV-Vis Diode array of **17** spectrum at 5.03 min with characteristic peak at 679.53 nm for Cy5.5(1S) dye

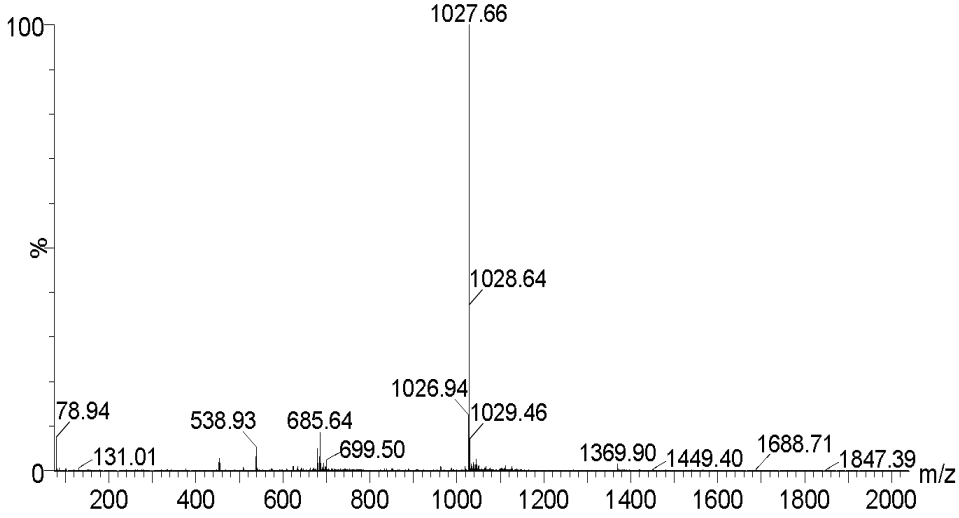

Positive Ion Mass spectrum of **17** at 5.03 min, product 1027.66 m/z $(M+2H^+)/2$

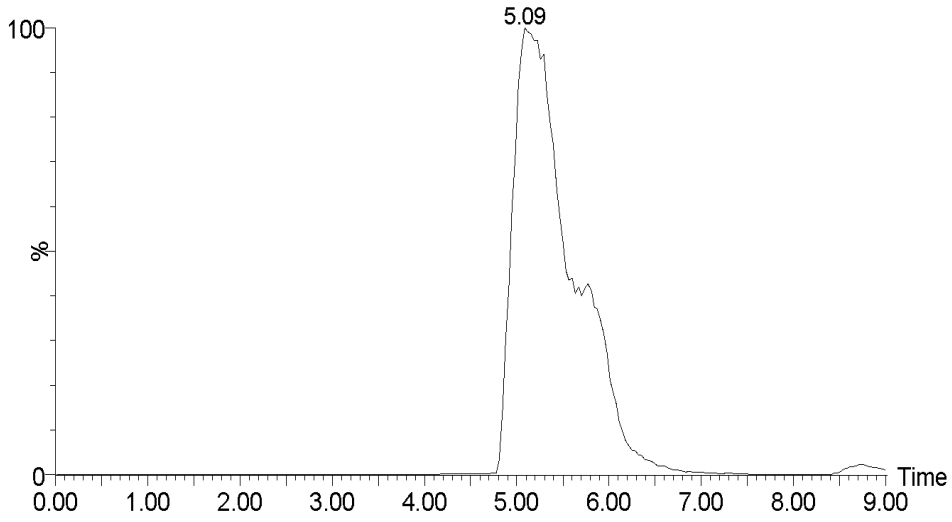

Positive Ion Extracted (Single) Ion Chromatogram (XIC) for Positive Ion at 1027.66 amu

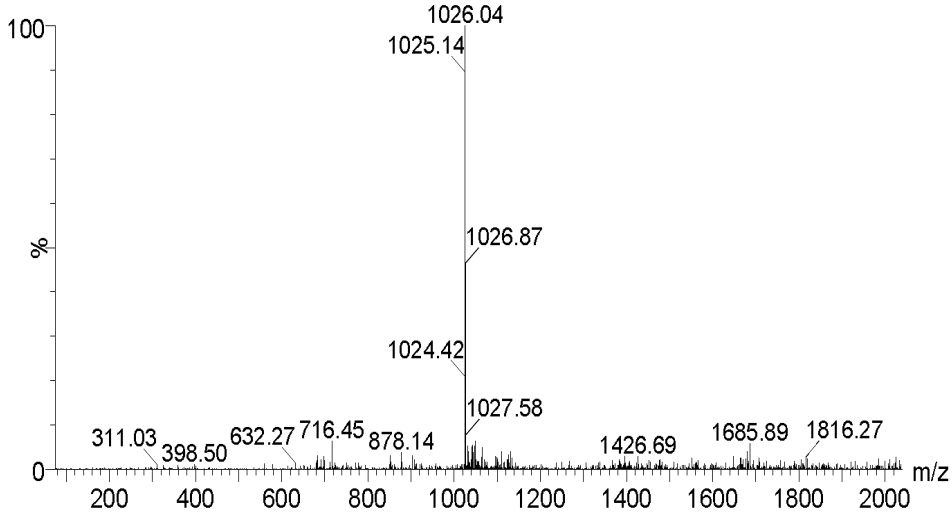

Negative Ion Mass spectrum of **17** at 5.03 min, product 1026.04 m/z $(M+2H^+)/2$

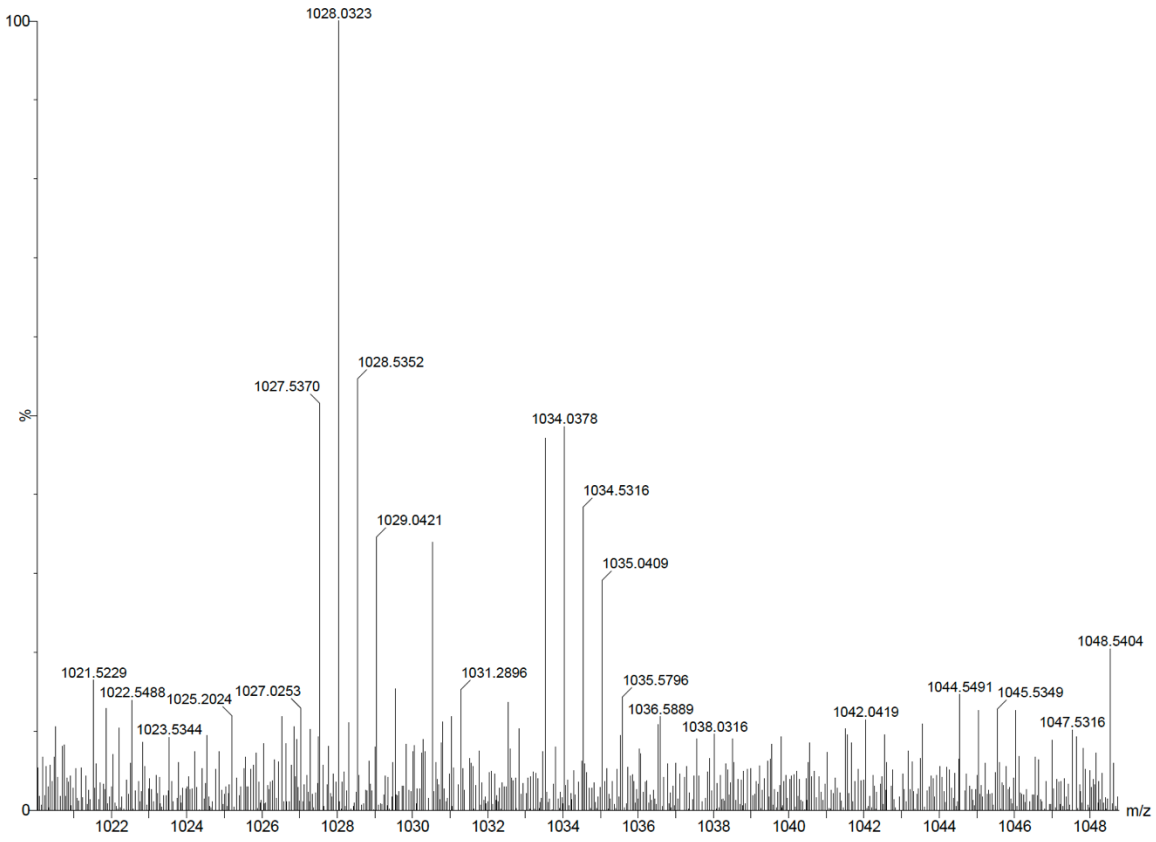

HRMS Positive Ion Mass Spectra of product **17** (Calc. MW 2053.05759, ½ mass 1027.53674, Found 1027.5370)

Compound 18: Fmoc-Gd(DOTA)-Cy5.5(1S)-Trp-d-Nle-Glu-Ala-Ala-Tyr(tBu)-Gln-d-Lys-Phe-Leu-NH_2 (Dual Modal Product)

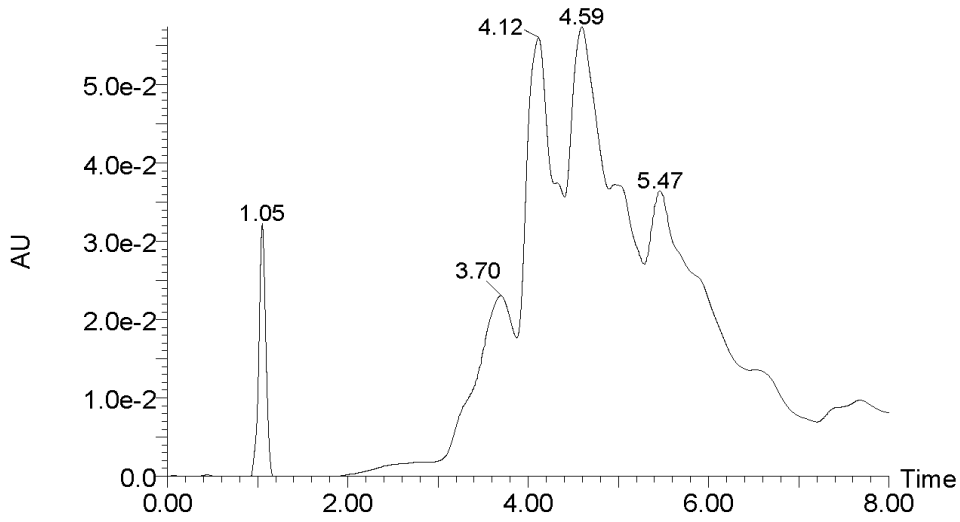

Single Wavelength Chromatogram of **18** at 680, main peak at 4.59 min

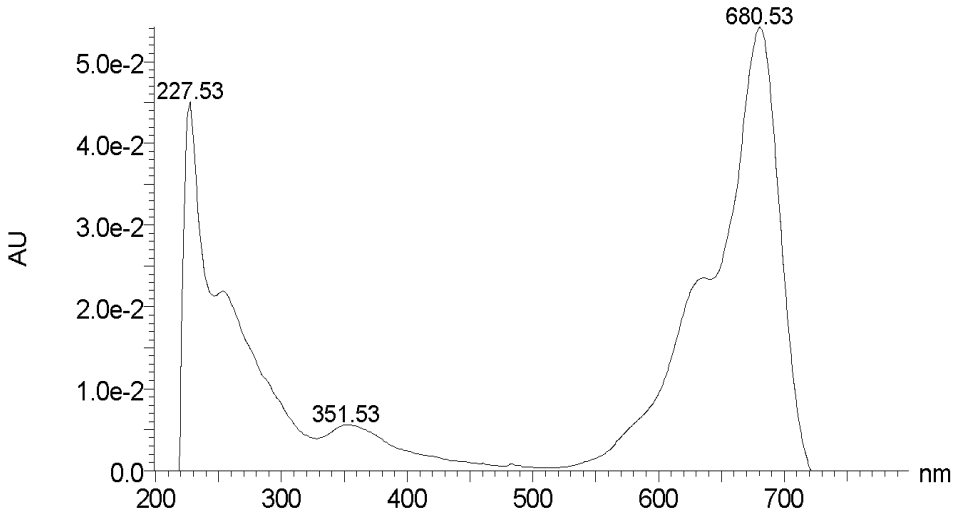

UV-Vis Diode array of **18** spectrum at 4.59 min with characteristic peak at 680.53 nm for Cy5.5(1S) dye

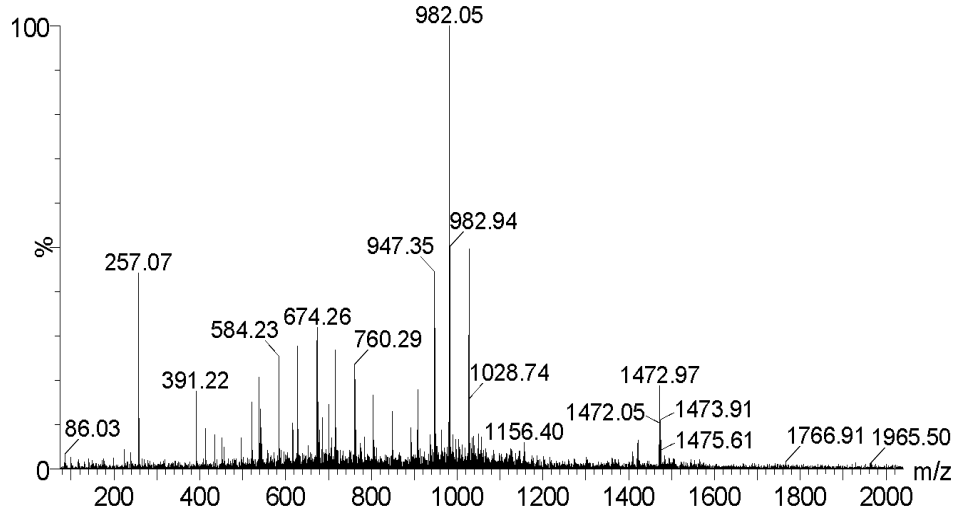

Positive Ion Mass spectrum of **18** at 4.59 min, product 1473.97 m/z $(M+2H^+)/2$ and 982.05 m/z $(M+3H^+)/3$

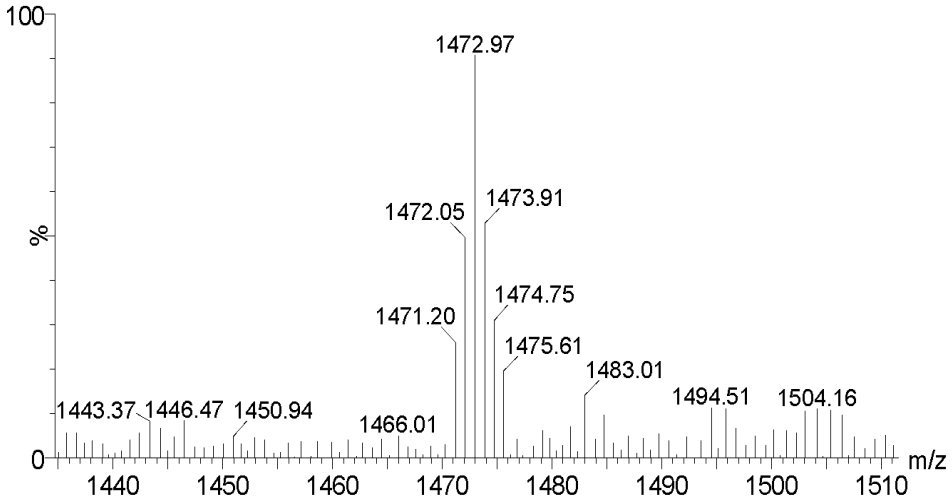

Positive Ion Mass spectrum of **18** at 4.59 min, product 1472 m/z $(M+2H^+)/2$ (showing Gd Trend)

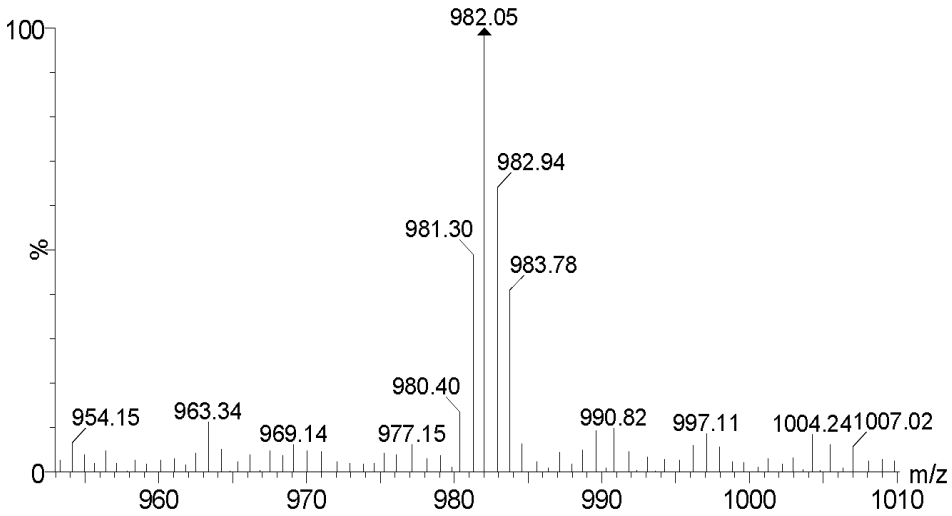

Positive Ion Mass spectrum of **18** at 4.59 min, product 982.05 m/z $(M+3H^+)/3$ (showing Gd Trend)